August 9, 1984

ANL Analysis of ZPPR-13A

compiled by P. J. Collins and S. B. Brumbach

ANL--97003542

Applied Physics Division
Argonne National Laboratory
P. O. Box 2528
Idaho Falls, ID 83403-2528

Work supported by the U. S. Department of Energy under Contract W-31-109-Eng-38.

TABLE OF CONTENTS

DISCLAIMER

Portions of this document may be illegible in electronic image products. Images are produced from the best available original document.

TABLE OF CONTENTS (cont.)

LIST OF FIGURES

LIST OF FIGURES (cont.)

LIST OF FIGURES (cont.)

Page

LIST OF TABLES

LIST OF TABLES (cont.)

LIST OF TABLES (cont.)

LIST OF TABLES (cont.)

LIST OF TABLES (cont.)

1.0 INTRODUCTION

The ZPPR-13 experiments provide basic physics data for radial-heterogeneous LMFBR cores of approximately 700 MWe size. Assemblies ZPPR-13A, ZPPR-13B and ZPPR-13C comprised the JUPITER-II cooperative program between US-DOE and PNC of Japan. The measurements were made between August 1982 and April 1984. The core designs and the measurements were planned jointly by the two parties with substantial input from U.S. industrial interests (GE-ARSD, W-AESD) to ensure coverage of the design requirements.

This report describes in detail the results of the ANL analyses of phases 13A

The data were compiled primarily for discussions at the Third Jupiter Analysis Meeting to be held at ANL-West between September 11th and 14th, 1984.

The Jupiter-I program covered experiments in conventional cores of similar size to ZPPR-13. ANL analyses of these data are described in Ref. 1 (ZPPR-9) and Ref. 2 (ZPPR-10).

The ZPPR-13 assemblies possessed the common features of a large central blanket zone, two internal blanket rings and three fuel zones of the same average enrichment. The cores were surrounded radially and axially by uranium oxide/sodium/steel blanket regions and by steel reflectors. The core height was 0.916 m and the fissile loading was about 2500 kg in each assembly.

The fuel and internal blanket arrangements for the ZPPR-13 series are shown in Fig. 1.1.

The physical characteristics of the ZPPR-13A are given in Table 1.1. The values in Table 1.1 refer to the reference critical configurations

In the design of the cores, the basic internal blanket arrangements were chosen first. Small adjustments were made to fuel and blanket boundaries to obtain peak/average power densities which were within reasonable limits, generally less than 1.3; but little attempt was made at optimization.

The experimental program was designed to follow changes in core properties in progressing from a simple benchmark, ZPPR-13A, to a power reactor design, A major concern in the large heterogeneous cores is the ability to predict spatially varying parameters. Consequently, measurement of reaction rate distributions and control rod worths comprised the principal measurements in each phase. Data on most other integral parameters were taken in ZPPR-13A The measurements made in each assembly are shown in Table 1.2.

The analysis of ZPPR-13 used ENDF/B-IV data for two reasons. First, for consistency with past analysis of ZPPR so that the ZPPR-13 cores could fill in gaps in the existing data base. Second, because at the start of the program the ENDF/B-V data were in the process of revision.

The reference model for each phase was three-dimensional (xyz) diffusion theory calculated with 28 group data. Since a vast number of calculations were required for analysis of control rod worths and for reduction of the experimental data, these were made in two-dimensional (xy) geometry and 8 groups. However, 28 group xyz calculations were also made for the principal rod banks in each phase. Two-dimensional models were also used to study asymmetry effects and transport corrections. These calculations will be described in detail in the subsequent sections.

In addition to the reference calculation, three special studies have been made for ZPPR-13A:

(i) Comparisons of calculations with ENDF/B-IV data and ENDF/B-V.2 (the second and final revision).

(ii) A Monte Carlo calculation with the VIM code.

(iii) Calculations with the recently developed nodal-diffusion and nodal-transport codes.

These studies will be reported as special topics.

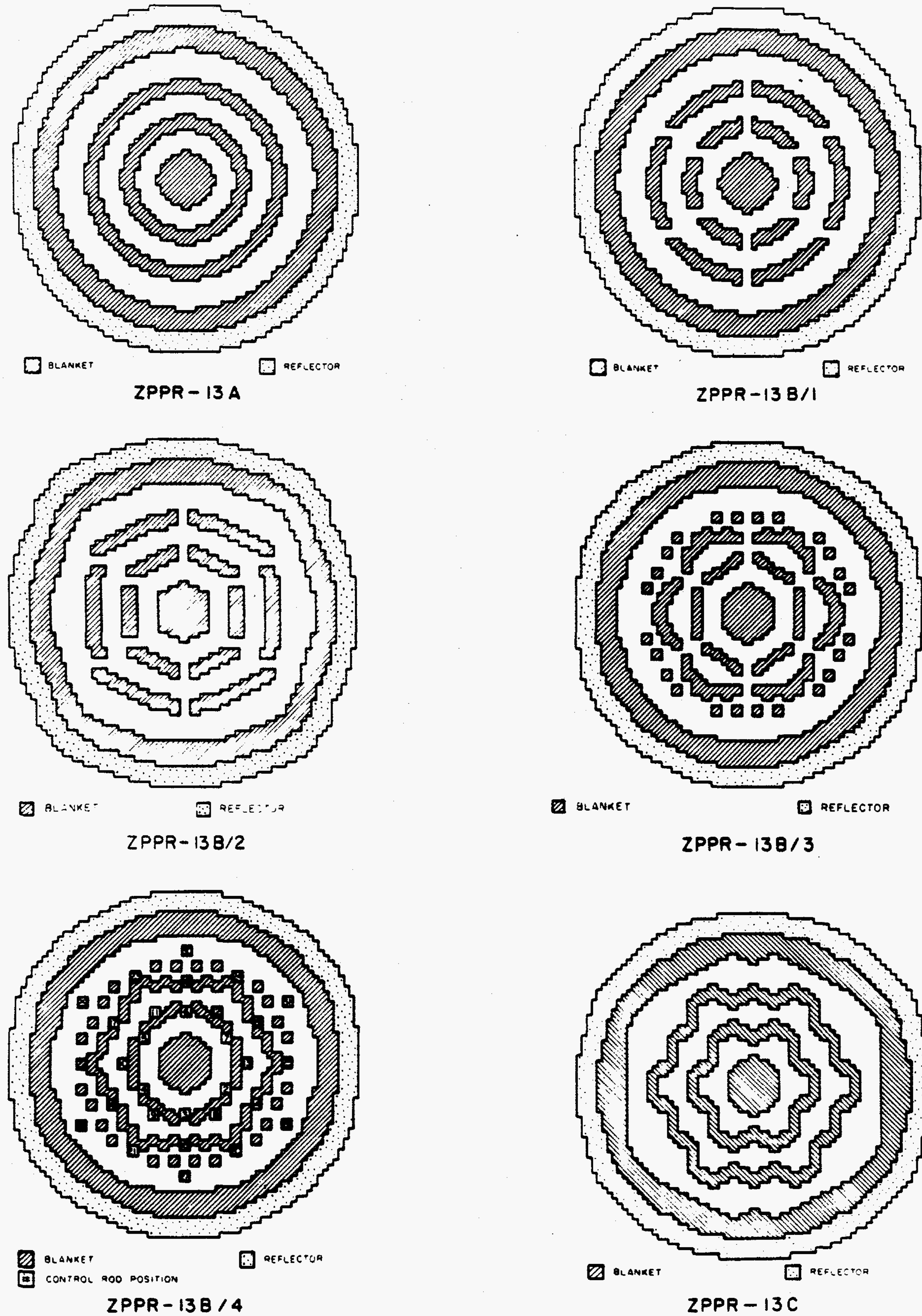

Fig. 1.1. Core/blanket configurations for the ZPPR-13 cores.

TABLE 1.1. Physical Characteristics of ZPPR-13A

	ZPPR-13A
Core Volume, L[a]	5715.472
Effective Radius, m[a]	1.995
^{239}Pu Mass, kg	2435.060
Total Fissile Mass, kg	2513.073
^{238}U Mass, kg[b]	
Core Regions	8332.193
Internal Blanket	16313.678
Radial Blanket	21572.243
Axial Blanket	10200.764
Total Fuel Drawers	2880
Total Internal Blanket Drawers	1216
Fraction of Double-Fuel-Column Drawers[d]	0.72

[a]Fuel plus internal blanket zones.

[b]Internal and radial blankets are ± 788 mm. Core region is ± 458 mm. Axial blanket is ± 458 to ± 788 mm.

[c]Includes sodium-filled control rod positions.

[d]Core average.

JAIIA4

TABLE 1.2. The Experimental Program in ZPPR-13A

	ZPPR-13A
Date of first critical	8-5-82
Approach to critical	●
Criticality	●
Reaction Rates:	
Detailed xy	●
Limited xy	●
Axial	●
Control Rod Worths:	
Single Rods	●
Rod Banks	●
Rod Interactions	
Pin Rods	
Large Rod Sizes	
CPR/Fuel Reactivity	●
Sodium Void	●
Doppler Coefficient	●
Reactivity Samples:	
Traverses	●
Drawer Oscillator	●
Kinetics Measurements	●

[a]ZPPR-13B/2 was subcritical by 3.6$. Reaction Rates were measured with the 64 in-core fission chambers.

JAIIA5

2.0 DESCRIPTION OF THE ASSEMBLIES AND MEASUREMENT TECHNIQUES

2.1 General Features of Cell Designs and Core Loadings

Previous experience with smaller heterogeneous cores (350 MWe) and larger homogeneous cores (700-900 MWe) had indicated the need for maximum simplicity and uniformity in cell designs. The following constraints were imposed at the outset:

(i) Use of a single type of fuel throughout -- the ZPPR Pu/U/Mo metal fuel using plutonium with 11% ^{240}Pu content. This limited the core sizes to a little less than 2500 kg.

(ii) Use of cells symmetric in placement of plutonium and uranium plates within a drawer.

Five basic cell designs were used in all cores of the series: single-fuel-column, double-fuel-column, internal and radial blanket, axial blanket and steel reflector. The plate loadings of the cells are shown in Fig. 2.1, 2.2 and 2.3.

In practice, many detailed variations about the basic cell loadings were necessary because of inventory limitations and operational/experimental requirements. These were:

(i) Variations in piece length distributions making up the fuel and sodium columns in a drawer.

(ii) Variations in ZPPR fuel by "vendor type" (Vendor-65, Vendor-63).

(iii) Variations in sizes of individual uranium oxide, uranium metal and steel plates.

(iv) Narrow drawers required to accommodate the ZPPR safety/shim rod blades.

(v) Special drawers for in-core fission chambers.

(vi) Thermocouple drawers.

Initially, narrow blanket drawers and blanket detector drawers contained less ^{238}U than standard blanket drawers. This mass difference and other small variations in drawer loading had significant effects on the measured parameters, as will be discussed in detail in subsequent sections.

Other, less important, deviations from an ideal, uniform, loading imposed by inventory limitations occurred in the upper reaches of the axial blanket and in the radial reflector.

Changes in fuel enrichment were achieved by changing the ratios of single-fuel-column (SFC) drawers to double-fuel-column (DFC) drawers. Exactly the same ratio could not be obtained in each fuel region, but these proportions were made as close as possible. All fuel and blanket loadings were symmetric in the four quadrants, but the SFC and DFC drawers were not symmetric about the quadrant bisector (resulting in differences of several percent in fluxes between the x and y axes). This latter feature was not regarded as important since analyses would necessarily be made in xy or xyz geometry and little uncertainty in the evaluation of the data was expected. Other asymmetries were caused by the narrow drawers and detector drawer placements. The former are constrained by locations available in the ZPPR machine. The latter were placed in asymmetric positions in order to provide maximum utility in coverage of the whole core.

2.2 The Assemblies

ZPPR-13A was designed to be a benchmark core for the series. Internal blanket zones were continuous and all regions had closely cylindrical outlines. The reactor loadings prohibit direct use of an rz model for detailed comparison with experiment, but the calculation of reactor-average properties (k_{eff}, β_{eff}) are reasonably accurate and transport/diffusion theory corrections are facilitated in this geometry.

ZPPR-13B/1 retained the basic zone outline of 13A, but gaps were introduced into the two internal blanket rings as a first step in the progression towards more prototypic cores. Reaction rates and control rod worths were measured for comparison with analyses of ZPPR-13A, Fig. 2.4 compares fission rates in -13A. This figure explains the changes in most measured parameters.

2.3. Experimental Techniques and Uncertainties

Most of the experimental methods used in ZPPR-13 have been in standard use at ZPPR and are described in the TM reports. Several refinements were found necessary due to the sensitivity of the larger heterogeneous cores. Some new techniques for sample reactivity worth measurements were used in ZPPR-13, following results from the ANL diagnostic core series in ZPR-6, ZPR-9 and ZPPR-12. This section summarizes the principal points relevant to the analysis and the uncertainties estimated for each type of measurement.

2.3.1 Critical Mass (k-effective)

Uncertainties in the experimental critical mass are due to imprecision in material masses and locations, and core temperatures. For convenience in the analysis, adjustments are made for the reactivity of inserted shim rods, parked shim and safety rods and to a uniform temperature of 293 K. The adjustments are conveniently expressed in Δk units using a calculated value for β_{eff}. A number of less tractable features of the assembly are normally assigned experimental uncertainties. These are often relatively small and need be only crudely estimated.

The current assessment of uncertainties for experimental values of k_{eff} in ZPPR-13 is shown in Table 2.1. The total uncertainty of about 0.04% Δk (1σ) is dominated by knowledge of the fuel mass. Consequently this varies but little among all Pu/U oxide LMFBR criticals built at ZPPR. Many of the large uncertainties are correlated among the assemblies.

2.3.2 Reaction Rate Measurements with Foils

Four reaction rate types were measured in ZPPR-13 with foils: $^{239}Pu(n,f)$, $^{235}U(n,f)$, $^{238}U(n,\gamma)$, $^{238}U(n,f)$. The number of available plutonium foils and their recycle time limits their use to a few traverses in the principal assemblies of the series. However, experience has shown that equivalent information on the ability to predict spatial power distributions in core regions is obtained with ^{235}U foils. Thus extensive use is made of ^{235}U. For convenience in the analysis and to provide data directly relating to principal components of the neutron balance in the assemblies, the basic reaction rates measured in the foils are converted to "plate-average" and to "cell-average" quantities using measurements with several foils in the unit cells and "split-plates", i.e. plates of half-thickness to include central foils or "cell-averaging foils".

The uncertainties in measured reaction rates may be considered in three categories:

(i) Statistical uncertainties in the foil counting (these also include components for foil placement and correction for other isotopes).

(ii) Uncertainties in the cell-average/foil factors.

(iii) Uncertainties due to absolute calibration.

For analysis of reaction rate distributions between cells of the same type, the statistical uncertainty is the major component. Measurements with multiple foils in cells at different locations generally indicate good separability between the cell fine-structure and the overall reactor reaction rates.

For comparison of a given reaction rate in different cells, the uncertainties in cell-average factors should be considered. For reaction rate ratios the calibration uncertainties must be taken into account together with the correlation implicit when a common denominator reaction, usually $^{239}Pu(n,f)$, is used.

Typical statistical uncertainties are about 0.8% for the three non-threshold reactions and about 1.5% for $^{238}U(n,f)$ within the fuel and internal blanket regions. In the radial, axial and the large internal blanket the statistical uncertainties for the $^{238}U(n,f)$ reaction rate deteriorate rapidly with penetration, increasing from 2% to 20% or more. This is due to the attenuation of the high energy flux and to the increasing importance of corrections for ^{235}U content in the foil.

Uncertainties in the cell-average/foil factors are due to statistics in the fine-structure measurement, calculated adjustments for gross reactor gradients and to the split-plate/whole-plate factor (Stanford-Robinson experiment). These uncertainties are about 2%.

Uncertainties in the foil calibration are estimated to be 1.5%. However systematic differences between ANL and UK techniques(3) of 3% in the ^{238}U capture to ^{239}Pu fission ratio, of which 2% is due to the plutonium fission calibration, have yet to be explained.

Foil irradiations are made at a reactor power of approximately 1 kW. The reactor is controlled by ZPPR shim rods, which are narrow blades of 93% enriched B_4C inserted in 1/2 in. spaces in the matrix created by use of drawers of only 3/4 normal width. The excess reactivity is kept to a minimum and for ZPPR-13 was in the range of 6¢ to 13¢. The shim rods produce perturbations in reaction rates at the midplane of about 1%. To facilitate their modelling in the calculations, eight symmetrically disposed shim rods (four in each half) are used in the irradiation with equal insertion. The shim-rod perturbations have been checked in several cases using the 64 fission chamber system.

2.3.3 Reaction Rate Measurements with the In-core Fission Chambers

The statistical precision obtainable with the sixty-four in-core fission chambers can be very high. In practice an uncertainty of about 0.1% is usually obtained to avoid overly long counting times in far-subcritical states. For reactivity measurements, using countrate ratios in each chamber, only the statistical uncertainties need be considered.

Because of the extensive core-coverage afforded by the fission chamber system, the fission chambers have been calibrated against ^{235}U foils placed in normal cells in positions symmetric to the fission chambers. The calibration takes into account the variation in mass of the fission chamber deposits and the electronic biases. The calibration has been discussed by Ikegami.[4] Uncertainties in the calibration are estimated to be 1.5%.

2.3.4 Reactivity Measurements

Large-scale reactivity measurements of control rod worths, zone sodium voiding and drawer substitutions are measured relative to a reference configuration by the modified-source-multiplication (MSM) technique.[5] A reference state, subcritical by 10¢ to 20¢, is established and the reactivity scale (in dollars) is measured by inverse-kinetics analysis of the power history following a "rod-drop". The only calculated input required are the λ_i values from the delayed neutron analysis. The experimental reactivity is insensitive to these data and an uncertainty of 0.7% is estimated from the statistical analysis.

Calculated values for "detector efficiencies" and "effective source ratios" are provided for determination of reactivity relative to the chosen reference. A linear least-squares fit of the reactivity estimate from each detector versus efficiency ratio (ϵ) results in a statistical uncertainty for the system reactivity of about 0.1%. Measurements of asymmetric perturbations in ZPPR-13 showed the need for improved estimates of the effective source ratio (S_R). These can be obtained by an iterative method in which the cross sections in the perturbed region are adjusted until a good fit to the detector countrates (relative to those in the reference) is obtained. Numerical tests have shown that the result could be achieved by the relation $(1-\epsilon^2) \approx (1-S_R)$ (Ref. 6), thus eliminating the need for multiple calculations. The source ratios vary in the range 0.7 (for control rod banks worth about $20) to 1.1. As a result of the numerical tests, an uncertainty of 0.04 $(1-S_R)$ was assigned with a minimum uncertainty of 0.3%. Additional uncertainty components arise from corrections for the (relative) ZPPR interface gap, temperature, and ^{241}Pu decay. These are relatively small components for control rod worths, but may dominate in the case of sodium void reactivities.

2.3.5 Small-sample Reactivity Worths

Small-sample reactivity worths were measured in ZPPR-13 using three techniques. These techniques were the radial and axial tube, the shim blade and the long-drawer oscillator. Radial tube measurements are made at the reactor midplane. The oscillator tube is accommodated by pushing the drawers along one row of both assembly halves back from the interface about 6.4 mm. The axial tube is accommodated by using a special drawer with 12.7 mm of material removed from the center of the drawer. Small, encapsulated samples, usually with cylindrical or annular geometry are oscillated in and out of the core. Because of the perturbation caused by the presence of the tube, sample worths are also measured by other techniques. One new technique used in ZPPR-13 measurements is the shim-blade oscillator. A sample, normally a foil of fissile material, is attached to a (0.9 mm thick) stainless steel blade which is oscillated axially in the air gap between the top of the contents of a drawer and the matrix tube. Special drawers with a bottom thickness of 0.25 mm instead of the normal 0.75 mm are used to increase the thickness of the air gap to 2 mm. Foils up to 0.5 mm thick are placed in a shallow depression in the blade and covered with 0.05 mm thick stainless steel to protect the samples during oscillation. In the long-drawer-oscillator technique, a special drawer, is loaded with core material and special samples of interest. The sample zone is oscillated axially in and out of the core. Sample worths are inferred from worth differences with and without the samples. For all techniques, worths are derived from the inverse-kinetics analysis of the output of the two experimental ex-core BF_3 chambers.

All three sample worth techniques were used in ZPPR-13, but only the axial- and radial-tube measurement data have been processed and none of the measurements have been adequately analyzed.

Statistical uncertainties in the tube-oscillator technique range from 0.2 - 0.6% for high worth samples. Other, larger, systematic uncertainties arise from uncertainties in temperature, sample position and half closure. These systematic uncertainties are estimated to be about 1-2% for high-worth samples.

2.3.6 Doppler Coefficient

The Doppler measurements at ZPPR use a cylindrical sample, sealed in Inconel, 305 mm long and 25.4 mm in diameter with a 3 mm hole in the center to accommodate thermocouples. Samples are heated in vacuum by a heating element wrapped around the Inconel capsule. Measurements are made in a single matrix location by oscillating the sample axially into and out of the core. Worth is inferred from inverse-kinetics analysis of the output of the two experimental ex-core BF_3 chambers. Uncertainties in measured values are estimated to be about 2-4%, based mostly on measurement reproducibility.

2.3.7 Summary of Experimental Uncertainties

Table 2.2 summarizes the uncertainties in the various measured quantities discussed in this report. For the sample worth measurements and the Doppler measurements, the random uncertainties are relatively small. For these measurements it is likely that not all sources of systematic uncertainty have been quantified or, perhaps, even identified. Thus, the Doppler, and small sample worth uncertainties are estimated from experience in reproducing results of similar measurements.

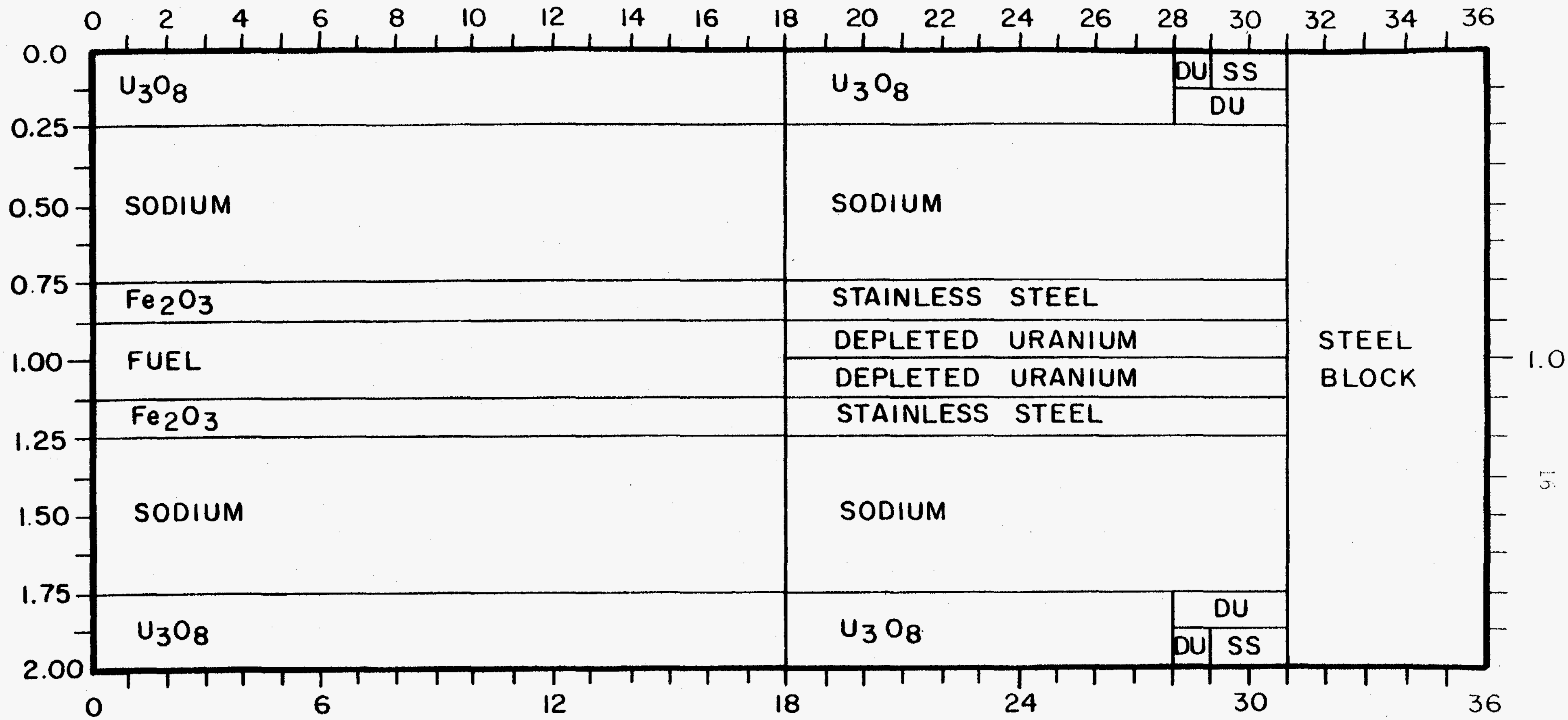

Fig. 2.1. Typical loading pattern for a single-fuel-column drawer.

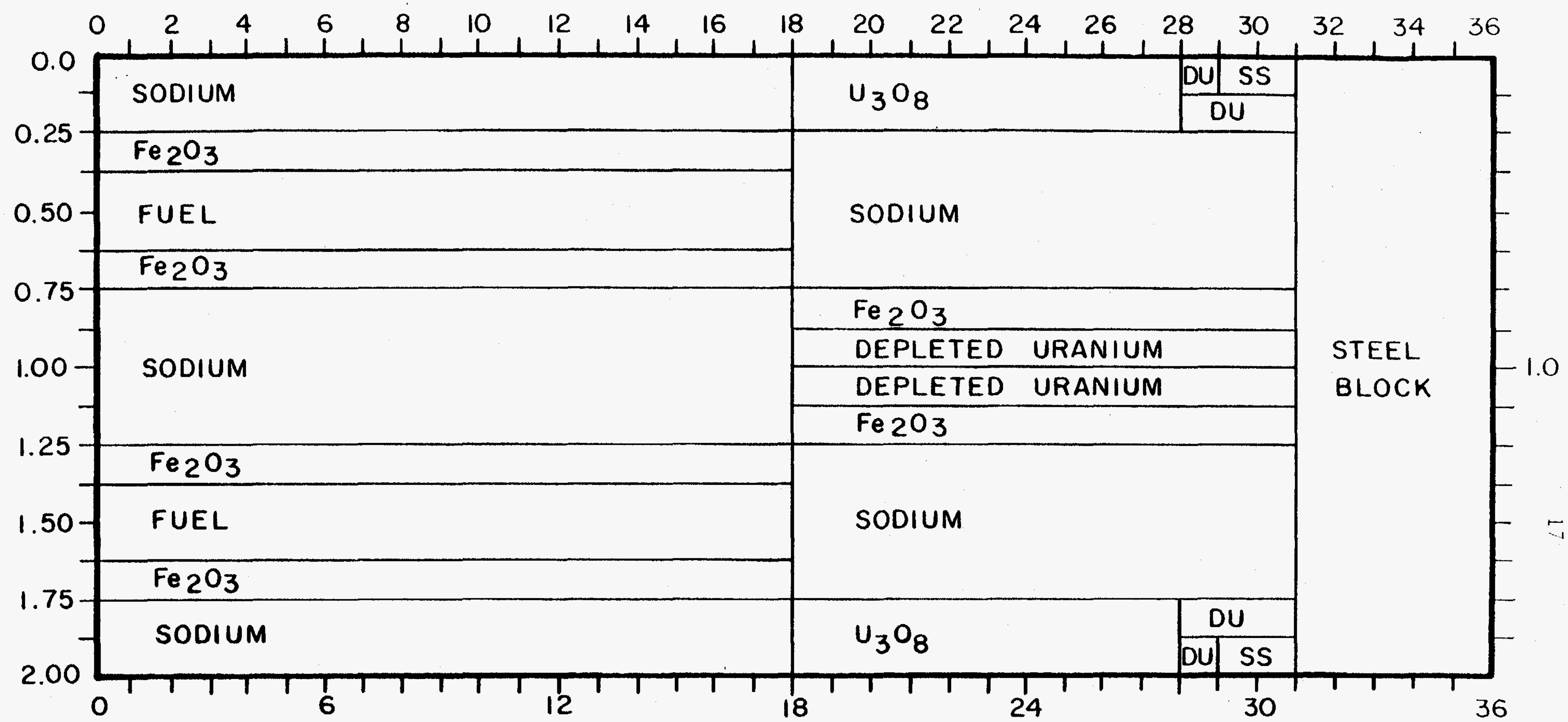

Fig. 2.2. Typical loading pattern for double-fuel-column drawer.

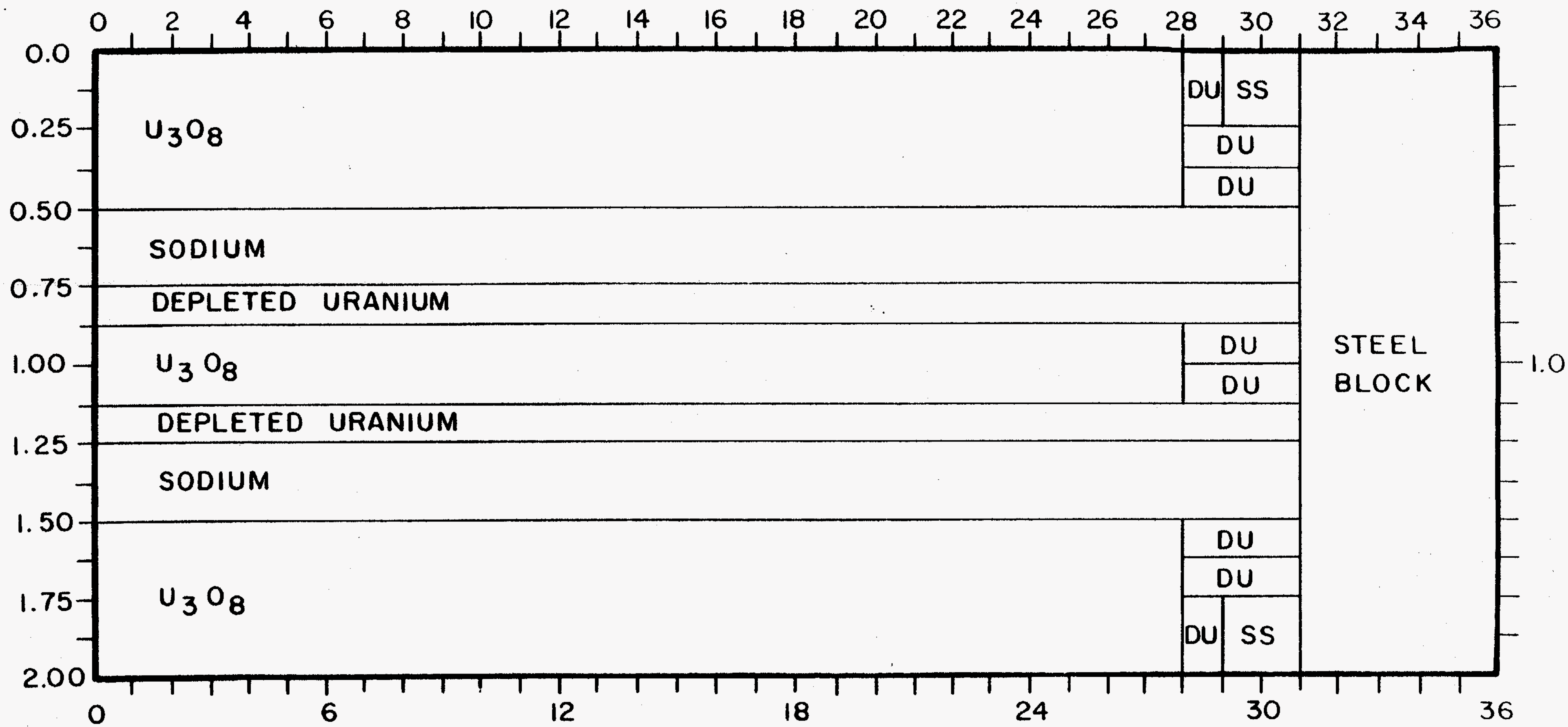

Fig. 2.3. Typical loading pattern for a blanket drawer.

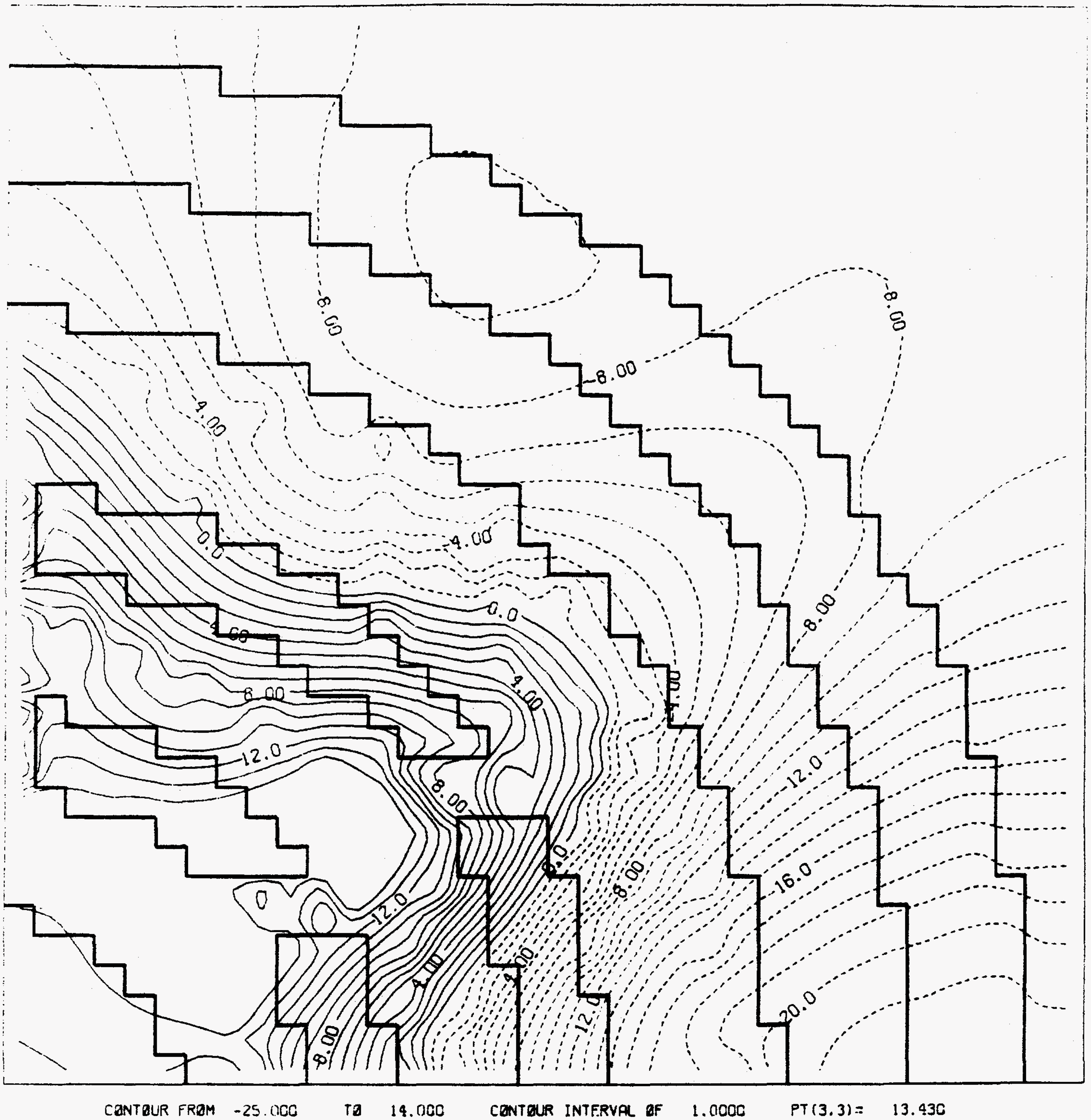

Fig. 2.4. Calculated percent change in ^{235}U fission rates, ZPPR-13B/1 compared to ZPPR-13A.

TABLE 2.1. Estimated Uncertainties for Experimental k_{eff} Values in ZPPR-13

		Estimated 1σ Uncertainty, % Δk
		13A
a.	Measured excess:	
	period measurement	0.0008
b.	Calculated β_{eff}	0.0025
c.	Configuration reproducibility	0.0005
d.	Material location	0.0066
e.	Interface gap	0.0149
f.	Core temperature adjustment:	
	thermocouple calibration	0.0017
	average temperature	0.0033
	temperature coefficient	0.0024
g.	^{241}Pu decay of fuel[a]	0.0100
h.	Void slots:	
	shim/PSR drawers	0.0066
	fission chambers	0.0090
i.	Isotopic composition	0.0320
j.	Humidity	0.0002
k.	PSR blades parked in plenum	0.0040
	Statistical sum	0.0395

[a]Uncertainty in calculated decay from fabrication date

JAII-A17

TABLE 2.2. Summary of Experimental Uncertainties

Measured Parameter	Typical Uncertainties (1σ) Random (Statistical)	Correlated
Critical Mass		
(keff)	0.01%	0.04%
Reaction Rate Distributions		
Core F9, F5, C8	0.8%	2%
F8	1.5%	2%
Blankets F9, F5, C8	1-2%	2%
F8	2-30%	2%
Reaction Rate Ratios (Core region)		
F5/F9, C8/F9	1%	2%
F8/F9	1.5%	2%
Control Rod Worths	0.1% to 0.5%	1%
Sodium Void Reactivity	0.2%	1%
Sample Traverses		
High worth (fissile, ^{10}B)	0.05 Ih/kg	1-2%
Low worth and scattering samples		
Drawer Oscillation	<0.5%	1-2%
Doppler Effect	<1%	2-4%

JAIIA16

3.0. CALCULATION METHODS

3.1 Cross Section Processing

Calculations for ZPPR-13 used the ENDF/B-IV data. The generation of a multigroup library which includes treatment of heterogeneity effects in the unit cells used methods similar to those for JUPITER-I analysis[1,2], with the following steps:

(i) Processing the ENDF/B files into a 2082 group library for the MC^2-II code is done by the Methods and Computation Group in Illinois using the ETOE code. This library is used in all neutronics calculations (with ENDF/B-IV) within the Applied Physics Division at ANL.

(ii) Calculation of a 2082 group spectrum with MC^2-II and production of an "intermediate library" in 226 groups. This calculation was done once only, using the double-fuel-column composition.

(iii) Calculation of resonance shielding and flux fine-structure for each cell type using the SDX code with 226 groups, homogenization of the cross sections in each cell by flux-volume weighting and collapse to 28 groups.

These methods are described in more detail in Refs. 1 and 2. Several differences were invoked for ZPPR-13, principally as a result of studies in ZPPR-11 and ZPPR-12. These were:

(i) Improved treatment of resonance shielding for narrow resonances in iron, nickel, chromium, manganese, molybdenum, and sodium, following modifications to the MC^2/SDX codes. For ZPPR-13, data for these isotopes were shielded for the homogeneous cell compositions. Heterogeneous treatment is possible but leads to difficulties in equivalence theory between adjacent plates with the same isotopes. These improvements give an increase in k_{eff} of 0.1% for the ZPPR cores which contain similar volume fractions of steel.

(ii) Cell calculations were made with group-dependent bucklings. The bucklings were obtained from a prior xyz calculation for ZPPR-13A using microscopic cross sections generated for ZPPR-11. The 28 group fluxes were edited in the DIF3D code to provide the average leakages and bucklings for all occurrences of a given cell in a given zone of the reactor. The bucklings in the subset of 28 groups were used in the 2000 groups for MC^2 and in the 226 groups for SDX. Some further details of the calculations were:

(a) The option to scale collision probabilities was used (rather than to add DB^2 to Σ_{tr}).

(b) Since the one-dimensional cell models used "mid-cell densities and thicknesses", the impressed bucklings produced a k_{eff} of about 1.1. A modification to the codes was made to scale the bucklings by a constant factor to achieve the reactor k-effective of 0.980. Since a given cell type will have a variety of neighboring cell-types in the actual loading, it is obvious that this prescription does not match any location exactly. It is further obvious that prediction of the correct flux shape within the cell would require consideration of the different leakages on the "left" and "right" sides of the cell. An improved scheme would require processing of an impracticably large number of cells and vast complications in the application of the data in the reactor model. The average bucklings are a compromise, but have been shown to give improvements in calculations of the threshold fission rate and in sodium void reactions.

The cell calculations for ZPPR-13A used bucklings generated for each cell in each radial zone. Differences of about 1% in flux-advantage factors for a given cell between the zones were noted. It was decided to use different cross sections in each zone although the effectiveness, compared with a simple method of using an average buckling for all zones of the same type is not obvious. In addition, cross sections for the large central blanket were generated for inner and outer regions. The following processed cross sections were generated:

- central blanket inner region (CBI), outer region (CBØ)
- fuel ring one, single column (F1 SC), double column (F1 DC)
- blanket ring one (B1)
- fuel ring two, F2 SC and F2 DC
- blanket ring two (B2)
- fuel ring three (F3 SC and F3 DC)
- radial blanket (RB)
- axial blanket (AB), using bucklings in the 18 in.-28 in. region of the double-fuel-column drawer. The axial blanket cell of the single-fuel-column drawer and axial blanket cells remote from the core were not processed, but the data from the principal cells were mixed with the appropriate homogeneous compositions.
- cross sections for the steel reflector regions were taken for the steel cross sections in the radial blanket.

The input data for the MC^2-II calculation and for SDX calculations of the two fuel cells in ring 2 are shown in Appendix A.

Microscopic cross sections processed for ZPPR-13A were used in all other assemblies with no additional cell calculations. Macroscopic cross sections for each phase were "remixed" with the appropriate average atomic densities. These densities are given in Appendix B. The date for ^{241}Pu decay was fixed at January 1, 1982 for the library and was not adjusted for each assembly.

3.2 Comparison of Results using the Buckling-Recycle Method and Asymptotic Cell Processing

Cross sections were generated using the method used for conventional cores using the same SDX cell models as above, but with a buckling search to critical for fuelled-cells and a zero buckling for blanket cells. These cross sections were compared with the data generated with the reactor bucklings, in an rz-model of ZPPR-13A. The calculations were done by M. Kawashima.

The k-effective values for the rz model differed by only 0.05%:

Buckling-recycle data k = 0.977775

Asymptotic data k = 0.977225

A comparison of radial reaction rate distributions was made with the rz model. Figs. 3.1 and 3.2 compare the radial reaction rate distributions. Differences are about 1% for the three non-threshold reactions, but about 5% for ^{238}U fission. Changes for this reaction type significantly improve agreement with experiment.

A similar improvement was shown for analysis of ZPPR-7.(7) In that case cross sections were generated for a two-drawer cell-model with adjacent fuel and blanket cells.

3.3 Anisotropic Diffusion Coefficients

Anisotropic diffusion coefficients were generated by the Benoist method. One-dimensional cell models were used in which the plate regions were "stretched" over the lattice pitch. Sodium-plate regions included both steel clad and sodium core. The perpendicular matrix and drawer structure was "smeared" uniformly into all plates.

The anisotropic diffusion coefficients are implemented in the DIF3D code as "modifier factors" which multiply the cell-average diffusion coefficients calculated with the SDX code (D_{SDX}). Modifier factors for ZPPR-13 are shown in Table 3.1. The modifiers are defined as the ratios of D_x (perpendicular to plates) and D_y (parallel to plates), which is the same as D_z in the one-dimensional model, to the D_{SDX}. Previous analysis used the ratios of D_x and D_y to the homogeneous diffusion coefficient D_{hom} (see Ref. 8).

Figure 3.3 shows the effect of plate streaming on calculated fission rates in ZPPR-13A. This figure shows the ratio of ^{235}U fission for an xy calculation with anisotropic D's to a calculation with the D_{SDX}'s. The fluxes are normalized to the same total fission source in the reactor. Inclusion of streaming modified the fission distributions in the core by up to 1%. Effects on reactivity worths are approximately twice those shown for fission rates. Inclusion of streaming generally improves agreement with experiment. The effects in the heterogeneous cores are quite complex. Since the peak fluxes are in the second fuel ring, streaming effects flatten the fission distributions both towards the core center and outwards into the radial blanket.

Since anisotropic diffusion coefficients are used in all calculations, corrections for streaming are not shown separately as in previous analyses. The effect on calculated k_{eff} is about -0.3% (-0.1% Δk in the xy-plane and -0.2% Δk in the z-direction). For sodium void analysis, the Benoist diffusion coefficients increase the leakage contributions by 30% to 40%. Results of least squares fitting to experiment indicates that the Benoist method (in the cell model used here) overestimated the streaming effect in the sodium voided cells.

3.4 Reactor Models

Analysis of ZPPR-13A made more extensive use of three-dimensional (xyz) models than in the past. The reference method used was:

- ENDF/B-IV data in 28 energy groups.

- Diffusion theory in xyz geometry, one-eighth core model (one quadrant, half-height).

- Mesh spacing of 55 mm in the xy-plane (one mesh point per ZPPR drawer (1MPD)). The axial mesh-spacing was similar, but varied to match shim rod insertion (for reaction rate calculations) and axial zone boundaries. The core contained six equal intervals of 51 mm for the first 306 mm from the midplane, four intervals of between 25 mm and 50 mm up to the blanket boundary, and six intervals of 42 mm in the lower part of the axial blanket.

- Anisotropic diffusion coefficients were used in all calculations.

The xyz models are used for calculation of k_{eff}, reaction rates, sample traverses and sodium void reactivity. Two-dimensional models in xy and rz geometry are used to calculate mesh and transport effects and for special studies. Group and region dependent buckling terms for xy models are obtained from the leakages calculated in the xyz models. These generally lead to small errors in the xy k_{eff} (~0.01%) and in core-region reaction rates (tenths of a percent). Specification of an rz model is not unique in the cores with complex internal blanket and CRP arrangement. These models have been used to calculate transport corrections in ZPPR-13A and preliminary values of β_{eff} for all cores.

The xy and rz models for ZPPR-13A, are shown in Figs. 3.4 to 3.5 * Axial regions in the xyz models were the same as in the rz models.

A large number of calculations are required for control rod experiments, both to obtain calculated worths and to derive detector efficiencies and source ratios required for analysis of the experimental data. These calculations are made with the following method:

- ENDF/B-IV data in 8 energy groups.
- Diffusion theory in xy geometry, using quarter-, half- or full-plan models as required.
- Mesh spacing of 55 mm.

---

* Calculations for 13A used the average blanket drawers in these locations.

• Group and region dependent buckling terms derived from the leakages at the core/axial blanket interface (±458 mm).

The 8 group library is essentially the same as the 9 group library used in JUPITER-I analysis, and differs only in combination of the lowest energy group (upper energy 3 eV) with the group above. Group collapse is made for all regions in the reference model using the xyz fluxes. Data for control rods and CRPs are obtained from an xyz calculation with a bank of rods (or CRPs) fully inserted in the second fuel ring. These data are used for control rods (and CRPs) in all locations.

The buckling terms are obtained by repeating the xyz calculations (reference, rod bank and CRP bank) in 8 groups. The buckling terms are used in the same way as the collapsed data; bucklings for the reference model in all zones, and bucklings for the control rod (CRP) in all locations.*

In each phase of ZPPR-13, the principal control rod banks were calculated with xyz models in both 28 groups and 8 groups for comparison with results from the xy models. As will be seen in Section 6, the approximation in the two-dimensional models lead to errors in rod worths of less than 2%.

Energy group structures of the 2082, 226, 28 and 8 group data are shown in Table 3.2.

3.5 More Complex Reaction Models and Asymmetry Effects

The early measurements in ZPPR-13A showed unanticipated differences between measurements in what were thought to be symmetrically equivalent locations in the reactor. A series of investigations mounted to study this problem is described in Ref. 9.

One effect seen in this study was due to the variation in interface gap between the two halves of the ZPPR machine. Upon half-closure, the matrix

*Note that the buckling terms include effects of streaming in the z-direction, since the xyz model used anisotropic diffusion.

is in contact at the top of the core and separated by about 1 mm at the bottom. This has the effect of bringing fuel closer together at the top of the core than at the bottom. Fission rates at the top are about 1% higher and control rod worths are about 2% higher. This feature of the loading is exceedingly difficult to model in the calculations.

At a later stage, two features of the reactor loadings which affect the symmetry of the measurements were uncovered. These were:

(i) Asymmetries due to the loading of the "narrow drawers" used in blanket regions to accommodate the ZPPR safety/shim rod blades.

(ii) Asymmetries due to the loadings of fission-chamber drawers in blanket regions.

In both of these cases, a significant amount of uranium was removed from the cells. The effects were calculated using xy models (half xy-plan for (i) and full xy-plan for (ii)).

Perturbations in fission rates due to the narrow blanket drawers for ZPPR-13A are shown in Fig. 3.12. Note that in addition to the effect on left to right symmetry, there is a sensible difference between points on the x-axis and the y-axis.

Perturbations due to blanket fission chamber drawers are a little more subtle. These are shown in Fig. 3.13. The asymmetries largely result from a nonuniform distribution of the blanket fission chambers -- more are present in the upper-left-hand (ULH) quadrant of half-one than in the LRH quadrant. The perturbations affect fission rates between left and right sides and also between the top and bottom of the interface.

Correction for these two effects resulted in much improved consistency between C/E values on the left and right sides of the core.(10,11)

A remaining characteristic of the analyses with the reference models was a marked difference in predictions of experiments at the x-axis and at the y-axis. For example, C/E values for control rods CR25 (x-axis in F3) and CR28 (y-axis in F3) differed by 4% even after including the effects described above.[9] Diligent efforts by the ZPPR analysts, in the face of rising torrents of experimental data, eventually revealed that most of this problem was due to variation in the fissile masses in the individual loadings of a generic drawer-master. This feature had not been considered important in any previous ZPPR cores. It was found that perturbations in fission rates, compared with those calculated using homogenized compositions, arose from three principal effects:

(i) Use of two types of ZPPR fuel (Vendor 63 and Vendor 65) for which the fissile contents per plate differ by about 1%.

(ii) Use of four plutonium plates in a fuel column of a drawer instead of the more usual three plates (e.g. a 5 in., 5 in., 4 in., 4 in. loading compared with a 8 in., 6 in., 4 in. loading). This difference results in a decrease in fissile content of 0.5% to 1% compared with the average.

(iii) Variations in total uranium content among the various specific blanket drawer masters.

The variations in ^{239}Pu and ^{238}U for the ZPPR-13A masters are shown in Table 3.3.

Given a uniform distribution over the core of each master type, these variations would result in local perturbations only. However, it transpired that in ZPPR-13A, the drawers with higher or lower fissile content than average tended to be grouped in certain areas. Thus an overall perturbation in reactor fission rates was produced.

Effects due to variation in uranium content were somewhat surprising, since the uranium worth is considerably lower than that for plutonium and variations were only about 0.5% from the average. However, the different masters were loaded selectively in regions at the axes and centered around 45° to the axes. Figure 3.14 shows diagrammatically the locations of the most deviant masters for fuel drawers in ZPPR-13A.

Calculations have been made to test the effect of variation in the drawer masters using an xy model. A computer code (called McMASTERS) has been written which takes the assembly loading record (on tape), scans through the matrix and automatically writes most of the input required for the DIF3D code. Since some of the masters are different between half-one and half-two of the reactor (fission chamber locations, thermocouple locations, radial reflector), the code scans both half-one and half-two loadings and, for the xy model, uses an average composition for these cases. An auxiliary module (McADEN) writes the composition of each master in ARC system format for data mixing. These codes will eventually form part of a general system for setting up ARC system calculations from the reactor loading records.

The fission chamber drawers in blanket regions presented an additional twist, since the uranium was removed only from the first 8 in. of the drawer. For these drawers weighted average atomic densities, $\bar{N}$, were defined as:

$$\bar{N} = 0.545\ N(0\text{-}8\ \text{in.}) + 0.455\ N\ (8\ \text{in.} - 18\ \text{in.}).$$

The xy calculations were run in diffusion theory with the 55 mm mesh size and 28 group cross sections. To simplify the input, cross sections and bucklings processed for middle fuel ring (F2), second blanket ring (B2) and radial reflector (RR) were used throughout. The fission rates from the all-master model (AMM) were compared with those using the model with homogenized composition (HMM). The same microscopic cross sections and bucklings for F2 and B2 were used in the homogenized model.

Figure 3.15 shows the effects in ZPPR-13A of using individual masters for the fuel drawers. Figure 3.16 shows the effects of using individual masters for the blanket drawers. Figure 3.17 shows the effects of using all master, including narrow blanket drawers and blanket fission chamber drawers. In each case the fluxes are normalized to the same total fission source in the reactor.

It can be seen that the individual effects are additive, to a good approximation. That is, superposition of Figs 3.12, 3.13, 3.14, 3.15, and 3.16 reproduces the total perturbations in Fig. 3.17.

Perturbations to reactivity worths at different positions in the reactor are about double those for fission rates. Direct calculations for control rods CR25, CR28 and a bank of six rods in fuel ring 3 (6F3) for ZPPR-13A are shown in Table 3.4. Corrections to worths from the HMM model are within 0.2% of estimates from the fission rate perturbations in Fig. 3.17. Estimated corrections for control rods in other positions have been made from the fission rate data.

3.6 Sensitivities and Eigenvalue Separation

A key parameter for describing large, heterogeneous LMFBR designs is the neutronic coupling between the core zones. It has become customary to refer to heterogeneous cores as loosely coupled or tightly coupled, depending on the sensitivity of the power distribution to local perturbations. Decoupling is generally introduced in designs by isolating the individual core zones with thick internal blanket rings. The degree of coupling (or decoupling) can be quantified by several parameters, but not all of them give a good picture of overall reactor behavior. In planning the ZPPR-13 experiments, the (k_{ij})

matrix from the Avery theory of coupled reactors[12] and the eigenvalue spectrum were chosen as decoupling descriptors. In applying the Avery theory, the reactor is arbitrarily divided into two parts, and the coupling between them is described by the elements of the (2 x 2) k_{ij} matrix. The eigenvalue spectrum is particularly useful if nodal kinetic analysis to be used.

For ZPPR-13, only the separation between the fundamental and the first harmonic eigenvalues* were used for analysis of the eigenvalue spectrum. Previous experience had shown that the first harmonic eigenvalue was always for an azimuthal mode, even if there were only two fuel rings separated by an unusually thick blanket. Intuitively one might expect the core to be more radially decoupled, but in general azimuthal decoupling dominates for local perturbations.

Approximate solutions for the first harmonic eigenvalue were obtained by imposing a zero-flux boundary condition along the x or y axis in a 1/8-core, xy model of the assembly. Exact solutions were later obtained by stripping out the fundamental mode and solving directly for the first harmonic. It was demonstrated that the approximate solutions were sufficiently accurate provided that the zero-flux boundary condition was imposed along an axis where there was a natural minimum in the reference flux solution. Application of this knowledge made preliminary planning considerably easier.

For ZPPR-13, only the separation between the first two eigenvalues was considered as a measure of the relative decoupling. Table 3.5 gives the percentage separation

*Here we refer to the eigenfunction closest to the fundamental as the first harmonic.

Table 3.7 shows eigenvalue separation for ZPPR-13 cores, estimated for the 8 group models used for control rod analysis. Eigenvalues were obtained by forming a zero flux at the x-axis and at the y-axis in each case. In addition to the reference configuration, results are shown for control rod banks inserted in each ring in the subcritical states. The eigenvalue separations in the critical cores will depend on the changes made to bring the core critical. However, for a uniform increase in enrichment, it appears that the cores with control rods inserted may be far more sensitive than the references.

The response to a perturbation of the reactor (flux tilts) can be analyzed by an eigenfunction expansion. If ψ_i are the eigenfunctions of the reference reactor, with eigenvalues λ_n,

$$L\psi_n = (1/\lambda_n)M\psi_n$$

Wade[13] has shown that the fluxes, ϕ, in the perturbed case are given by:

$$\phi(r) = a_o\psi_o(r) + \sum_n \frac{\rho_n\lambda_n\lambda_n}{\lambda_o-\lambda_n}\psi_n(r)$$

where

$$\rho_n = \langle\psi_n^*, (-\delta L + \delta M)\ \phi\rangle/\langle\psi_n^*, M\psi_n\rangle$$

Thus, harmonics with the smallest eigenvalue separation dominate. Perturbations at the peak of the eigenfunction have maximum effect, while perturbations at the nodes will give zero contribution.

The sensitivities of the cores to errors in cross section data can also be characterized by the eigenvalue spectra. Only a limited number of results have been obtained for ZPPR-13 at this stage. Table 3.8 shows the results of a 5% increase in ^{238}U capture, uniformly in all regions, for ZPPR-13A

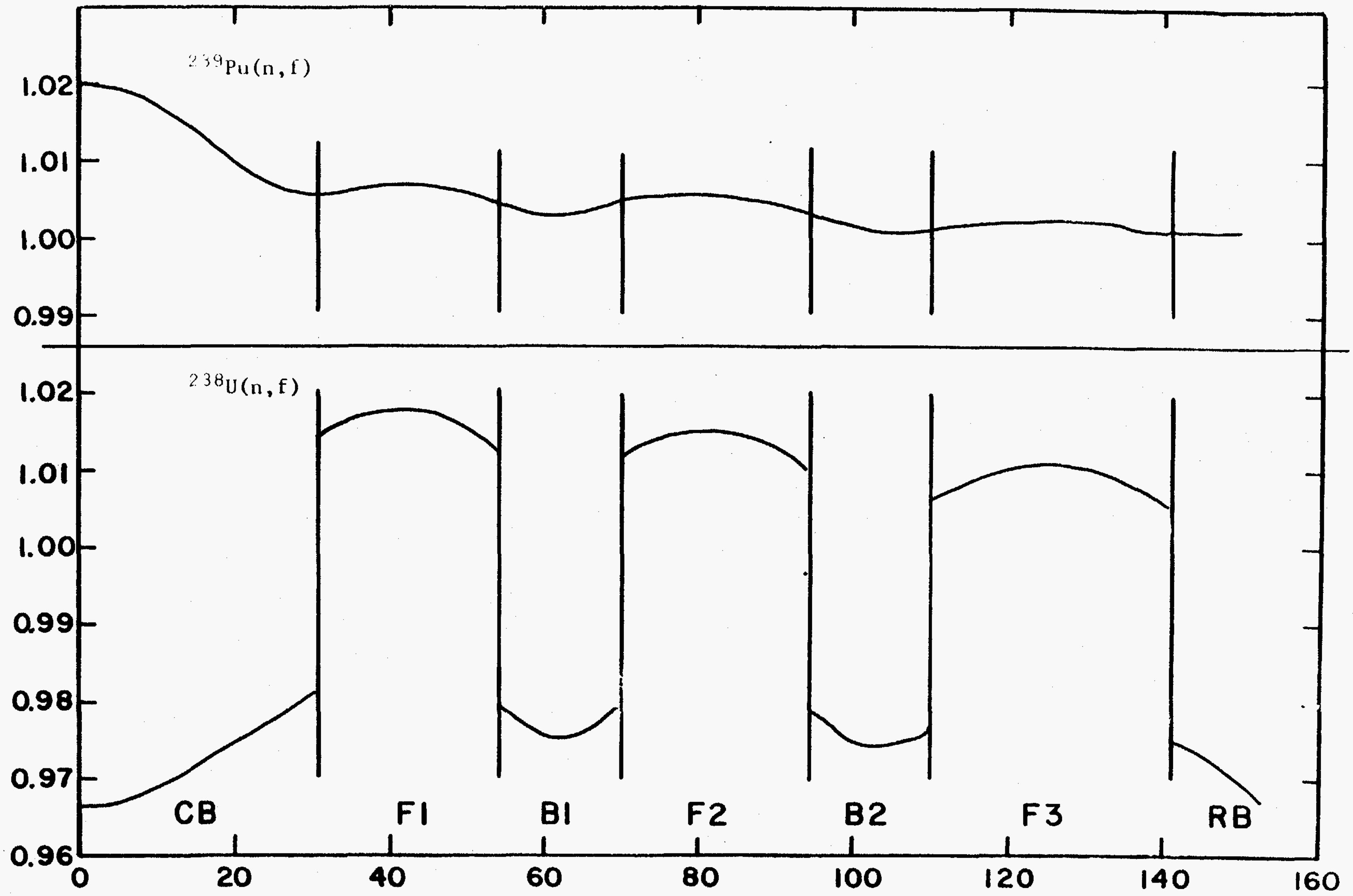

Fig. 3.1. ZPPR-13A: Ratios of reaction rates with "multibuckled cell data" to those with "Asymptotic cell data"; $^{239}Pu(n,f)$ and $^{238}U(n,f)$.

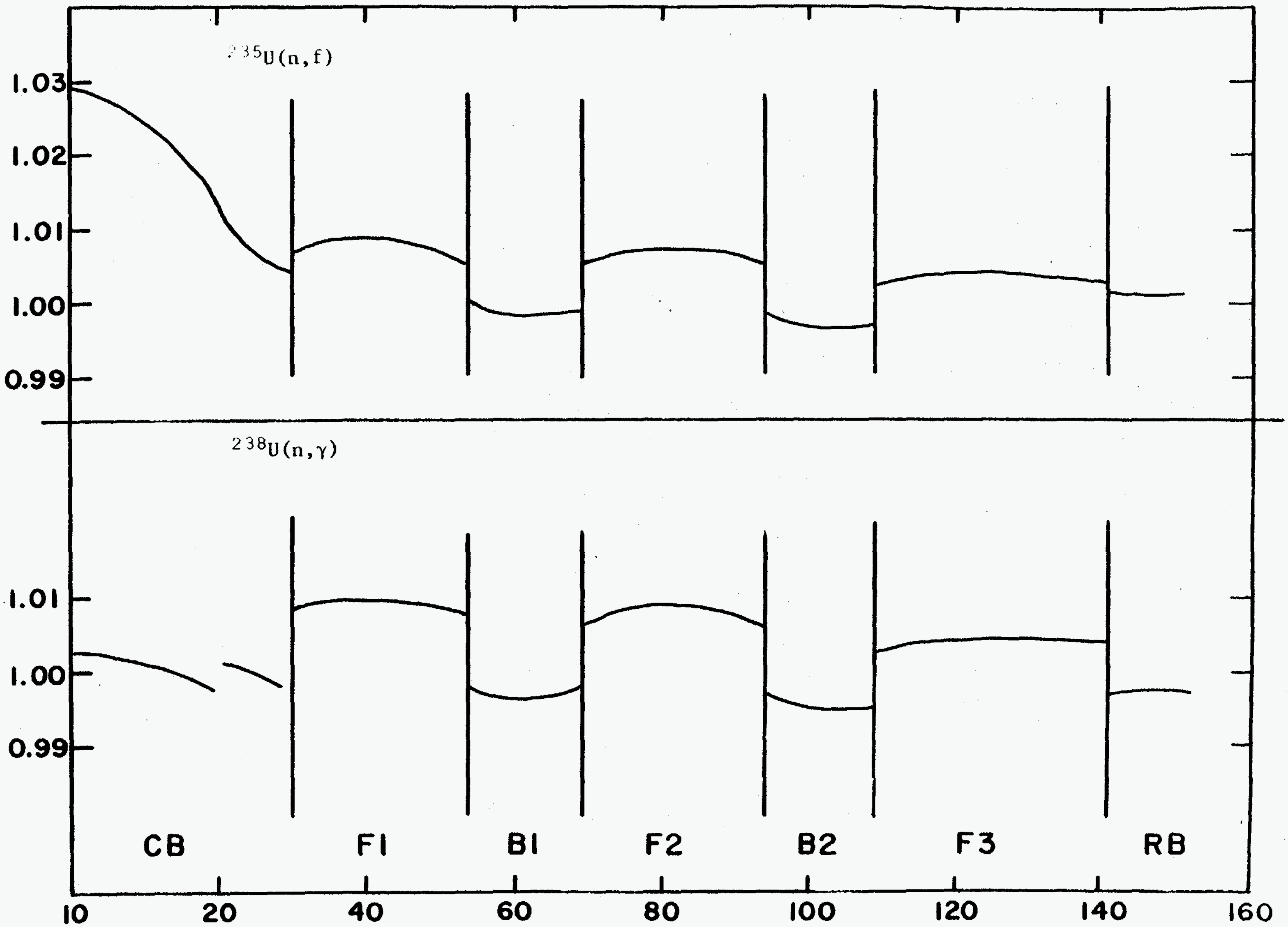

Fig. 3.2. ZPPR-13A: Ratios of reaction rates with "multibuckled cell data" to those with "asymptotic cell data"; $^{235}U(n,f)$ and $^{238}U(n,\gamma)$.

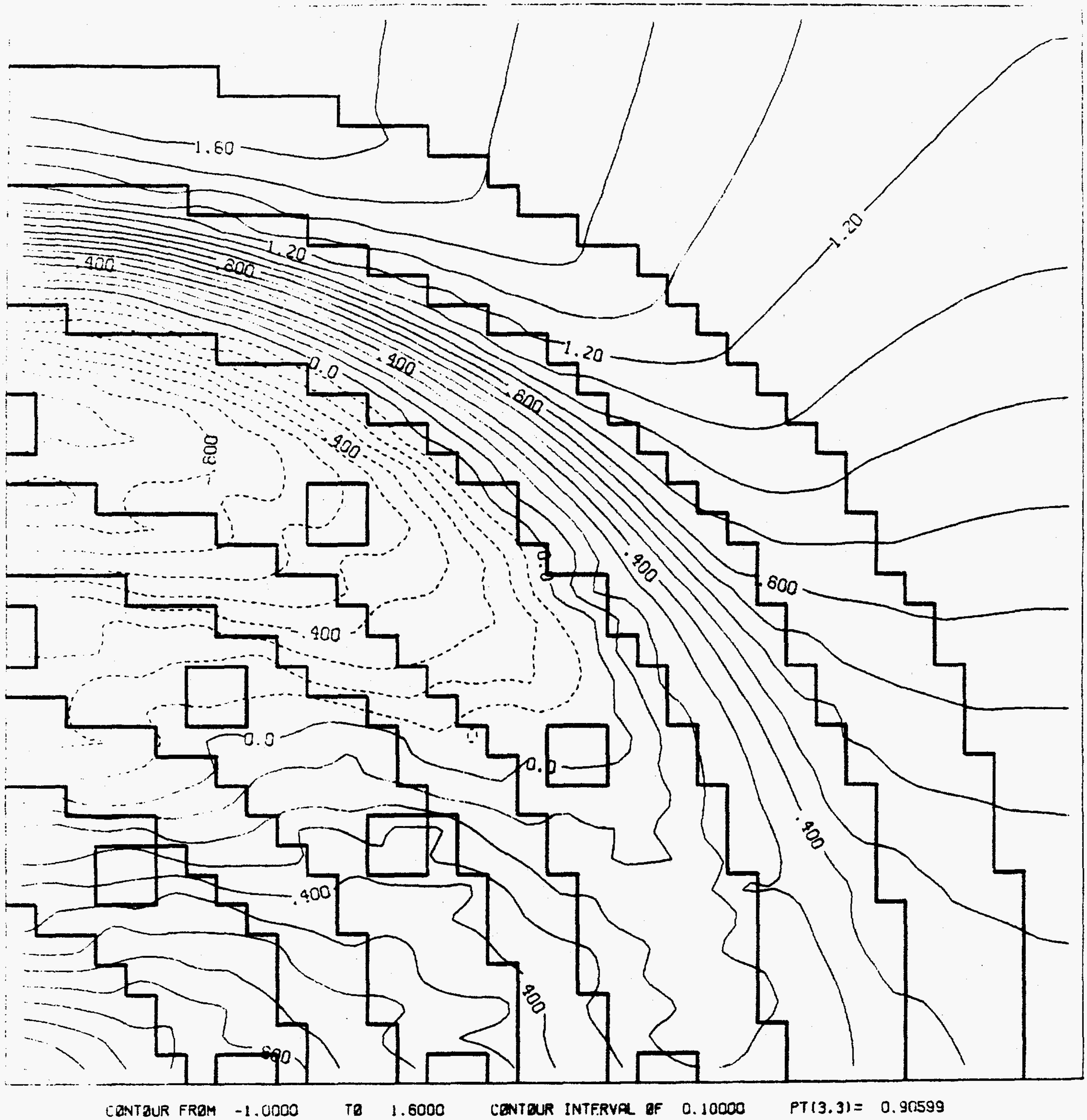

Fig. 3.3. Calculated percent change in ^{235}U fission rate in ZPPR-13A when plate streaming is included.

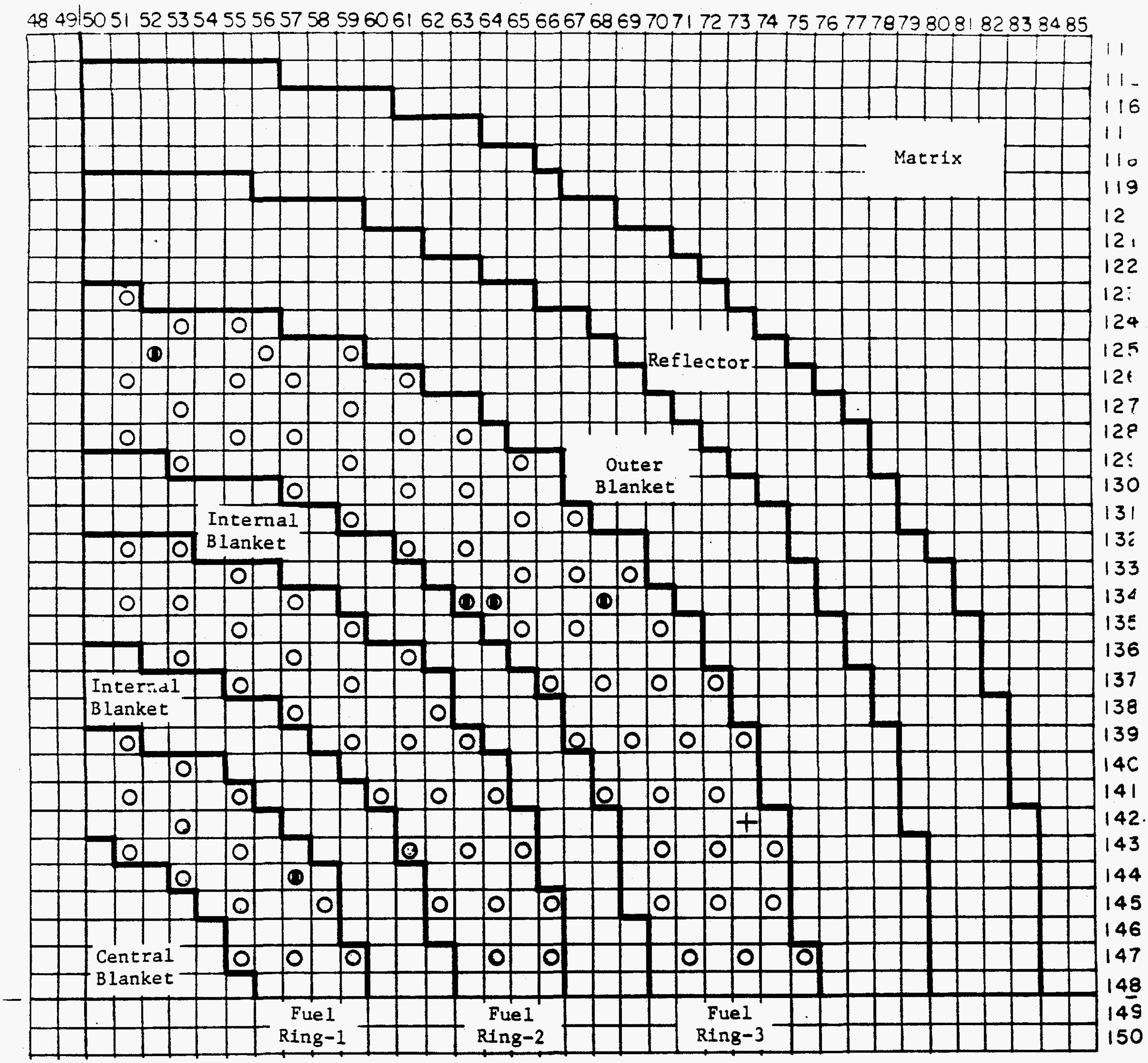

○ Single Column Fuel Drawer

● Single Column Fuel - Poison Safety Rod

+ Replace with single column fuel drawer for subcritical reference for control rod experiments.

Fig. 3.4. XY Calculational Model for ZPPR-13A Critical Reference.

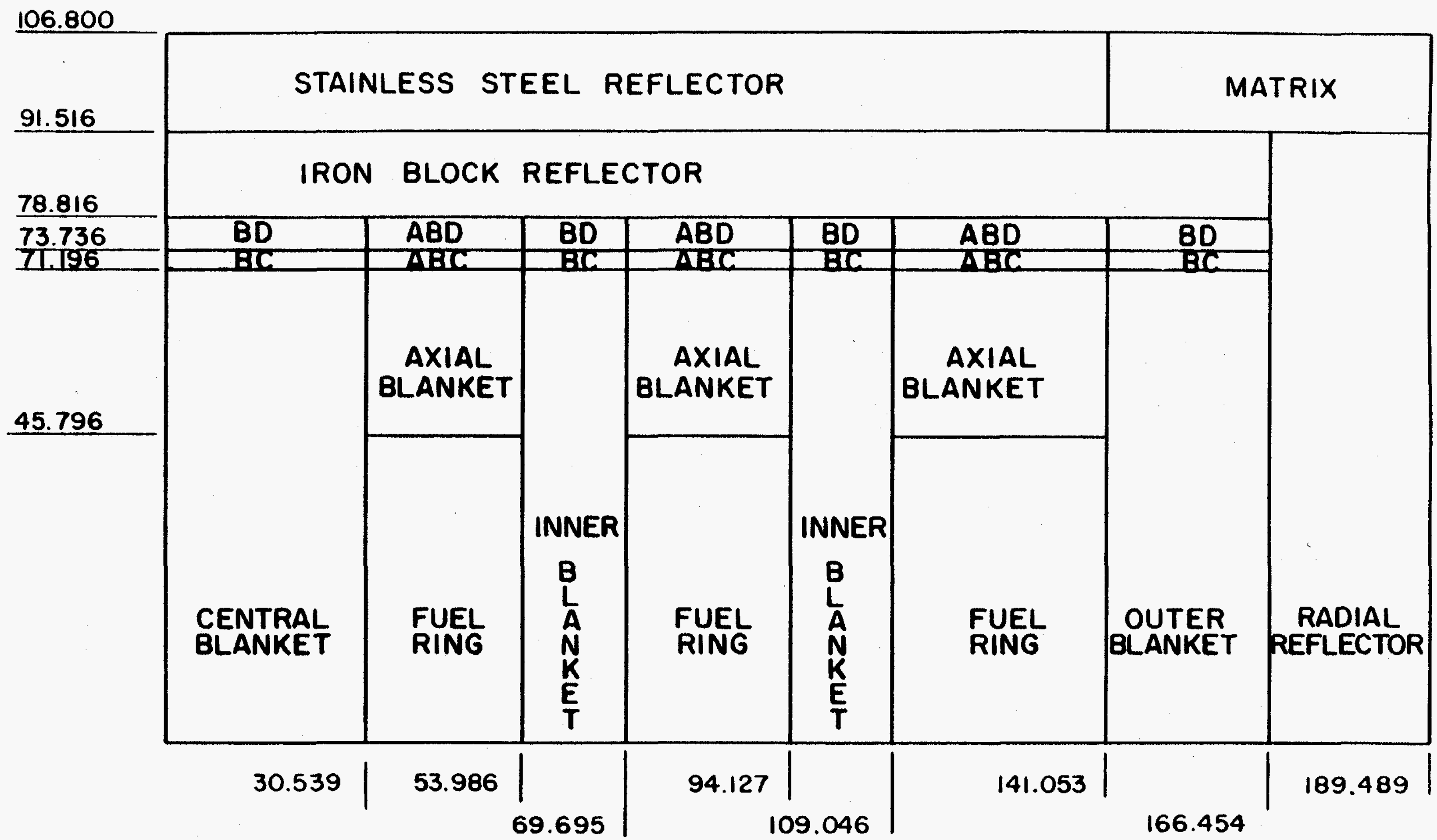

Fig. 3.5. R-Z Calculational Model for ZPPR-13A Critical Reference (dimensions in cm)

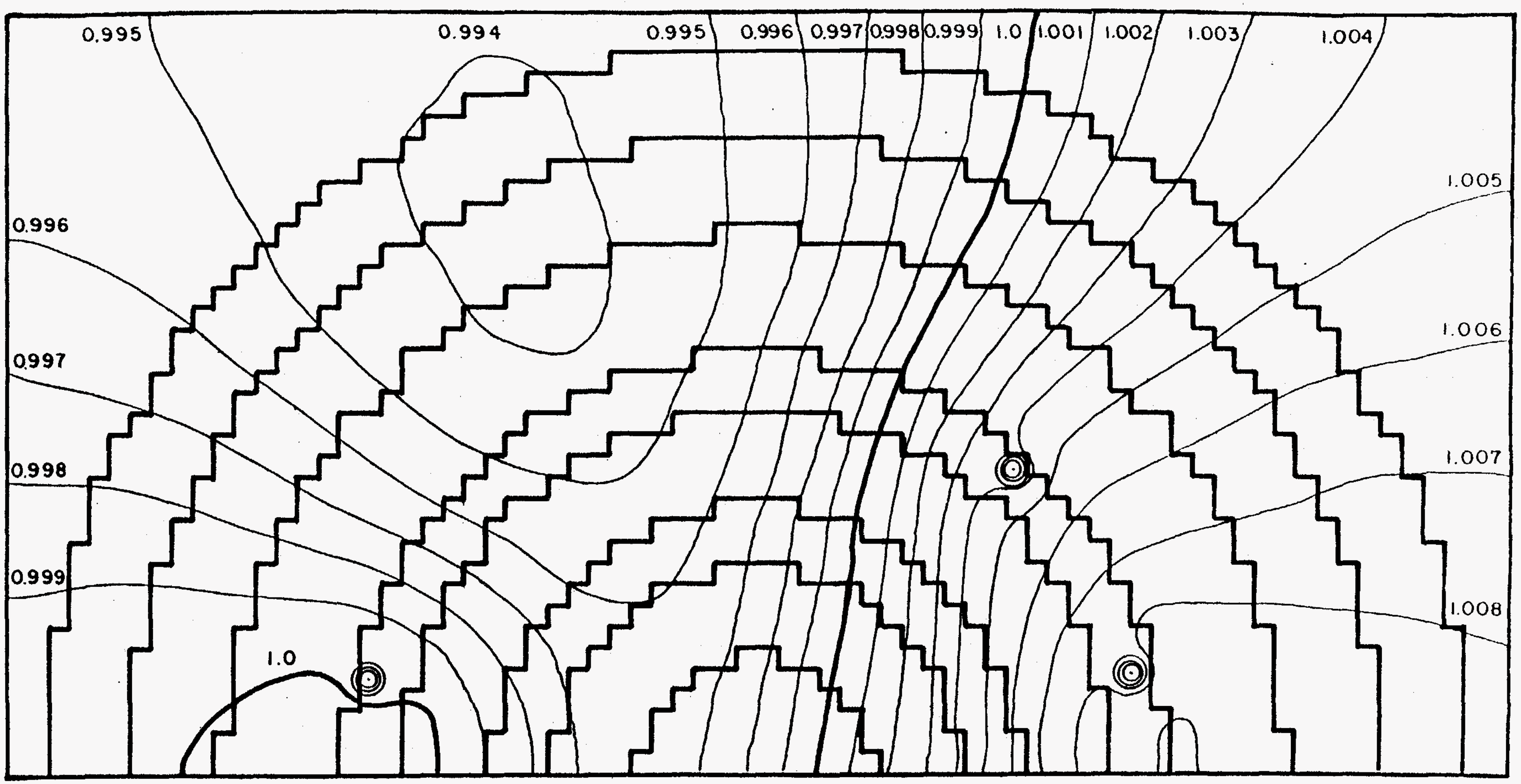

Fig. 3.12. ZPPR-13A. Correction Factors for ^{235}U Fission Rates Due to Narrow Drawers in Blankets

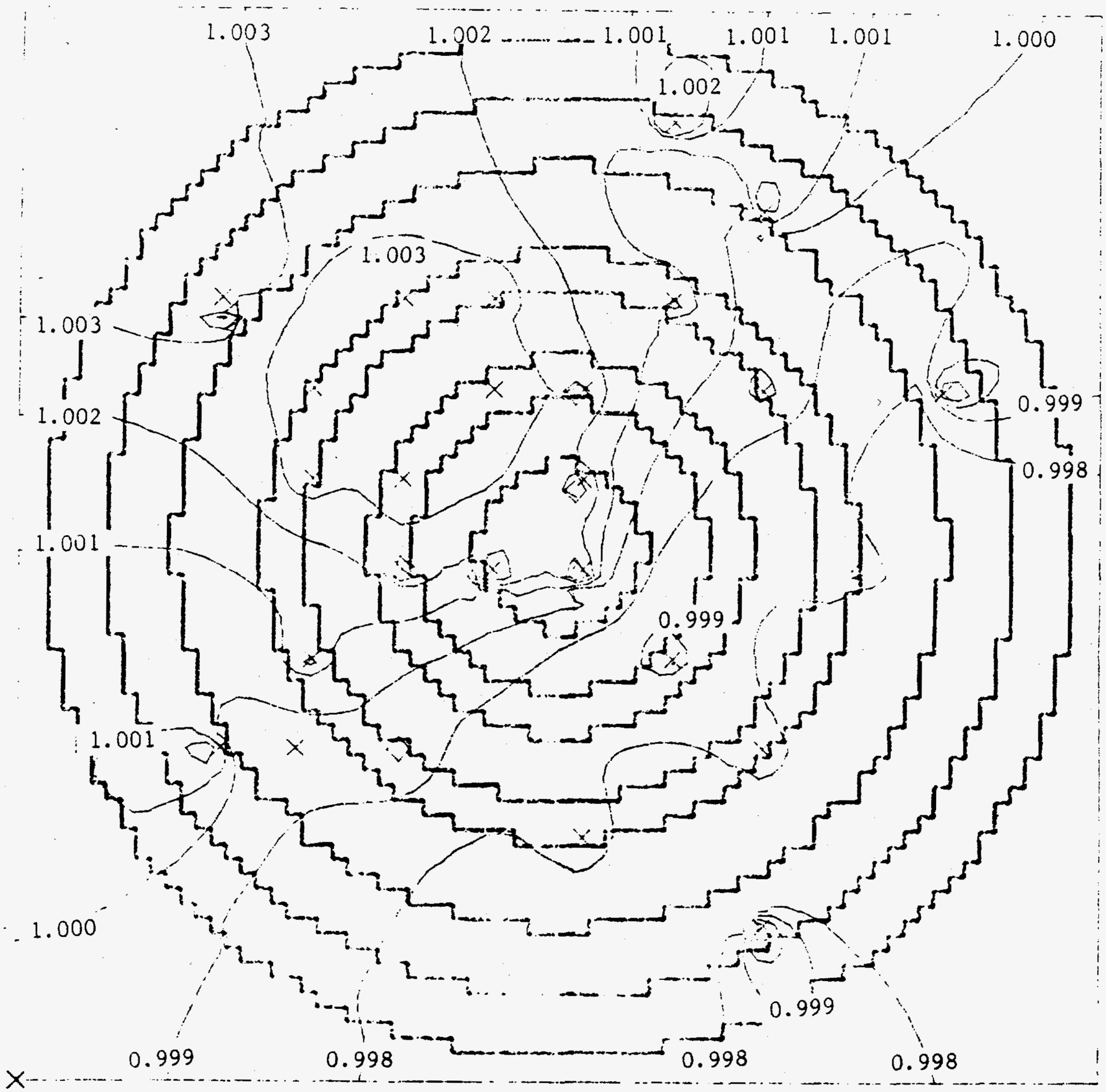

Fig. 3.13. Perturbation in ^{235}U fission rates in ZPPR-13A due to detector-drawers in blankets.

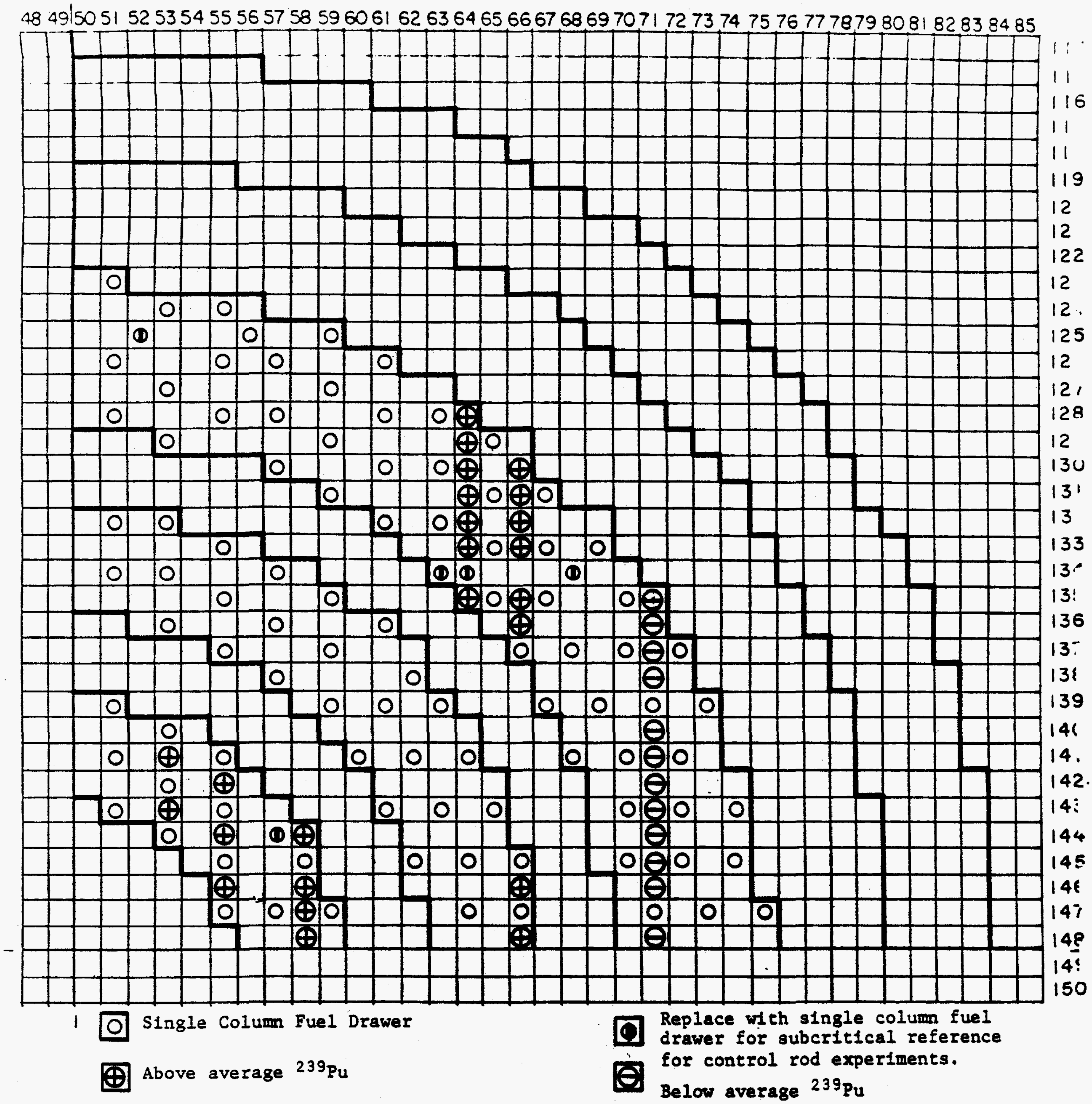

Fig. 3.14. ZPPR-13A: Locations of drawers with slightly greater or less than average fissile mass.

Fig. 3.15. Percent change in ^{235}U fission rate in ZPPR-13A using specific fuel drawer masters compared to homogenized master.

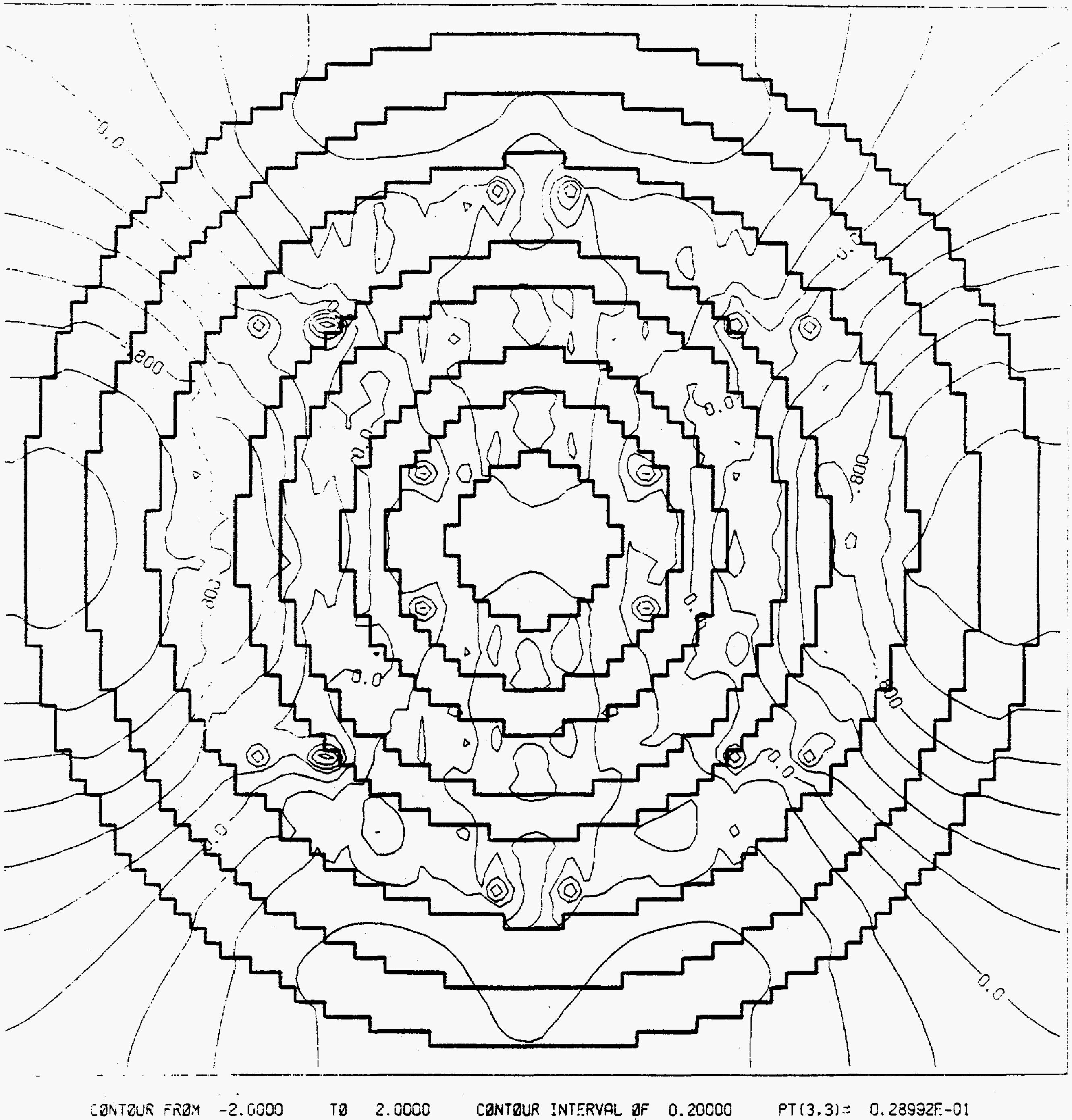

Fig. 3.16. Percent change in ^{235}U fission rate in ZPPR-13A using specific blanket drawer masters compared to homogenized masters.

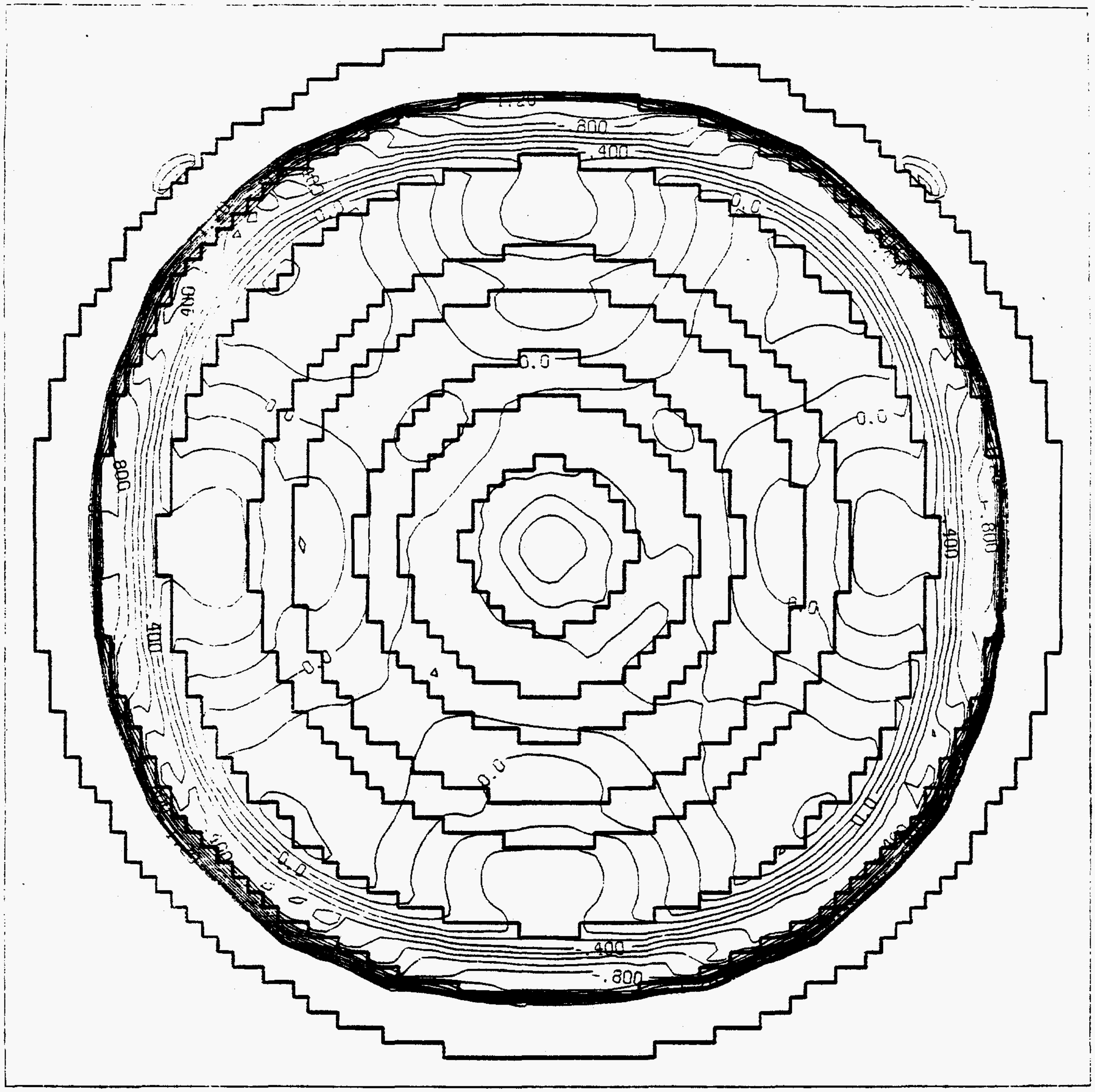

CØNTØUR FRØM -1.5000 TØ 1.4000 CØNTØUR INTERVAL ØF 0.10000 PT(3,3)= -2.2010

Fig. 3.17. Percent change in ^{235}U fission rate in ZPPR-13A using all-master model compared to homogeneous model.

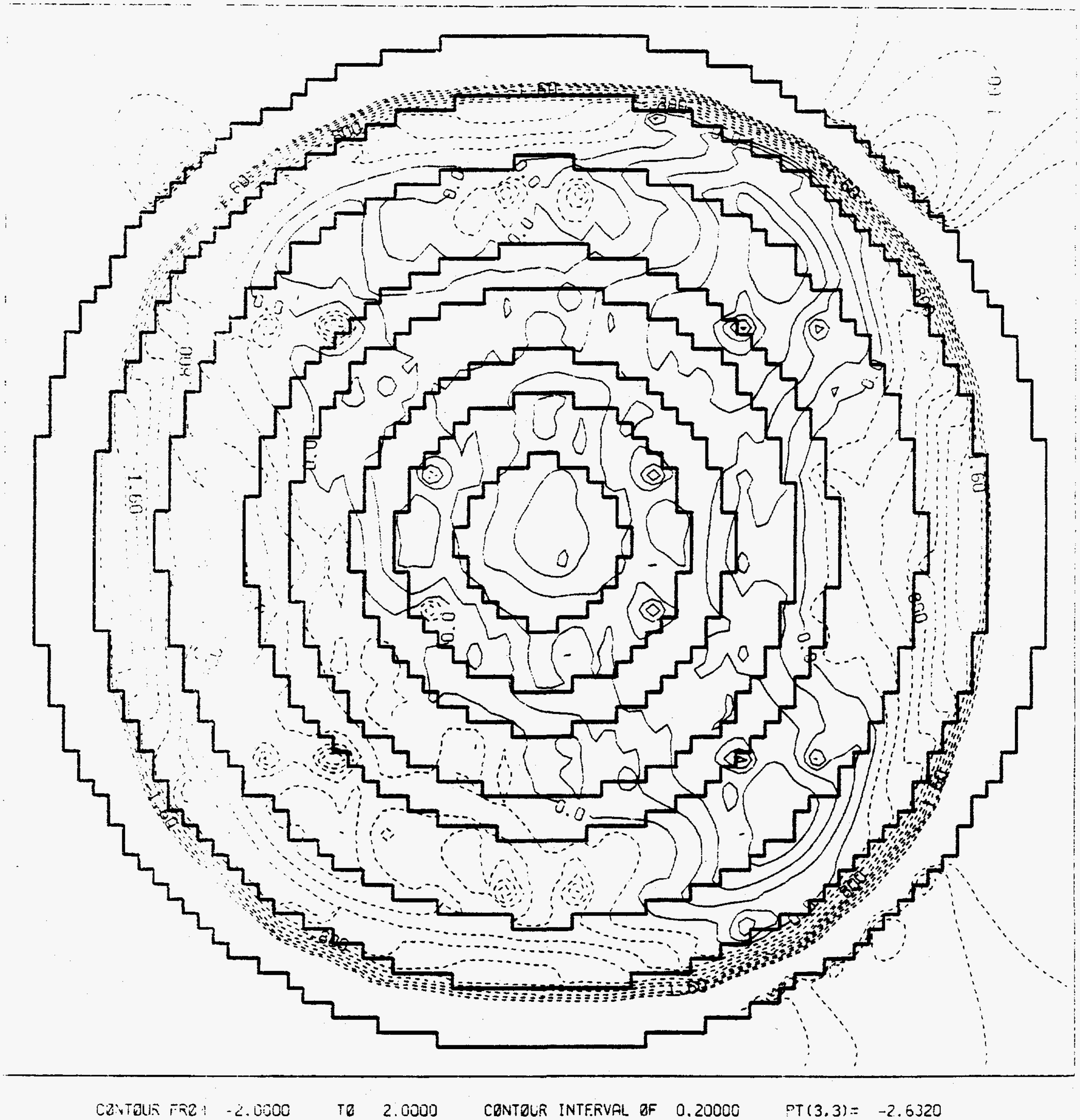

TABLE 3.1. Directional Diffusion Coefficient Modifiers for ZPPR-13A: D(Benoist)/D(Heterogeneous)[a]

Group	Double Column Fuel		Single Column Fuel		Radial Blanket		Axial Blanket		Voided Double Column Fuel		Voided Single Column Fuel		Voided Radial Blanket	
	X	Y,Z	X	Y,Z	X	Y,Z	X	Y,Z	X	Y,Z	X	Y,Z	X	Y,Z
1	1.0178	1.0305	1.0212	1.0376	1.0028	1.0090	1.0133	1.0330	1.0193	1.0486	1.0208	1.0636	1.0021	1.0156
2	1.0161	1.0307	1.0193	1.0384	1.0018	1.0087	1.0107	1.0326	1.0182	1.0506	1.0195	1.0683	1.0014	1.0165
3	1.0110	1.0262	1.0139	1.0327	1.0015	1.0083	1.0078	1.0293	1.0118	1.0470	1.0137	1.0650	1.0013	1.0167
4	1.0069	1.0255	1.0081	1.0309	1.0004	1.0093	1.0049	1.0306	1.0087	1.0516	1.0100	1.0735	1.0004	1.0214
5	1.0063	1.0311	1.0064	1.0338	1.0008	1.0157	1.0066	1.0360	1.0066	1.0717	1.0066	1.0982	0.9999	1.0372
6	1.0030	1.0161	1.0031	1.0157	1.0007	1.0069	1.0036	1.0196	1.0041	1.0622	1.0045	1.0847	1.0009	1.0303
7	1.0042	1.0451	1.0045	1.0516	1.0011	1.0270	1.0055	1.0565	1.0067	1.0992	1.0076	1.1385	1.0020	1.0570
8	1.0034	1.0343	1.0035	1.0378	1.0016	1.0178	1.0047	1.0444	1.0066	1.0891	1.0075	1.1244	1.0031	1.0465
9	1.0035	1.0440	1.0040	1.0478	1.0016	1.0224	1.0058	1.0574	1.0059	1.0983	1.0074	1.1330	1.0028	1.0495
10	1.0046	1.0476	1.0056	1.0553	1.0021	1.0235	1.0079	1.0658	1.0076	1.0998	1.0097	1.1386	1.0035	1.0486
11	1.0043	1.0441	1.0052	1.0489	1.0020	1.0205	1.0077	1.0598	1.0081	1.1061	1.0108	1.1461	1.0039	1.0509
12	1.0054	1.0522	1.0093	1.0706	1.0032	1.0240	1.0118	1.0793	1.0079	1.1029	1.0133	1.1486	1.0049	1.0435
13	1.0027	1.0482	1.0039	1.0525	1.0021	1.0244	1.0062	1.0631	1.0068	1.1098	1.0102	1.1474	1.0045	1.0531
14	1.0029	1.0409	1.0068	1.0553	1.0025	1.0217	1.0090	1.0633	1.0056	1.0908	1.0125	1.1432	1.0044	1.0466
15	1.0035	1.0365	1.0142	1.0700	1.0049	1.0257	1.0143	1.0702	1.0076	1.0836	1.0252	1.1609	1.0080	1.0467
16	1.0032	1.0108	1.0054	1.0160	1.0027	1.0121	1.0094	1.0203	1.0061	1.0829	1.0209	1.1534	1.0075	1.0469
17	1.0168	1.0352	1.0213	1.0532	1.0401	1.1063	1.0182	1.0497	1.0060	1.0923	1.0209	1.1635	1.0074	1.0498
18	0.9955	1.0347	0.9999	1.0472	1.0001	1.0161	1.0030	1.0515	1.0063	1.1070	1.0161	1.1640	1.0060	1.0478
19	1.0001	1.0625	1.0076	1.0891	1.0033	1.0274	1.0114	1.0901	1.0055	1.1082	1.0161	1.1664	1.0060	1.0462
20	1.0000	1.0692	1.0080	1.0969	1.0038	1.0275	1.0131	1.0935	1.0038	1.1110	1.0143	1.1668	1.0058	1.0437
21	1.0006	1.0596	1.0151	1.1093	1.0064	1.0349	1.0178	1.1003	1.0041	1.0896	1.0224	1.1657	1.0083	1.0468
22	0.9956	1.0871	1.0072	1.1169	1.0050	1.0337	1.0183	1.1151	0.9999	1.1303	1.0141	1.1878	1.0071	1.0495
23	0.9934	1.0860	1.0044	1.1129	1.0044	1.0290	1.0151	1.1015	0.9977	1.1294	1.0107	1.1826	1.0063	1.0438
24	0.9857	1.0909	0.9979	1.1154	1.0041	1.0282	1.0134	1.0981	0.9918	1.1362	1.0050	1.1861	1.0065	1.0436
25	0.9820	1.1030	0.9934	1.1233	1.0039	1.0270	1.0137	1.0942	0.9895	1.1517	0.9996	1.1949	1.0057	1.0414
26	0.9998	1.0871	1.0097	1.1174	1.0047	1.0378	1.0172	1.1332	1.0068	1.1345	1.0178	1.1930	1.0078	1.0577
27	0.9497	1.1373	0.9753	1.1445	1.0046	1.0321	1.0114	1.1212	0.9657	1.2112	0.9856	1.2350	1.0082	1.0534
28	1.0029	1.0806	0.9959	1.1139	1.0037	1.0262	1.0136	1.0926	1.0059	1.1284	1.0034	1.1895	1.0055	1.0412

[a]In ZPPR, the x-direction is perpendicular to the plates in the unit cells. The y- and z-directions are parallel to the plates and are equivalent in the models used to represent the ZPPR cells.

File MR3/B3,4

TABLE 3.2. Energy Structure of the Cross Section Sets used for ZPPR-13 Analysis

Energy Boundary	8-Group Number	28-Group Number	226-Group Number[a]	2082-Group Number[a]
14.191 MeV				
6.065		1	36	102
3.679		2	49	162
2.231	1	3	66	222
1.353		4	80	282
820.9 keV	2	5	93	342
497.9		6	105	402
302.0		7	116	462
183.2	3	8	128	522
111.1		9	140	582
67.38		10	144	642
40.87	4	11	150	702
24.79		12	157	762
15.03		13	164	822
9.119	5	14	168	882
5.531		15	172	942
3.355		16	178	1002
2.035	6	17	185	1062
1.234		18	191	1122
748.5 eV		19	193	1182
454.0	7	20	195	1242
275.4		21	197	1302
167.0		22	199	1362
101.3		23	201	1422
61.44		24	203	1482
37.27		25	205	1542
22.60		26	207	1602
13.71		27	209	1782
Thermal	8	28	226	2082

[a]The MC^2-II library used 2082 groups with a lethargy width of 1/120. The SDX intermediate library had 226 groups with a variable lethargy width. JAII2B14

TABLE 3.3. Variation in Average Composition of Drawer Masters in ZPPR-13A

Master	Type	Number[a]	Deviation in Mass from Average, % ^{239}Pu	Deviation in Mass from Average, % ^{238}U	Character[b]
101	SCF	179/181	+0.07	+ 0.05	V63 8-4-6
102	SCF	178/182	+0.01	- 0.00	V63 7-5-6
103	SCF	16/16	+0.24	+ 0.02	V63 5-5-8
701	SCF	3/1	+0.07	+ 0.05	FC V63 8-4-6
705	SCF	6/2	+0.01	- 0.00	FC V63 7-5-6
801(802)	SCF	18/18	-1.02*	- 0.52	PSR V63 5-5-4-4
201	DCF	111/111	-0.08	+ 0.07	V65 7-5-6
202	DCF	172/168	+0.07	+ 0.18	V65 5-5-8
203	DCF	250/252	-0.00	+ 0.13	V65 8-4-6
207	DCF	59/59	+0.92*	- 0.33	V63 5-5-8
208	DCF	40/40	+0.67*	- 0.47	V63 7-7-4
209	DCF	40/40	-1.18*	- 1.08	V65 5-5-4-4
210	DCF	31/30	-0.05	+ 0.10	V65 6-6-6
211	DCF	86/85	+0.07	+ 0.18	V65 5-5-8
212	DCF	175/174	-0.20	- 0.01	V65 7-7-4
213	DCF	56/56	-0.08	+ 0.07	V65 7-5-6
218	DCF	8/8	-0.35*	- 1.58	V63 5-5-4-4
702	DCF	1/1	-0.08	+ 0.07	FC V65 7-5-6
706	DCF	1/1	+0.92*	- 0.33	FC V63 5-5-8
707	DCF	1/2	-0.05	+ 0.10	FC V65 8-6-6
708	DCF	2/7	+0.07	+ 0.18	FC V65 5-5-8
709	DCF	6/4	-0.00	+ 0.13	FC V65 8-4-6
711	DCF	1/1	-0.60*	- 0.49	TC V65 7-7-4
712	DCF	0/1	-0.20	- 0.01	V65 7-7-4
501	IB/RB	275/274	---	+ 1.02	RB inner IB2(x)
502	IB	72/71	---	+ 1.03	CB edge 45°
503	RB	278/280	---	+ 0.91	Middle of RB
504		75/74	---	+ 1.02	IB(y)
505	IB	172/169	---	- 0.63	B2 45°
506	IB	150/150	---	-.0.63	B1 x and y
507	IB	70/71	---	- 0.63	CB center & axes
508	RB	167/168	---	- 0.63	RB outer zone
509	RB	72/72	---	- 0.63	RB outside
510	RB	16/16	---	- 0.63	RB outside
511	RB	47/48	---	- 0.63	RB outside
703	IB/RB	12/13	---	- 7.71	FC distributed
803(804)	IB	6/16	---	-25.72	PSR

[a]Number in half-1 and half-2.

[b]V63 = Vendor 63 fuel, V65 = Vendor 65 fuel, FC = Fission chamber drawer, PSR = Narrow drawer for PSR, TC = thermocouple drawer. a-b-c = fuel piece distribution a in., b in., c in. from midplane.

*Major deviation in ^{239}Pu.

JAIIA15

TABLE 3.4. Perturbation in Control Rod Worths in ZPPR-13A due to Variations in Master Loadings

Control Rods	Worth by AMM Model, $[a]	Worth by Homogeneous Model, $	Ratio (Correction)	Estimated Correction from Fission Rates[b]
CR22	0.7406	0.7458	0.993	0.995
CR25	0.8537	0.8708	0.980	0.981
CR28	0.7466	0.7458	1.001	1.000
CR31	0.8462	0.8708	0.992	0.990
6 R3	7.363	7.385	0.997	0.997

[a]Calculations 28G XY 1MPD WBD, β = 0.3294%.

[b]Square of ^{235}U fission rate ratio in AMM to HMM.

JAII#2A7

TABLE 3.5. Characterization of the Eigenvalue Spectrum in ZPPR-13 Series of Assemblies

Assembly	% Separation Between k_0 and k_1[a]
13A	2.66

[a]k_{eff} of the fundamental mode solution (k_0) and the first azimuthal harmonic solution (k_1).

TABLE 3.7. Eigenvalue Separation for ZPPR-13 Core

Assembly	Zero Flux Axis	Subcritical Reference	Control Rod Banks[a]		
			F1	F2	F3
ZPPR-13A	y	0.0266	0.0175	0.0147	0.0396
	x	0.0293	0.0205	0.019	0.0254
	x+y	0.0808	0.0653	0.0528	0.1041

[a]Calculated for subcritical cores. The banks contained six control rods in F1, twelve in F2 and twelve in F3

TABLE 3.8. Sensitivity of Fission Rates in ZPPR-13A

Zone	Percent Change in Fission Rate for 5% Increase in ^{238}U Capture[a]	
	ZPPR-13A	
	y-axis	Zone Average
F1	-1.2	-1.2
F2	-0.5	-0.4
F3	+0.4	+0.5

[a]Calculations for design models, not the final configurations, normalized to same total power.

JAII#2A7

4.0 CRITICALITY PREDICTIONS, BETA, REACTIVITY COEFFICIENTS

4.1 Analysis of k-effective

The experimental values for k_{eff}, after adjustment to a core with all shim and safety rods removed and to a temperature of 293K, are given in Table 4.1. The estimated uncertainties (Table 2.1) are about 0.04% Δk, but several of the larger components are correlated among the assemblies.

The results of the diffusion theory calculations are given in Table 4.2. Several small corrections are applied to the reference results. The correction of -0.032% Δk, for streaming in the airgap above the plates in each drawer, was estimated for ZPPR-8 and has been used for all subsequent cores. Corrections for ^{239}Pu, ^{240}Pu, ^{241}Pu and ^{238}U loadings were derived by comparing the isotopic masses edited from the xyz model with those from the ZPPR fuel inventory system. The small differences in mass were converted to Δk using atom-density sensitivity coefficients calculated for ZPPR-13A (Section 4.3). The correction for ^{241}Pu is shown separately since this is mainly due to having a fixed date for decay calculation in the cross section library.

The diffusion theory C/E results are similar for all phases and span a range of 0.976 to 0.979.

A number of transport calculations have been made for ZPPR-13A in xy, rz and r geometry. These used a fine mesh, equivalent to 27 mm in the xy plane (or four meshes per drawer). Axial buckling terms for xy models were derived from the reference xyz solution and buckling terms for r models were derived from an rz solution. Two-dimensional models were calculated with S_4 angular quadrature and one-dimensional models used, in addition, S_{16} quadrature with a finer mesh (equivalent to nine meshes per drawer). The mesh and transport corrections are given in Table 4.3.

The estimated transport correction for ZPPR-13A is relatively large in comparison with that for conventional cores. The xy and r models show that this results principally from the annular geometry. The results in the two geometries differ by 0.2%. The transport option of the DIF3D code was used for xy geometry and the ONEDANT code was used for r geometry. It is not clear at this stage that this difference is due wholly to the better geometric representation in the xy model. Effects due to insufficiently refined mesh size and angular quadrature, and in the application of the buckling terms, may be different in the two geometries and codes. The effects of finer mesh in the r dimension and of higher order quadrature in the transport calculations are fairly small.

Using the rz transport correction with the available mesh and angular refinements, the correction to the reference xyz diffusion solution is estimated to be +0.76% Δk. The corrected C/E value for ZPPR-13A is then 0.9857.

Table 4.4 compares the k_{eff} results for a number of ZPPR cores. Diffusion calculations for the heterogeneous cores with no plutonium in the blankets (BOC cores) are about 0.5% Δk lower than for the EOC-cores or the conventional cores. After transport corrections are applied, the results for all cores fall in the range 0.984 to 0.987. The corrected result for ZPPR-13A, 0.986 is in good agreement.

4.2 <u>Delayed Neutron Parameters</u>

Delayed neutron parameters for ZPPR-13 were calculated with the ENDF/B-V delayed neutron data (with reactor fluxes calculated using ENDF/B-IV cross sections). The original calculations used reactor models in rz geometry. The calculations were repeated using the three-dimensional models in xyz geometry using the VARI3D editor. Parameters from both models are shown in Table 4.5.

For ZPPR-13A, the β_{eff} values from rz and xyz models are in close agreement as would be expected from the cylindrical design of the core.

4.3 Reactivity Coefficients

Reactivity coefficients for the most important heavy isotopes were calculated for ZPPR-13A using the rz model. The reactivities were calculated for a 1% increase in density in each region of the core (mass or number-density sensitivity coefficients). These are shown in Table 4.6. The results have been used to make small corrections to k_{eff} for differences in masses between the calculations and the actual loadings.

TABLE 4.1. Experimental Values for k_{eff} in the ZPPR-13 Reference Core

Assembly	Measured Excess, %δk	Temperature Correction to 293K, %δk	PSR Correction[a] %δk	Corrected k_{eff}
13A	0.0221	0.0238	0.0040	1.000499

[a]Estimated correction for B_4C poison safety blades which were fully withdrawn.

JAIIB7

TABLE 4.2. Reference Diffusion Theory k_{eff} Calculations for ZPPR-13

	ZPPR-13A
<u>Reference Calculations</u>	
xyz 28 groups	0.97891
<u>Corrections</u>	
Uniform axial mesh[a]	-0.00003
Air gap streaming	-0.00032
^{241}Pu decay	-0.00004
Fuel loading	+0.00007
<u>Corrected Calculation</u>	0.97859
C/E	0.9781

[a]The xyz models used a variable axial mesh to accommodate the ZPPR shim rods. A correction is made to a uniform mesh of 51 mm in the core region.

JAIIB8

TABLE 4.3. Mesh and Transport Corrections Derived for ZPPR-13A

Correction	Source	Value, Δk
Mesh in xy-plane 55 mm to 27 mm	xy models r models	-0.0016 -0.0014
Total transport: diffusion to S_4 with mesh equivalent to 27 mm	rz diffusion and S4 models	+0.0087
Transport in xy-plane: diffusion to S_4 with mesh 27 mm or equivalent	xy models r models	+0.0073 +0.0051
S_4 to S_{16} quadrature with mesh equivalent to 27 mm	r models	+0.0002
Transport mesh in xy-plane: ~27 mm to ~18 mm with S_{16} quadrature	r models	+0.0003

TABLE 4.4. Comparison of k_{eff} Results for a Range of ZPPR Cores

	Diffusion Theory k_{eff}			Transport Theory k_{eff}		
	No.	Mean	S.D.	No.	Mean	S.D.
Physics Benchmarks						
ZPPR-2	1	0.9828	---	1	0.9854	---
ZPPR-9	1	0.9827	---	1	0.9842	---
ZPPR-7A	1	0.9761	---	1	0.9855	---
ZPPR-13	5	0.9777	0.0010	1	0.9857	---
Cores with CRPs						
Small conventional	3	0.9789	0.0007	3	0.9844	0.0007
Large conventional	3	0.9794	0.0007	3	0.9846	0.0011
Small heterogeneous[a]						
BOC	6	0.9751	0.0022	3	0.9868	0.0023
EOC	4	0.9787	0.0008	2	0.9863	---

[a]Results from ZPPR-7 and ZPPR-11. Beginning-of-cycle (BOC) cores have no plutonium in blanket regions. The end-of-cycle (EOC) cores simulated plutonium buildup.

JAIIB9

TABLE 4.5. Calculations of β_{eff} and ℓ for ZPPR-13

Assembly	rz Calculation: Prompt Neutron Lifetime (ℓ), 10^{-7} sec	rz Calculation: β_{eff}, %	xyz Calculation: β_{eff}
ZPPR-13A	4.049	0.3296	0.3294

JAIIB9

TABLE 4.6. Mass Sensitivity Coefficients for ZPPR-13

Assembly	Isotope	Percent Δk/k Per Percent Increase in Mass
ZPPR-13A	^{239}Pu	0.541
	^{240}Pu	0.0110
	^{241}Pu	0.00780
	^{238}U	-0.175

JAIIB7

5.0 ANALYSIS OF REACTION RATE MEASUREMENTS

Reaction rates were calculated with the xyz diffusion models and 28 group cross sections, as described in Section 3.4. The effects of the banked shim control rods were approximated in the model by adding boron to the fuel in the shim location, to the appropriate shim-insertion depth, and using a shielding factor derived to reproduce the measured shim reactivity to within 10%. This method was deemed sufficiently accurate since reaction rate perturbations at the midplane are generally less than 1%. The model is estimated to be accurate to 0.1% at the midplane.

Figure 5.1 shows the calculated perturbation in fission rates due to the shim rods in ZPPR-13A. In this case the effects are quite small with relative perturbations of 0.5% at the most. The calculated shim rod reactivity was 5¢.

The effects due to anisotropic diffusion vary up to 1% as shown in Section 3.3. In the absence of other perturbations, comparison of C/E values for reaction rates at equivalent positions on the x and y axes of ZPPR-13A should provide a test of the accuracy of calculated shim rod and streaming effects. Other ZPPR-13 cores have more complex internal blanket geometry.

Corrections for the variations in drawer compositions have been applied by multiplying the reaction rates calculated with the xyz model, R (xyz), by the ratio of reaction rates from the all-master xy model, R(AMM) to the reaction rate for the homogenized-master xy model, R(HMM) as follows:

$$R(\text{corrected}) = R(xyz) \times R(AMM)/R(HMM)$$

In the case of axial traverses, the result at each axial position is multiplied by the ratio calculated at the midplane from the xy models.

The experimental measurements are given in units of 10^{-18} fissions or captures per atom per second at a reactor power of approximately 1 watt. However, the normalization of the measurements is accurate only to about 20%.

For comparison with experiment, the calculated values are normalized to give an average C/E value of unity for all available measurements of fission in ^{239}Pu within the fuel regions. The normalization is not quite equivalent between different cores because the number of measurements for plutonium fission is limited and different traverses may be chosen in each case. Further, the plutonium measurements are normally made in one quadrant only and do not allow for asymmetries in the cores. The actual C/E results cannot be compared from core to core to better than a few percent; only the comparisons of the reaction rate distributions and reaction rate ratios are relevant.

Two foil irradiations were made in each of the assemblies ZPPR-13A, The two sets of data have been combined into one group for the present analysis. A number of ^{235}U foils were irradiated in common locations for each pair of measurements. Except for ZPPR-13A, the results for the "common foils" were in satisfactory agreement with the experimental statistics. The results for 13A showed a small bias. The original data for the separate irradiations have been preserved in the monthly TM reports.

The cross sections used to calculate reaction rates are cell-averaged for each cell type. In the case of plutonium in blanket zones, special cross sections resonance shielded for the 0.13 mm thick foils are generated. These show improvements over infinitely-dilute cross sections of up to 1% in the internal blankets and several percent in the soft spectrum regions of the radial and axial blankets.

For convenience in displaying the results, the following abbreviations are used to show the distinctive reactor zones:

CB for center blanket

F1, F2, F3, for fuel rings one, two and three

B1, B2 for the first and second internal blanket rings

RB for the radial blanket

AB for the axial blanket

In addition, the single-fuel-column drawers in the fuel zones are designated as F1 S, etc. This distinction is useful since systematic differences in C/E results for reactions in ^{238}U are evident between the single- and double-fuel-column drawers.

As an aid in visualizing the analysis of the reaction rates, the results in the summary tables and figures show mean C/E values for groups of adjacent measurements in the same zone. Very little loss of information is incurred by this condensation since any variation in C/E values over a range of several drawers is masked by experimental statistics. The detailed tables show the standard deviation of the C/E distributions for the chosen groups of foils. These data are not usually of statistical significance, due to the small number of results in the group, but are given as an indication of the spread in results. The standard deviations may be compared to the experimental statistics of 0.5% to 1% for the non-threshold reactions.

Radial reaction rate distributions along the x-axis of ZPPR-13A are shown in Figs. 5.2 and 5.3. The threshold fission rate, $^{238}U(n,f)$, a monitor of the flux variations in the MeV range, varies quite dramatically between the fuel and blanket rings. This presents a definite challenge to analysis in heterogeneous cores. Its accurate prediction is sensitive to cell-processing methods and to transport effects. In contrast, the non-threshold reactions are quite benign. These variations are typical of the reaction rates in all phases of ZPPR-13 and similar to those in in other heterogeneous cores.[7]

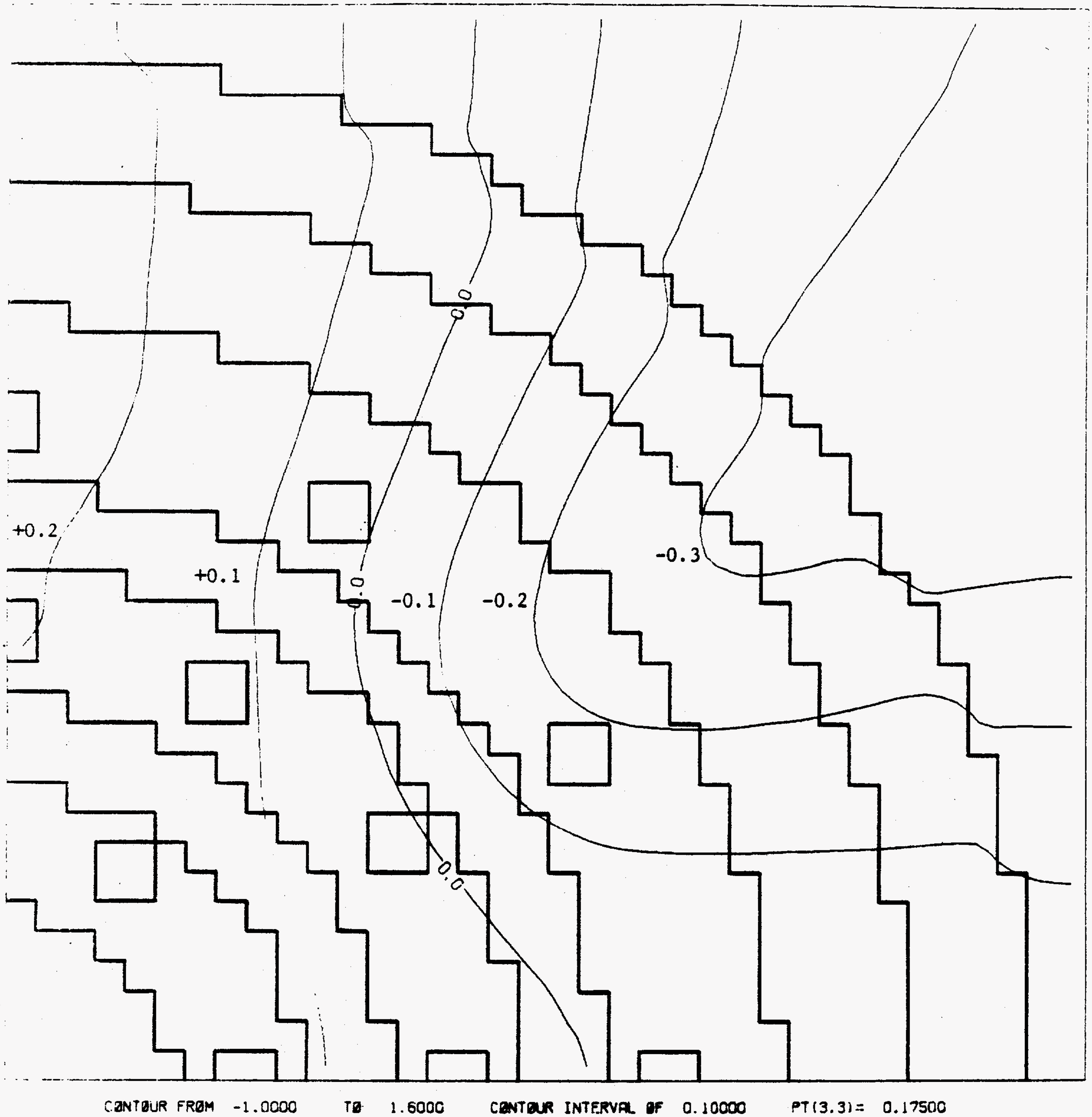

Fig. 5.1. Percent change in ^{235}U fission rate in ZPPR-13A caused by partially inserted shim rods.

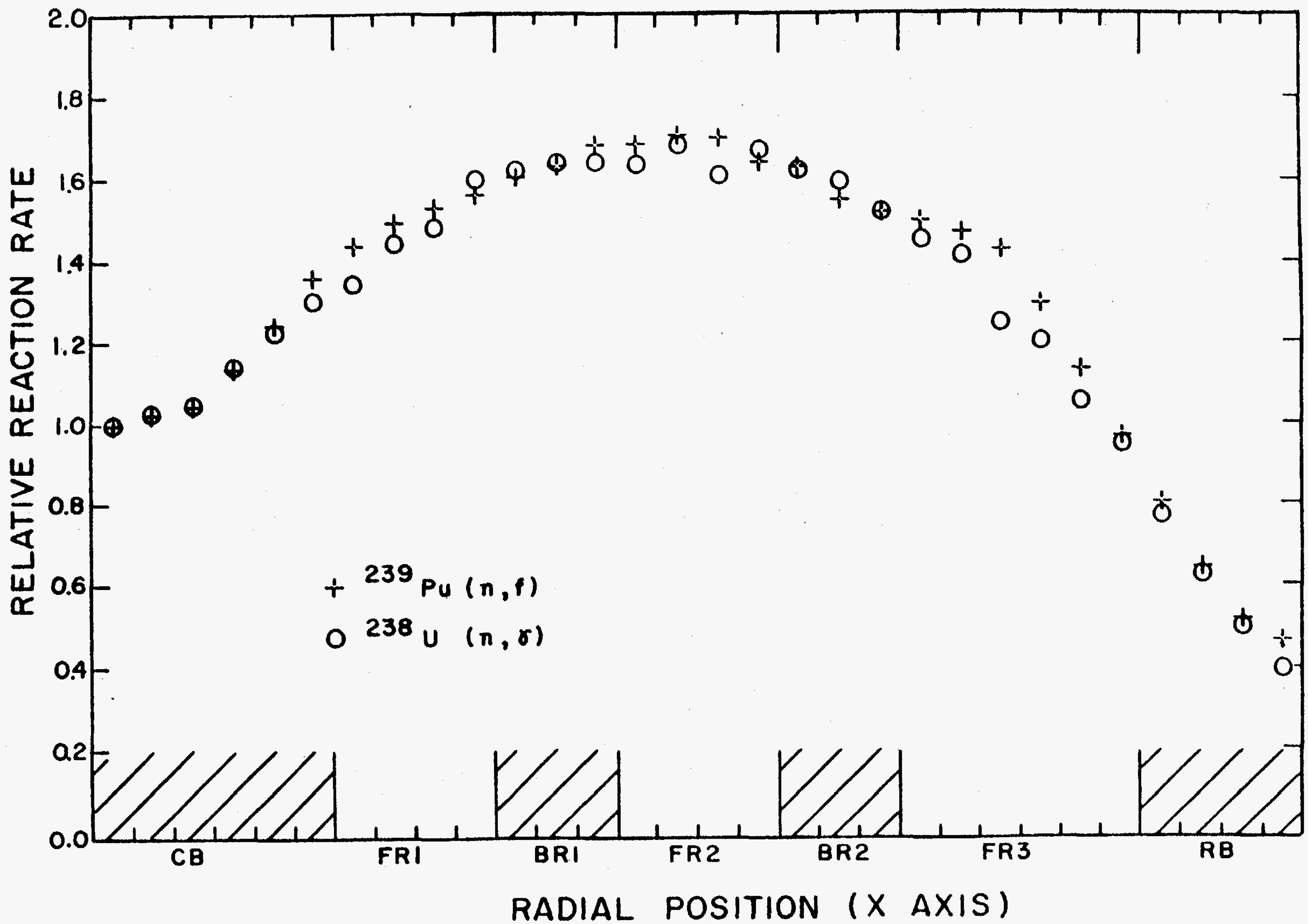

Fig. 5.2. Radial variation of ^{239}Pu fission and ^{238}U capture in ZPPR-13A.

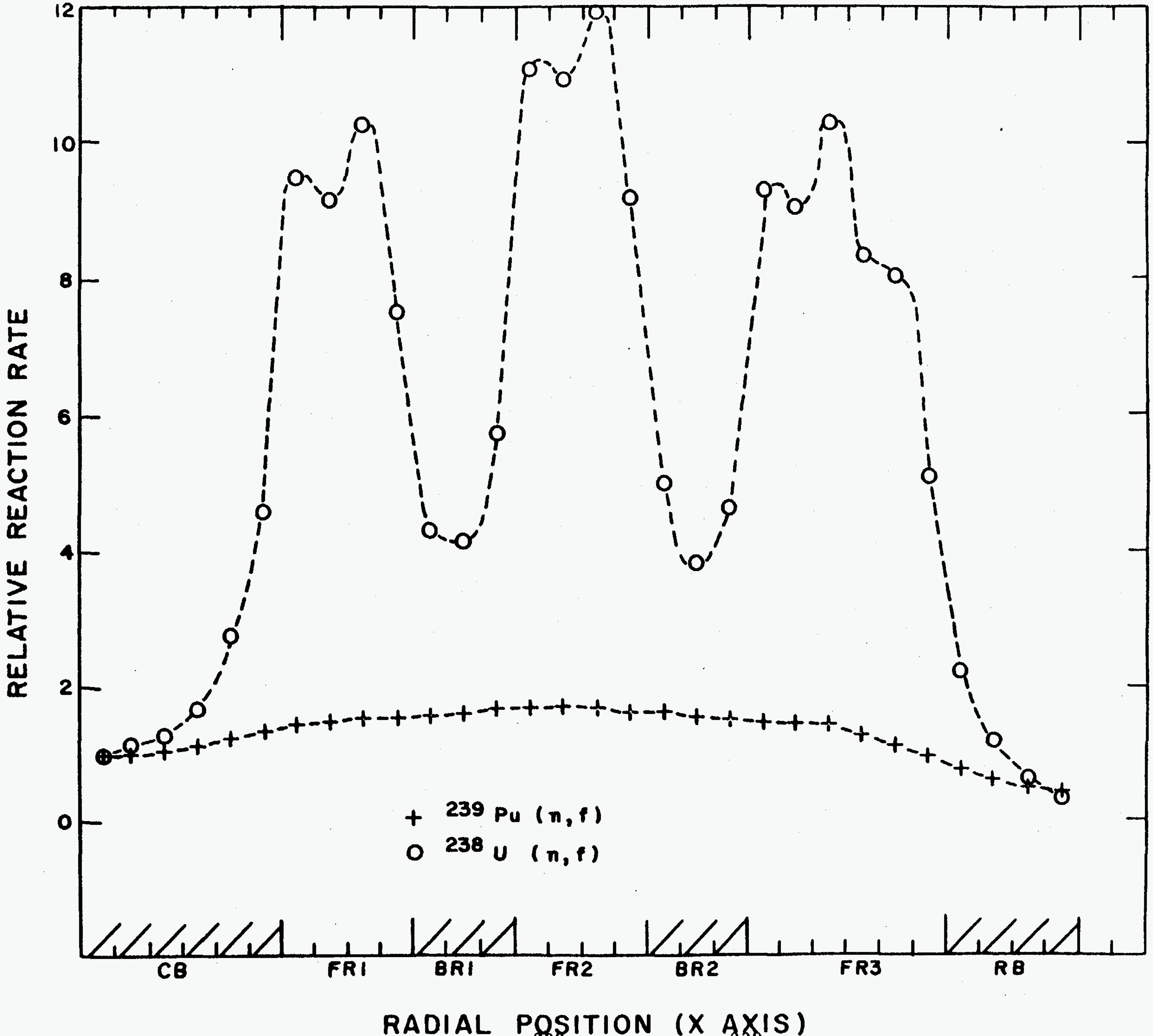

Fig. 5.3. Radial variation of ^{239}Pu fission and ^{238}U fission in ZPPR-13A.

5.1 Diffusion Theory Analysis for ZPPR-13A

The locations of the foil measurements in ZPPR-13A are shown in Figs. 5.4 and 5.5. The data fall into several groups:

(i) Traverses along the principal axes in the upper left hand (ULH) quadrant for all four reaction types.

(ii) Axial traverses for the four reactions in three locations in fuel zones.

(iii) Extensive data for ^{235}U fission in all four quadrants to test the symmetry of fission distributions.

(iv) A number of special measurements of ^{235}U fission including twelve axial traverses, measurements near the interface in the radial reflector and measurements in locations symmetric to fission chamber deposits for calibration purposes.

The two irradiations in ZPPR-13A were separated by an interval of over three months. Several other experiments took place between the two foil measurements, not the least of which were extensive sodium-void studies and "drawer-pushing" excercises.(9) There were 102 ^{235}U foils in the same locations for the two irradiations. The average of the ratios of the countrates in the first set divided by those in the second set (weighted with statistical uncertainties) was 1.0023 ± 0.0008 (1σ). This indicates a slight bias between the two measurements, but it is not considered too large to prohibit combination of the two sets of data.

The k_{eff} values for the xyz calculation models were:

- reference core 0.978908
- with shim rods inserted 0.978757
- shim rod reactivity 0.015% Δk

The measured shim reactivities were 0.015% Δk and 0.021% Δk for the two irradiations. The single calculation was regarded as adequate since perturbations to midplane reaction rates were less than 0.4% (Fig. 5.1).

The analysis of radial and axial reaction rate distributions is summarized in Tables 5.1 to 5.7. These results are a condensation of the detailed data in Appendix C. The conclusions are as follows:

(i) Radial reaction rate distributions are obtained for all four reaction types only in the upper left hand quadrant. Table 5.1 shows the mean C/E results in each radial zone.

The three non-threshold reactions show a similar monotonic increase in C/E with increasing radius. Reaction rates in fuel ring two (F2) are overpredicted by 2% relative to F1 and reaction rates in F3 are overpredicted by between 4.5% and 5% relative to F1.

The ^{238}U fission rates also show a radial misprediction. However, C/E results in adjacent fuel and blanket zones differ by about 15%. This result is entirely expected with diffusion theory calculations.

(ii) More than 300 ^{235}U foils were irradiated near to the midplane, covering all four quadrants of the reactor. These results are displayed in Table 5.2 to show the azimuthal variations in prediction. The results are also illustrated in Fig. 5.6. The azimuthal variation in C/E is about 3% in the third fuel ring (F3). The highest value is 1.066 on the negative x-axis and the lowest value is 1.036 near the top of the core. Results at the bottom of the core are about 1% higher than at the top and results on the RHS are generally lower than on the LHS.

(iii) Table 5.3 shows a summary of results for the 64 foils in locations symmetric to the in-core fission chambers. Results are averaged for each radial zone. These data are sufficient to identify the radial mispredictions of fission rates as can be seen by comparison with the results from all ^{235}U foils, shown in the last column of the table.

(iv) Axial traverses were made adjacent to or inside each of the twelve positions designated as control rod locations in the outer fuel ring. The average C/E results in these locations, shown in Table 5.4, provide data on the azimuthal variation covering all four quadrants. The results show a similar variation to those in Table 5.3 although values in the same regions tend to be higher by 0.5% to 1%.

(v) Tables 5.5, 5.6 and 5.7 give an analysis of axial reaction rate distributions. In order to remove biases in C/E values due to position in the core and reaction type, the tables show the C/E values at each z-position relative to a core average value. Since the foil locations are irregularly-spaced, an axially-weighted core-average is used (this is only a little different from the unweighted average (see results in Appendix C)). With this normalization, all results except ^{238}U fission show a similar trend.

The C/E results at the top of the core near the axial blanket interface are 1% low, on average, relative to the mean over the core height. The results in the axial blanket have consistent C/Es, within statistics, over the range 480 mm to 690 mm from the midplane. The results for ^{238}U capture appear less consistent between the core region and the blanket. In the axial blanket above the single-fuel-column drawer (Table 5.5) the C/Es are about 2% higher, but above the double-fuel-column drawer (Table 5.6) the C/Es are about 5% lower than the core average. The ^{238}U fission values across the core/axial blanket interface show a marked discontinuity of 5% to 10% in the same sense as found in the radial distributions.

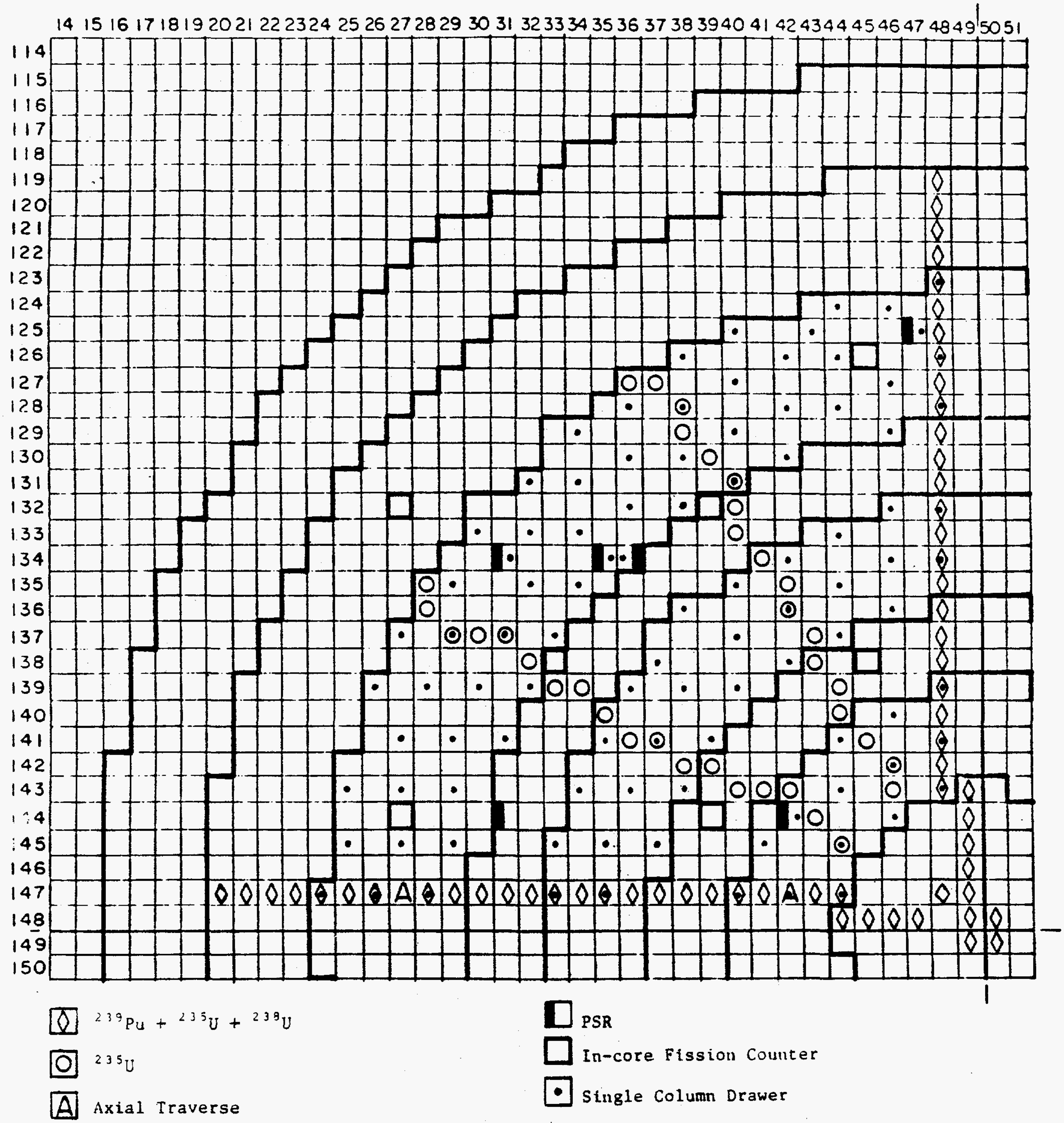

Fig. 5.4. Foil Locations in ZPPR-13A Irradiation No. 1.

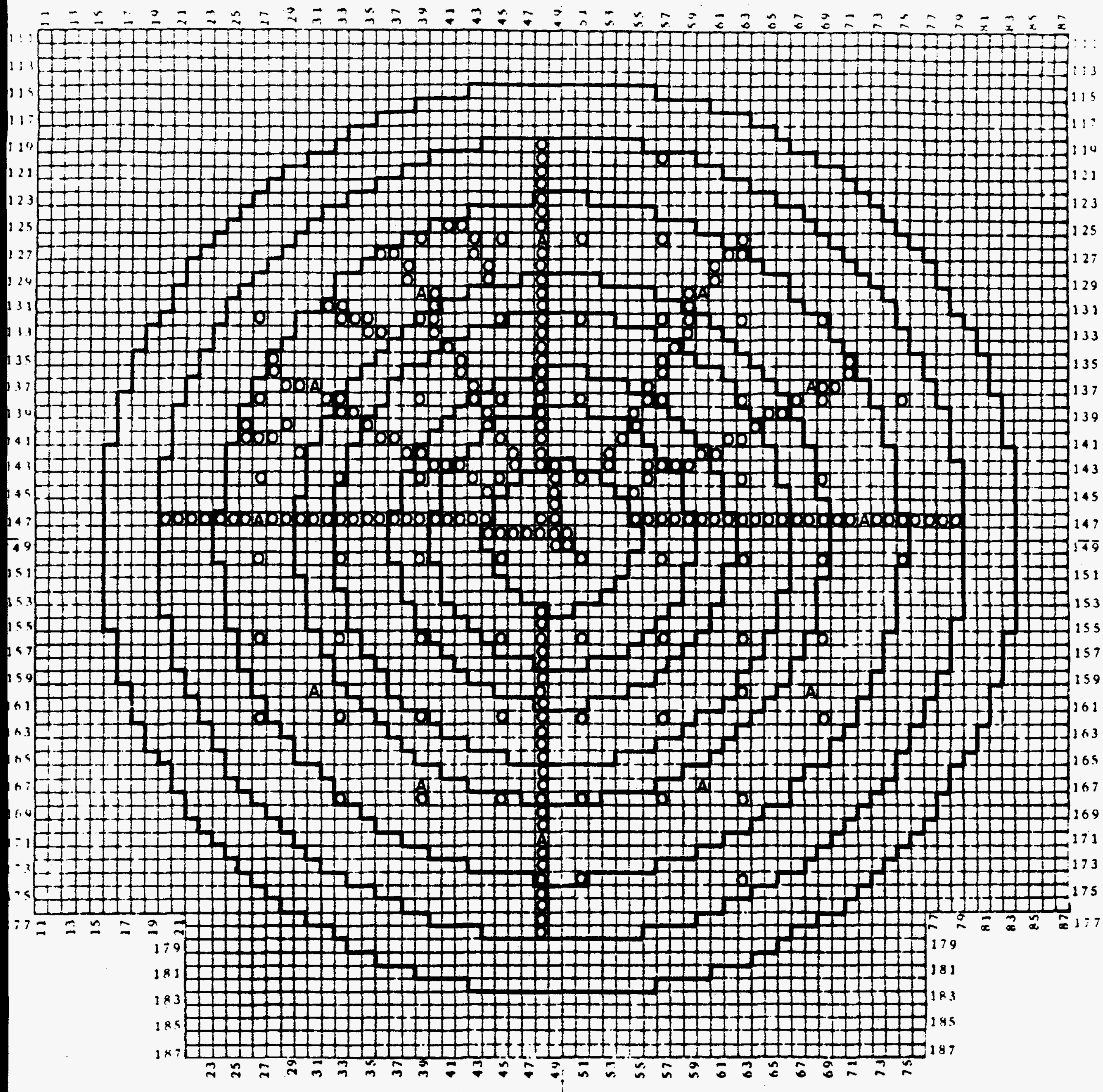

A Axial Traverse

O ^{235}U Foil

Fig. 5.5. Foil Locations in ZPPR-13A Irradiation No. 2.

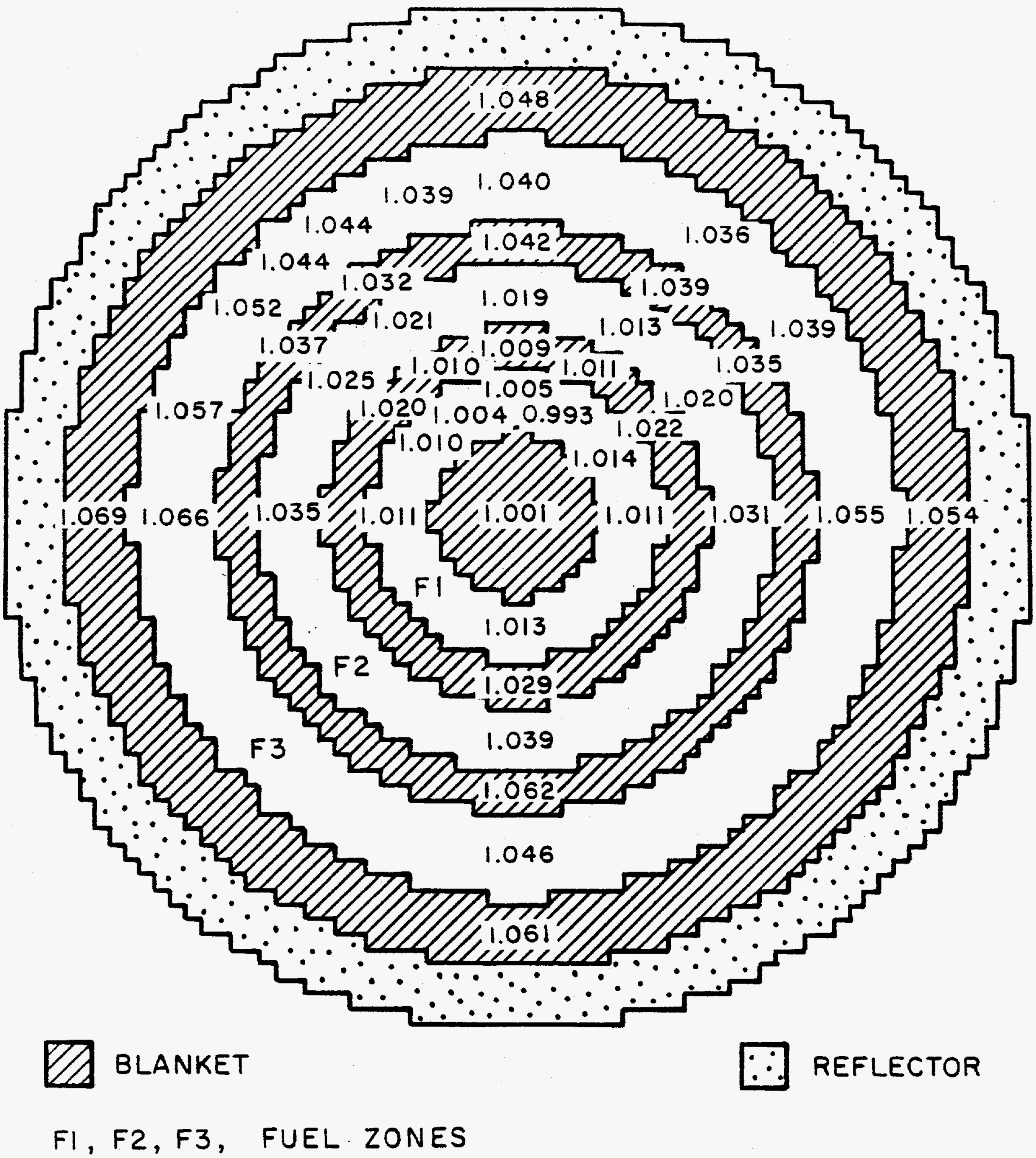

Fig. 5.6. Ratios of calculation to experiment for ^{235}U fission rates in ZPPR-13A.

TABLE 5.1. ZPPR-13A: Summary of Radial Reaction Rate Analysis

Zone	Number of Data	$^{239}Pu(n,f)$ Mean C/E	$^{239}Pu(n,f)$ S.D.[b]	$^{235}U(n,f)$[a] Mean C/E	$^{235}U(n,f)$[a] S.D.[b]	$^{238}U(n,\gamma)$ Mean C/E	$^{238}U(n,\gamma)$ S.D.[b]	$^{238}U(n,f)$ Mean C/E	$^{238}U(n,f)$ S.D.[b]
CB	14	0.969	0.011	1.005	0.007	1.045	0.007	0.961	0.089
F1	10	0.974	0.011	1.008	0.009	1.048	0.015	0.908	0.029
B1	6	0.987	0.008	1.013	0.006	1.050	0.007	1.060	0.019
F2	8	0.996	0.017	1.027	0.013	1.067	0.018	0.913	0.031
B2	6	1.022	0.018	1.051	0.012	1.077	0.011	1.091	0.034
F3	12	1.020	0.023	1.053	0.014	1.099	0.025	0.966	0.039
RB	8	0.997	0.025	1.058	0.014	1.095	0.019	1.003	0.092

[a]Includes only results at the x-axis and y-axis in the ULH quadrant for consistency with the other reactions.

[b]Standard deviation of the C/E distribution.

JAI12A24

TABLE 5.2. ZPPR-13A: Summary of Radial Fission Rate Analysis for ^{235}U

Azimuthal Position[a]	Mean C/E by Radial Zone[b] F1	B1	F2	B2	F3	RB
Negative x-axis	1.011	1.017	1.035	1.060	1.066	1.069
π/12	---	---	---	---	1.057	---
π/6	1.010	1.020	1.025	1.037	1.052	---
3π/12	---	---	---	---	1.044	---
π/3	1.004	1.010	1.021	1.032	1.044	---
5π/12	---	---	---	---	1.039	---
Positive y-axis	1.005	1.009	1.019	1.042	1.040	1.048
2π/3	1.014	1.022	1.020	1.035	1.039	---
5π/6	0.993	1.011	1.013	1.039	1.036	---
Positive x-axis	1.011	1.024	1.031	1.066	1.055	1.054
Negative y-axis	1.013	1.029	1.039	1.062	1.046	1.061
All Data:						
Number	38	29	43	31	140	22
Mean C/E	1.008	1.018	1.024	1.045	1.046	1.061
S.D.	0.011	0.012	0.013	0.014	0.014	0.014

[a]Approximate azimuthal positions with respect to the negative x-axis of ZPPR half 1.

[b]Mean C/E values for groups of three to six foils in fuel zone 1 (F1), blanket ring 1 (B1), etc. JAII2A25

TABLE 5.3. ZPPR-13A: Summary of Analysis for the Fission Chamber Calibration Foils

Zone	Number of Results	Mean C/E	S.D.	Mean C/E Using all Foil Data
CB	3	1.004	0.002	1.005
F1	5	1.000	0.013	1.008
B1	5	1.018	0.014	1.018
F2	11	1.019	0.010	1.024
B2	11	1.039	0.011	1.045
F3	23	1.042	0.015	1.046
RB	6	1.069	0.014	1.061

JAII2A26

TABLE 5.4. ZPPR-13A: Summary of Analysis of ^{235}U Fission Near Control Positions in Fuel Ring 3

Matrix Position	Control Position[a]	Orientation	Mean C/E[b]	S.D.
147-27	25	0 (-x)	1.062	0.012
137-31	26	$\pi/6$	1.045	0.005
130-39	27	$\pi/3$	1.025	0.010
126-48	28	$\pi/2$ (+y)	1.035	0.004
130-60	29	$2\pi/3$	1.029	0.006
137-68	30	$5\pi/6$	1.041	0.008
147-72	31	π (+x)	1.051	0.009
160-68	20	$7\pi/6$	1.049	0.006
167-60	21	$4\pi/3$	1.034	0.007
171-48	22	$3\pi/2$ (-y)	1.046	0.004
167-39	23	$5\pi/3$	1.033	0.013
160-31	24	$11\pi/6$	1.057	0.013

[a]Positions used for measurement of control rod worths in ZPPR-13A. Positions near the axes were adjacent to control positions, the remainder were inside the control positions.

[b]Mean result for seven or ten axial positions, depending on location. See detailed tables. JAII2A27

TABLE 5.5. ZPPR-13A: Axial Reaction Rate Analysis in Matrix 147-42

Zone	Z, mm	F9	F5	C8	F8
F1 S	77	1.015	1.008	1.018	1.002
	128	1.009	1.002	1.001	1.008
	204	0.999	0.997	0.999	1.060
	280	0.998	1.002	1.003	1.004
	331	0.988	1.010	0.982	0.969
	382	0.979	0.984	0.991	0.971
	433	0.999	0.988	0.984	0.950
AB	483	0.991	1.006	1.027	0.998
	534	1.004	1.001	1.024	1.004
	610	0.981	0.986	1.017	0.89
	687	0.966	0.999	1.007	0.81
Core Average[a]		0.984	1.017	1.034	0.956
	S.D.	0.012	0.010	0.013	0.035

[a]Weighted average over 0 to 458 mm. JAII2A26

TABLE 5.6. ZPPR-13A: Axial Reaction Rate Analysis in Matrix 147-27

Zone	Z, mm	F9	F5	C8	F8
F3	77	1.011	1.011	1.015	1.026
	128	1.003	1.010	1.008	1.000
	204	1.015	1.006	1.002	1.011
	280	0.985	0.992	0.985	0.997
	331	0.988	0.990	0.990	0.980
	382	0.988	0.992	0.974	0.981
	433	0.995	0.987	1.013	0.973
AB	483	0.982	1.014	0.952	1.105
	534	1.011	0.995	0.945	1.113
	610	0.966	1.002	0.955	0.94
	687	0.972	0.998	0.952	0.67
Core Average[a]		1.028	1.059	1.124	0.956
	S.D.	0.012	0.011	0.017	0.018

[a]Weighted average over 0 to 458 mm.

JAII2A28

TABLE 5.7. Summary of Axial ^{235}U Fission Rate Analysis

Z, mm	147-27	137-31	130-39	126-48	130-60	137-68
13	1.014	1.004	0.997	0.998	1.005	1.006
77	1.010	1.001	1.004	1.001	1.010	0.987
128	1.009	1.005	1.023	1.002	---	---
204	1.006	1.000	1.003	1.006	---	---
280	0.992	1.000	0.997	1.002	0.997	1.001
331	0.990	0.996	0.993	0.997	0.999	0.999
382	0.992	0.995	0.994	0.993	0.993	0.997
433	0.987	0.995	0.982	0.999	---	---
Core Average[a]	1.059	1.044	1.026	1.036	1.027	1.040

Z, mm	147-72	160-68	167-60	171-48	167-39	160-31
13	1.005	0.995	1.007	0.999	1.009	1.008
77	1.005	1.003	1.008	0.996	1.010	1.019
128	1.008	---	---	1.000	---	---
204	1.007	---	---	1.004	---	---
280	1.003	1.003	0.998	1.001	1.000	0.999
331	0.992	1.004	0.995	1.001	0.997	0.987
382	0.994	0.999	0.994	0.998	0.996	0.989
433	0.980	---	---	0.995	---	---
Core Average[a]	1.050	1.050	1.032	1.047	1.030	1.054

Average of all results at 13 and 77 mm = 1.004
Average of all results at 382 and 433 mm = 0.993

[a]Weighted average over 0 to 458 mm.

JAII2A29

5.5 Reaction Rate Ratio Analysis

Reaction rate ratios relative to fission in ^{239}Pu have been analyzed for all matrix positions in which all three foils were irradiated. Detailed results are given in the appendices. Note that the experimental values are not adjusted to a common location in the cell. The ^{235}U foils are separated from the plutonium foils by 27.7 mm and the ^{238}U foils are separated from plutonium foils by 13.8 mm. The adjustments would be about 1% for ^{235}U and 0.5% for $^{238}U(n,\gamma)$. Variations in ^{238}U fission may be much larger. Calculations are interpolated to the given foil locations to obtain appropriate C/E values. The C/E values are insensitive to mispredictions of the global flux shapes in the core since these are similar for all reactions. For a given cell type, the standard deviations of the C/E distributions are only a little larger than the statistical uncertainties of the measurements.

A summary of the reaction rate ratio analysis for ZPPR-13A is given in Table 5.13 Average results are given separately for single-fuel-column and double-fuel-column drawers and for blanket drawers since significantly different results may be obtained in different drawer types.

The conclusions are:

(i) Results are consistent between these cores and are similar to analysis of ZPPR-9 and ZPPR-10.

(ii) The average C/E for the ^{235}U fission ratio is 1.03 and varies by only a few tenths of a percent between SC fuel drawers, DC fuel drawers and blanket drawers except for the axial traverses in 13B/4 which are singularly out of line (C/E = 1.044).

(iii) The results for the ^{238}U capture ratio are significantly different between the drawer types:

SC fuel drawers <C/E> = 1.06

DC fuel drawers <C/E> = 1.09

Internal Blankets <C/E> = 1.07

(iv) The results for the ^{238}U fission ratios are also different.

For radial traverses:

SC fuel drawers <C/E> = 0.95 to 0.97

DC fuel drawers <C/E> = 0.92 to 0.93

Internal Blankets <C/E> = 1.07 to 1.08

The ^{238}U fission results are improved by fine mesh transport calculations.

TABLE 5.13. ZPPR-13A: Summary of Reaction Rate Ratio Analysis

Ratio	Traverse	Zone[a]	Number of Results	Mean C/E	Standard Deviation
$^{235}U(n,f)/^{239}Pu(n,f)$	Radial	Fuel DC	14	1.027	0.012
		Fuel SC	16	1.032	0.011
		Internal Blankets	26	1.033	0.014
	Axial	Fuel DC	7	1.028	0.007
		Fuel SC	7	1.034	0.013
$^{238}U(n,\gamma)/^{239}Pu(n,f)$	Radial	Fuel DC	14	1.091	0.012
		Fuel SC	16	1.060	0.014
		Internal Blankets	26	1.070	0.015
	Axial	Fuel DC	7	1.092	0.012
		Fuel SC	7	1.049	0.010
$^{238}U(n,f)/^{239}Pu(n,f)$	Radial	Fuel DC	14	0.915	0.018
		Fuel SC	16	0.953	0.024
		Center Blanket[b]	8	0.921	0.032
		Internal Blankets	18	1.078	0.023
	Axial	Fuel DC	7	0.933	0.012
		Fuel SC	7	0.970	0.033

[a]DC = double-fuel-column drawers; SC = single-fuel-column fuel drawers.

[b]Includes positions in interior of center blanket. Positions near the edge are averaged with the internal blanket rings.

JAII2B13

5.6 Transport Calculation

Transport calculations using a fine mesh (4MPD) have been calculated for the midplane reaction rates in ZPPR-13A using an xy model. The results for the xyz diffusion calculations have been adjusted first by the ratio of diffusion calculations in 4MPD relative to 1MPD and second by the ratio of the S_4 calculation with 4MPD to the diffusion calculation with 4MPD.

The transport corrections along the x-axis are given in Tables 5.16 to 5.19. Corrections are quite similar for the three non-threshold reactions; reaction rates in blanket regions are reduced by between 2% and 3% while values in fuel regions change by less than 0.5%. (Note that the transport results preserve the normalization to ^{239}Pu fission in the fuel zones). The mispredictions with radius are made marginally worse (0.3% to 0.5%) by transport corrections.

Transport corrections produce a marked improvement for $^{238}U(n,f)$. Calculated values in fuel regions are increased by between 1% and 3%, values in the internal blankets are decreased by between 6% and 13%. C/E results between the fuel zones F1 and F2 remain lower than those in blanket zones B1 and B2 by 5%.

Studies for ZPPR-7, using fuel/blanket coupled-cell models achieved agreement in predictions of ^{238}U fission between fuel and blanket drawers to within 2%.[7] Calculations for ZPPR-13 with multi-drawer models might also produce improved predictions.

TABLE 5.16. ZPPR-13A: TRANSPORT CORRECTED REACTION RATES FOR 239PU(N,F)

MATRIX POSITION	ZONE	EXP.	REFERENCE C/E	MEAN C/E (S.D.)	CORRECTIONS A MESH	S4	CORRECTED C/E	MEAN C/E (S.D.)
147 49	CB	4.473	0.959		1.009	0.967	0.936	
147 48	CB	4.588	0.966		1.009	0.966	0.940	
148 47	CB	4.669	0.980		1.008	0.966	0.954	
148 46	CB	5.095	0.979		1.007	0.964	0.951	
148 45	CB	5.610	0.975	0.973	1.005	0.969	0.949	0.948
148 44	CB	6.118	0.980	(0.009)	1.003	0.974	0.958	(0.008)
147 44	F1 S	6.146	0.958		1.003	0.988	0.949	
147 43	F1	6.434	0.971		1.001	1.003	0.975	
147 41	F1	6.895	0.974	0.968	1.002	1.001	0.978	0.965
147 40	F1 S	7.023	0.968	(0.007)	1.004	0.984	0.957	(0.014)
147 39	B1	7.222	0.984		1.005	0.966	0.955	
147 38	B1	7.350	0.992	0.991	1.005	0.965	0.962	0.964
147 37	B1	7.559	0.998	(0.007)	1.003	0.974	0.975	(0.010)
147 36	F2	7.567	0.997		1.002	1.001	0.999	
147 35	F2 S	7.709	1.015		1.000	1.003	1.018	
147 34	F2	7.654	1.007	1.009	1.001	1.006	1.014	1.010
147 33	F2 S	7.403	1.017	(0.009)	1.002	0.990	1.008	(0.008)
147 32	B2	7.343	1.016		1.003	0.970	0.988	
147 31	B2	6.985	1.040	1.035	1.004	0.964	1.005	1.005
147 30	B2	6.847	1.048	(0.017)	1.002	0.973	1.022	(0.017)
147 29	F3	6.764	1.022		1.000	1.000	1.022	
147 28	F3 S	6.611	1.045		0.997	1.006	1.048	
147 26	F3 S	5.818	1.047		0.996	1.006	1.049	
147 25	F3	5.102	1.059	1.039	0.997	1.009	1.065	1.040
147 24	F3 S	4.388	1.023	(0.016)	0.998	0.994	1.014	(0.021)
147 23	RB	3.628	1.037		1.000	0.973	1.009	
147 22	RB	2.911	1.016		1.002	0.968	0.985	
147 21	RB	2.339	1.009	1.007	1.005	0.972	0.986	0.984
147 20	RB	2.095	0.967	(0.029)	1.009	0.981	0.957	(0.021)

A CORRECTIONS WERE NOT CALCULATED IN POSITIONS 147-42 AND 147-27 .

TABLE 5.17. ZPPR-13A: TRANSPORT CORRECTED REACTION RATES FOR 235U(N,F)

MATRIX POSITION	ZONE	EXP.	REFERENCE C/E	MEAN C/E (S.D.)	CORRECTIONS A MESH	S4	CORRECTED C/E	MEAN C/E (S.D.)
147 49	CB	5.306	1.000		1.009	0.968	0.977	
147 48	CB	5.429	1.003		1.008	0.968	0.979	
148 47	CB	5.524	1.011		1.008	0.968	0.986	
148 46	CB	5.981	0.996		1.006	0.968	0.970	
148 45	CB	6.324	1.003	1.006	1.004	0.973	0.980	0.982
148 44	CB	6.557	1.020	(0.009)	1.002	0.977	0.999	(0.010)
147 44	F1 S	6.492	1.021		1.003	0.986	1.010	
147 43	F1	6.684	1.004		1.003	0.998	1.005	
147 41	F1	7.235	0.996	1.008	1.004	0.996	0.996	1.003
147 40	F1 S	7.576	1.012	(0.011)	1.003	0.984	0.999	(0.006)
147 39	B1	7.987	1.012		1.003	0.971	0.986	
147 38	B1	8.155	1.018	1.017	1.003	0.971	0.991	0.992
147 37	B1	8.198	1.022	(0.005)	1.002	0.977	1.000	(0.007)
147 36	F2	7.977	1.020		1.003	0.997	1.020	
147 35	F2 S	7.970	1.045		1.000	0.997	1.042	
147 34	F2	7.942	1.029	1.035	1.002	1.001	1.032	1.033
147 33	F2 S	7.901	1.047	(0.013)	1.002	0.988	1.037	(0.009)
147 32	B2	7.936	1.058		1.000	0.975	1.032	
147 31	B2	7.797	1.061	1.060	1.001	0.971	1.031	1.033
147 30	B2	7.551	1.062	(0.002)	0.999	0.977	1.037	(0.003)
147 29	F3	7.061	1.058		1.001	0.998	1.057	
147 28	F3 S	6.765	1.069		0.997	1.002	1.068	
147 26	F3 S	5.897	1.066		0.995	1.004	1.065	
147 25	F3	5.257	1.071	1.065	0.998	1.006	1.075	1.063
147 24	F3 S	4.646	1.062	(0.005)	0.997	0.993	1.051	(0.009)
147 23	RB	3.935	1.083		0.998	0.978	1.057	
147 22	RB	3.255	1.069		1.001	0.973	1.041	
147 21	RB	2.667	1.065	1.069	1.005	0.974	1.042	1.047
147 20	RB	2.321	1.057	(0.011)	1.010	0.981	1.047	(0.007)

A CORRECTIONS WERE NOT CALCULATED IN POSITIONS 147-42 AND 147-27 .

TABLE 5.18. ZPPR-13A: TRANSPORT CORRECTED REACTION RATES FOR 238U(N,G)

MATRIX POSITION	ZONE	EXP.	REFERENCE C/E	MEAN C/E (S.D.)	CORRECTIONS A MESH	CORRECTIONS A S4	CORRECTED C/E	MEAN C/E (S.D.)
147 49	CB	0.6268	1.050		1.010	0.966	1.025	
147 48	CB	0.6521	1.041		1.009	0.967	1.016	
148 47	CB	0.6649	1.053		1.009	0.968	1.028	
148 46	CB	0.7207	1.049		1.007	0.970	1.025	
148 45	CB	0.7739	1.057	1.050	1.005	0.976	1.036	1.027
148 44	CB	0.8217	1.051	(0.005)	1.003	0.980	1.034	(0.007)
147 44	F1 S	0.8763	1.034		1.003	0.986	1.023	
147 43	F1	0.8544	1.067		1.005	0.993	1.065	
147 41	F1	0.9277	1.060	1.052	1.006	0.991	1.056	1.045
147 40	F1 S	1.0090	1.048	(0.014)	1.004	0.984	1.035	(0.019)
147 39	B1	1.0130	1.046		1.004	0.975	1.024	
147 38	B1	1.0330	1.055	1.053	1.004	0.975	1.032	1.032
147 37	B1	1.0330	1.059	(0.007)	1.003	0.980	1.040	(0.008)
147 36	F2	1.0250	1.086		1.005	0.992	1.083	
147 35	F2 S	1.0560	1.060		1.001	0.993	1.053	
147 34	F2	1.0120	1.094	1.080	1.004	0.995	1.092	1.074
147 33	F2 S	1.0500	1.078	(0.015)	1.003	0.988	1.068	(0.017)
147 32	B2	1.0210	1.079		1.002	0.978	1.058	
147 31	B2	1.0050	1.083	1.085	1.003	0.976	1.060	1.064
147 30	B2	0.9617	1.093	(0.007)	1.000	0.982	1.074	(0.009)
147 29	F3	0.9143	1.117		1.003	0.995	1.115	
147 28	F3 S	0.8874	1.089		0.997	1.000	1.086	
147 26	F3 S	0.7578	1.099		0.995	1.002	1.096	
147 25	F3	0.6627	1.135	1.110	0.999	1.002	1.136	1.106
147 24	F3 S	0.6026	1.109	(0.018)	0.997	0.993	1.098	(0.020)
147 23	RB	0.4870	1.125		0.999	0.981	1.103	
147 22	RB	0.3947	1.116		1.002	0.976	1.091	
147 21	RB	0.3114	1.109	1.110	1.005	0.974	1.086	1.088
147 20	RB	0.2540	1.088	(0.016)	1.009	0.977	1.073	(0.012)

A CORRECTIONS WERE NOT CALCULATED IN POSITIONS 147-42 AND 147-27 .

TABLE 5.19. ZPPR-13A: TRANSPORT CORRECTED REACTION RATES FOR 238U(N,F)

MATRIX POSITION	ZONE	EXP.	REFERENCE C/E	MEAN C/E (S.D.)	CORRECTIONS A MESH	S4	CORRECTED C/E	MEAN C/E (S.D.)
147 49	CB	0.0220	0.883		1.009	0.981	0.874	
147 48	CB	0.0255	0.897		1.010	0.935	0.847	
148 47	CB	0.0289	0.919		1.014	0.940	0.876	
148 46	CB	0.0378	1.065		1.021	0.866	0.942	
148 45	CB	0.0612	1.052	0.977	1.027	0.900	0.972	0.911
148 44	CB	0.1006	1.045	(0.086)	1.010	0.904	0.954	(0.051)
147 44	F1 S	0.1421	0.948		1.001	0.997	0.946	
147 43	F1	0.2089	0.895		0.989	1.036	0.917	
147 41	F1	0.2250	0.893	0.912	0.993	1.040	0.922	0.925
147 40	F1 S	0.1666	0.911	(0.025)	1.006	0.997	0.914	(0.015)
147 39	B1	0.0951	1.054		1.034	0.881	0.960	
147 38	B1	0.0910	1.072	1.059	1.035	0.875	0.971	0.971
147 37	B1	0.1267	1.050	(0.012)	1.021	0.917	0.983	(0.012)
147 36	F2	0.2419	0.884		0.992	1.036	0.909	
147 35	F2 S	0.2397	0.946		1.005	1.024	0.974	
147 34	F2	0.2618	0.919	0.920	0.995	1.046	0.957	0.942
147 33	F2 S	0.2020	0.931	(0.026)	0.997	0.998	0.927	(0.029)
147 32	B2	0.1102	1.045		1.037	0.904	0.980	
147 31	B2	0.0846	1.118	1.090	1.029	0.843	0.970	0.992
147 30	B2	0.1028	1.106	(0.039)	1.028	0.903	1.027	(0.030)
147 29	F3	0.2050	0.919		0.987	1.026	0.931	
147 28	F3 S	0.1988	1.032		1.000	1.015	1.047	
147 26	F3 S	0.1838	1.030		1.002	1.000	1.032	
147 25	F3	0.1773	0.977	0.987	0.991	1.028	0.995	0.997
147 24	F3 S	0.1125	0.979	(0.047)	0.998	1.002	0.979	(0.046)
147 23	RB	0.0493	1.112		1.022	0.893	1.015	
147 22	RB	0.0262	1.049		1.011	0.853	0.905	
147 21	RB	0.0141	1.004	1.029	1.000	0.922	0.926	0.945
147 20	RB	0.0079	0.952	(0.068)	0.986	0.994	0.933	(0.048)

A CORRECTIONS WERE NOT CALCULATED IN POSITIONS 147-42 AND 147-27 .

6.0 ANALYSIS OF CONTROL ROD WORTHS

The initial calculations of control rod worths used homogeneous atomic densities for each cell type and β_{eff} values calculated with rz reactor models. These data are recorded in the monthly ZPR-TM reports. The analysis for ZPPR-13A has now been improved in several respects:

(i) Corrections for variations in drawer loadings as described in Section 3.5.

(ii) Use of β_{eff} results from xyz calculations.

(iii) Revisions to experimental results following improvements to the effective source ratio in the McCRUNCH code (Section 2.3.4).

This section gives an analysis of all results in ZPPR-13A together with transport-corrected values for rod banks.

The experimental control rods occupied four ZPPR matrix positions in which the drawers were filled with both clad and unclad natural B_4C platelets for the first 457 mm (core region) and with sodium-filled plates for the second 457 mm (axial blanket region). Control rod position (CRP) drawers were filled with sodium-containing plates over their 914 mm length.

All control rod worths were measured relative to fuel. A number of measurements of the worths of CRPs relative to fuel were made in 13A both for single positions and for banks.

(v) The mean C/E for the 12 rods in FR2 (1.008) agrees well with the C/E for the bank of rods (1.010) which was measured at 20$ subcritical. Similarly the mean C/E for 12 rods in FR3 (1.038) compares with a C/E of 1.044 for the rod bank.

(vi) Control rod 13', which was adjacent to the blanket in FR2, has a worth lower than for CR13, by 5% , but the C/E results agree within 0.1%.

(vii) A remarkable discrepancy of 4% exists between predictions for rod 25 on the x-axis in FR3 and rod 28 on the y-axis. About 1% of this difference may be attributed to the ZPPR interface variation. The AMM model produced some improvement-from a 6% difference to a 4% difference.

(viii) The single rod measurements that were repeated in the second series, CR13, CR25 and CR28 gave worths that were higher than in the first measurements by 0.7%, 0.4% and 1.2% respectively. Comparison of the two subcritical references shows a difference of 2¢ after adjustment for relative ^{241}Pu decay, interface separation and temperature. Thus an uncertainty of about 1% is apparent due to unknown changes in core configuration (piece positioning in drawers and precise drawer positioning in matrix).

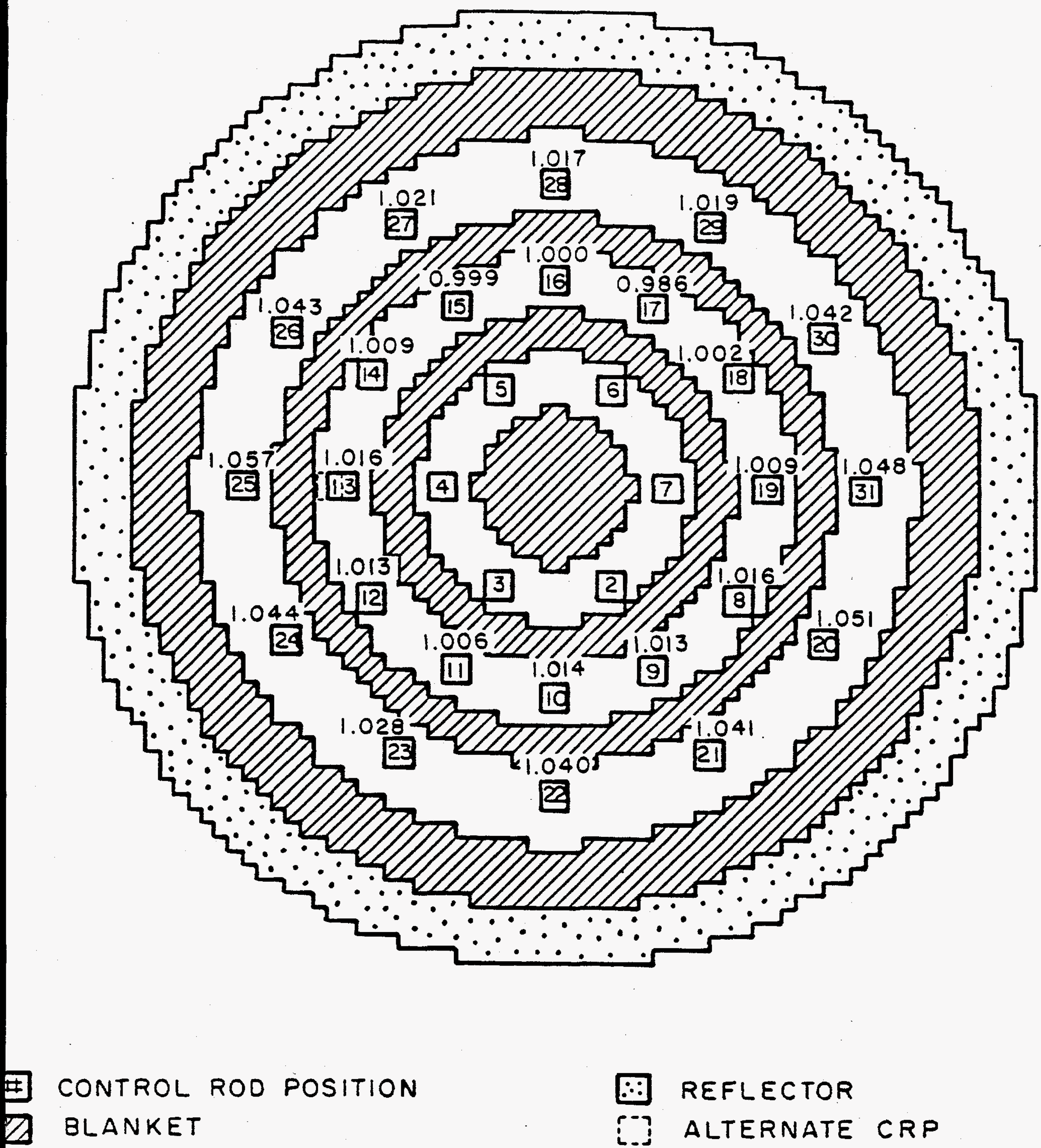

Fig. 6.1. Rod locations and C/E values for the worths of individual rods in ZPPR-13A.

TABLE 6.1. ZPPR-13A Comparison of xyz and xy Calculations for Control Rod Worths

Case	Geometry	Number of Groups	k-effective	Worth Relative to Reference, $	Error in[d] Worth, %
Reference	xyz	28	0.978324	---	---
12 CRP in F2	xyz	28	0.958703	6.349	---
12 CR in F2	xyz	28	0.919767	19.750	---
Reference[a]	xyz	8	0.979818	---	---
12 CRP in F2[a]	xyz	8	0.960103	6.360	+0.2
12 CR in F2[a]	xyz	8	0.920769	19.864	+0.6
Reference[b]	xy	8	0.979760	---	---
12 CRP in F2[b]	xy	8	0.959992	6.379	+0.5
12 CR in F2[b]	xy	8	0.920399	19.979	+1.2
6 CR in F1	xyz	28	0.961163	5.539	---
6 CR in F1[c]	xy	8	0.962359	5.601	+1.1
12 CR in F3	xyz	28	0.936091	13.996	---
12 CR in F3[c]	xy	8	0.936857	14.185	+1.4

[a]The 8 group xyz calculations used data collapsed for the reference xyz model in all zones except CRs and CRPs.

[b]The 8 group xy calculations used bucklings derived from the reference xyz model in all zones except CRs and CRPs.

[c]These calculations used the data generated for CRs in fuel zone 2 (F2).

[d]Error in worth relative to xyz calculation in 28 groups. File MR-A25

TABLE 6.2. Control Rod Worth Analysis for the First Series of Measurements in ZPPR-13A

Rods Inserted	k_{eff}[a]	Calculated Worth, $[b]	AMM Correction[c]	Measured Worth (E), $	Corrected C/E
Fuel Ring 1					
CR04	0.976385	1.071	1.010	1.097	0.986
6 CRs	0.962359	5.603	1.009	5.725	0.987
Fuel Ring 2					
CR13	0.975954	1.208	0.996	1.176	1.023
CR13'	0.976142	1.149	0.994	1.118	1.022
12 CRs	0.972077	19.984	1.004	19.869	1.010
6 CRs + 6 CRPs	0.938122	13.753	1.004	13.428	1.028
5 CRs + 7 CRPs	0.943729	11.830	1.004	11.522	1.031
Fuel Ring 3					
CR25	0.977044	0.861	0.981	0.796	1.062
CR28	0.977303	0.779	1.000	0.757	1.029
6 CRs	0.956800	7.436	0.997	7.082	1.047
12 CRs	0.936857	14.190	0.998	13.559	1.044
6 CRs + 6 CRPs	0.949957	9.721	0.998	9.095	1.067
5 CRs + 7 CRPs	0.953322	8.593	0.998	7.980	1.075

[a]Calculation 8G XY DT 1MPD WBD. k_{eff} for the reference subcritical core was 0.979760.

[b]Worth defined as $|\Delta k|/(k_1 k_2 \beta)$, with $\beta = 0.3294\%$.

[c]Correction for All-master model.

JAIIB14

TABLE 6.3. Worths of CRPs Relative to Fuel for the First Series of Measurements in ZPPR-13A

CRPs Inserted	k_{eff}[a]	Calculated Worth, $[b]	AMM Correction[c]	Measured Worth (E), $	Corrected C/E
Fuel Ring 1					
CRP04	0.978483	0.404	1.010	0.382	1.069
6 CRPs	0.973041	2.140	1.009	2.013	1.072
Fuel Ring 2					
CRP13	0.978145	0.512	0.996	0.449	1.135
CRP13'	0.978188	0.498	0.994	0.449	1.103
12 CRPs	0.959992	6.381	1.004	5.739	1.116
Fuel Ring 3					
CRP25	0.978566	0.378	0.981	0.313	1.185
12 CRPs	0.965200	4.674	0.998	4.079	1.144

[a]Calculation 8G XY DT 1MPD WBD. k_{eff} for the reference subcritical core was 0.979760.

[b]Worth defined as $|\Delta k|/(k_1 k_2 \beta)$, with $\beta = 0.3294\%$.

[c]Correction for All-master model.

JAIIB15

TABLE 6.4 Single Control Rod Worths for the Second Series of Measurements in ZPPR-13A

Control Rod	k_{eff}[a]	Calculated Worth, $[b]	AMM Correction[c]	Measured Worth (E), $	Corrected C/E
Fuel Ring 2					
CR08	0.976087	1.166	1.007	1.156	1.016
CR09	0.976119	1.156	1.006	1.148	1.013
CR10	0.976157	1.144	1.002	1.130	1.014
CR11	(CR09)	1.156	0.998	1.147	1.006
CR12	(CR08)	1.166	0.997	1.148	1.013
CR13	0.975954	1.208	0.996	1.184	1.016
CR14	(CR08)	1.166	1.003	1.159	1.009
CR15	(CR09)	1.156	1.006	1.164	0.999
CR16	(CR10)	1.144	1.009	1.154	1.000
CR17	(CR09)	1.156	1.012	1.174	0.996
CR18	(CR08)	1.166	1.010	1.175	1.002
CR19	(CR13)	1.208	1.003	1.201	1.009
Mean C/E for 12 control rods					1.008
S.D.					0.007
Fuel Ring 3					
CR20	0.977139	0.831	1.004	0.794	1.051
CR21	0.977233	0.801	1.006	0.774	1.041
CR22	0.977303	0.779	0.995	0.745	1.040
CR23	(CR21)	0.801	0.991	0.772	1.028
CR24	(CR20)	0.831	0.991	0.789	1.044
CR25	0.977044	0.861	0.981	0.799	1.057
CR26	(CR20)	0.831	0.997	0.794	1.043
CR27	(CR21)	0.801	1.001	0.785	1.021
CR28	(CR22)	0.779	1.000	0.766	1.017
CR29	(CR21)	0.801	1.011	0.795	1.019
CR30	(CR20)	0.831	1.004	0.801	1.042
CR31	(CR25)	0.861	0.990	0.813	1.048
Mean C/E for 12 control rods.					1.038
S.D.					0.013

[a]Calculation 8G XY DT 1MPD WBD. k_{eff} for the reference subcritical core was 0.979760.

[b]Worth defined as $|\Delta k|/(k_1 k_2 \beta)$, with $\beta = 0.3294\%$.

[c]Correction for All-master model.

JAIIB16

TABLE 6.5. Comparison of C/E Results for Single Control Rods in Left and Right Sides of ZPPR-13A

Rod Pair	Ratio of C/E on RHS to C/E on LHS			
	Reference Model	Narrow Drawers	Narrow Drawers + Blanket Detectors	All Masters
Fuel Zone 2				
15, 17	0.989	1.002	0.996	0.997
14, 18	0.984	1.003	0.995	0.993
13, 19	0.985	1.005	0.992	0.993
12, 8	0.993	1.012	1.010	1.003
11, 9	0.999	1.010	1.008	1.007
Fuel Zone 3				
27, 29	0.986	1.002	0.996	0.998
26, 30	0.990	1.011	1.003	0.999
25, 31	0.982	1.001	0.995	0.991
24, 20	0.992	1.013	1.008	1.007
23, 21	0.998	1.014	1.010	1.013
Mean	0.990	1.007	1.001	1.000
σ	0.006	0.005	0.007	0.007

JAIIB17

TABLE 6.11. Comparison of Control Rod Worths in ZPPR-13A

Control Rods	Assembly	Measured Worth, $	C/E[b]	Change in Worth, %
Fuel Ring 1				
6 CRs[a]	13A	5.73	0.987	---
Fuel Ring 2				
CR 16	13A	1.15	1.000	---
12 CRs	13A	19.87	1.010	---
Fuel Ring 3				
CR 25[c]	13A	0.798	1.060	---
CR 28[c]	13A	0.762	1.023	---
6 CRs (odd)	13A	7.08	1.047	---
6CRs (even)				
12 CRs	13A	13.56	1.044	---

[a]The inner ring rods were rotated by 30° in ZPPR-13B/1 relative to ZPPR-13A to align with blanket-ring gaps.

[b]Reference diffusion calculations, 8 groups, xy geometry.

[c]Control rod 25 is on the x-axis and control rod 28 is on the y-axis (in line with blanket-ring gaps). These rods were measured twice in ZPPR-13A and the mean result is used.

JAIIB23

6.3 Control Rod Interactions

The worths of rod banks in ZPPR-13A are compared with the sums of the individual rod worths in Table 6.12. The normalized interaction obtained by dividing by the average of the single rod worths is useful for comparison between different rings and between different cores. The normalized interaction of 37%/$ in FR2 is well predicted. Interaction of 56%/$ for 12 rods in FR3 and of 63%/$ for 6 rods in FR3 are overpredicted by 2% and 3%.

TABLE 6.12. Control Rod Interaction Effects in ZPPR-13A

	E[a]	C	C/E
Fuel Ring 2			
Worth of bank of 12 rods,$	19.869	20.064	1.010
Sum of individual rod worths,$	13.940	14.049	1.008
Interaction, %	42.5	42.8	1.007
Normalized interaction, %/$[b]	36.6	36.6	
Fuel Ring 3			
Worth of bank of 12 rods,$	13.559	14.162	1.044
Sum of individual rod worths,$	9.427	9.783	1.038
Interaction, %	43.8	44.8	1.023
Normalized interaction, %/$	55.8	54.9	
Worth of bank of 6 rods,$	7.082	7.414	1.047
Sum of individual rods,$	4.738	4.908	1.036
Interaction, %	49.5	51.1	1.032
Normalized interaction, %/$	62.7	62.4	

[a]The rod bank worths were measured in the first series and the individual rods in the second series. There are indications of a systematic difference between the results from the two series of about 0.7% (see text).

[b]Using the mean worth of a single rod in the bank. JAIIB25

6.4 Transport Calculations

Transport calculations have been made for rod banks in each of the three fuel rings in ZPPR-13A Transport calculations require a finer mesh than the 55 mm (1MPD) used in the reference diffusion calculations. The diffusion calculations were repeated with the number of mesh points doubled (4MPD). Calculations were then made with the S_4 transport option of DIF3D. Since the S_4 calculations used isotropic diffusions (NBD), the diffusion theory calculations were also repeated with this method. Results of these calculations are shown in Table 6.15.

For ZPPR-13A the effects of a finer mesh and higher order quadrature were investigated in a one-dimensional r model using the 1DANT code. This model, shown schematically in Fig. 6.4, modelled control-rod banks as annular regions. The rod-bank worths do not match those of the xy model very closely, as shown in Table 6.18, but transport corrections are similar. Table 6.19 shows the effects of S_{16} quadrature and fine mesh which are less than 0.5%.

The mesh and transport corrections are of opposite signs, but compensate one another to different degrees as a function of rod radius and blanket arrangement. In ZPPR-13A, the mesh and transport corrections increase the radial discrepancy between FR1 and FR3 by 2%,

Streaming effects are included in the reference calculations, but their effect can be seen from Table 6.15 These improve the results for the relative bank worths between FR1 and FR3 by 2% in 13A

Table 6.20 show the corrected results for the rod banks. The tables include corrections to 28 group xyz calculations for Table 6.14 to 6.15. The following conclusions are noted:

(i) For ZPPR-13A the corrected C/E results are 0.980 (FR1), 1.011 (FR2) and 1.059 (FR3). The discrepancy between the inner and outer rod positions is 8%.

Zone		Radius (cm)	Standard Calculation: Number of Intervals	Standard Calculation: Mesh Spacing (cm)	Fine Mesh Calculation: Number of Intervals	Fine Mesh Calculation: Mesh Spacing (cm)
	℄	0.0				
(inner)	Center Blanket	20.6750	8	2.5844	16	1.2922
(outer)		30.5390	4	2.4660	8	1.2330
	Fuel	43.1132	6	2.0957	12	1.0479
(CR) *	Ring 1	45.7373	2	1.3121	4	0.6561
		53.9860	4	2.0622	8	1.0311
	Blanket Ring 1					
		69.6950	6	2.6182	8	1.3091
	Fuel	81.5168	4	2.9555	8	1.4778
(CR) *	Ring 2	84.3286	2	1.4059	4	0.7030
		94.1270	4	2.4496	8	1.2248
	Blanket Ring 2					
		109.0460	6	2.4865	12	1.2433
	Fuel	120.4072	6	1.8935	12	0.9468
(CR) *	Ring 3	122.3282	2	0.9605	4	0.4803
- - - - -		125.6060	2	1.6389	4	0.8195
		141.0530	8	1.9309	16	0.9655
(inner)	Radial Blanket	154.7170	6	2.2773	12	1.1387
(outer)		166.4540	6	1.9562	12	0.9781
	Radial Reflector	189.4890	8	2.8794	16	1.4397
	Matrix	205.0	4	3.8778	8	1.9389

(*)(CR): fuel, CR absorber or CRP compositions.

Fig. 6.4. One-dimensional Model for Study of Higher-order Transport Effects in ZPPR-13A.

XA-8

TABLE 6.15. ZPPR-13A: Comparison of Diffusion and Transport Calculations for Control Rod Worths

Configuration[a]	Calculation[b]					k-effective	Worth, \$[c]
Reference	xy	8G	DT	1MPD	WBD	0.979760	---
	xy	8G	DT	4MPD	WBD	0.978267	---
	xy	8G	DT	4MPD	NBD	0.979207	---
	xy	8G	S4	4MPD	NBD	0.986457	---
	xyz	28G	DT	1MPD	WBD	0.978324	---
6 CRs in F1	xy	8G	DT	1MPD	WBD	0.962359	5.601
	xy	8G	DT	4MPD	WBD	0.960088	5.873
	xy	8G	DT	4MPD	NBD	0.961348	5.748
	xy	8G	S4	4MPD	NBD	0.969135	5.499
	xyz	28G	DT	1MPD	WBD	0.961163	5.539
12 CRs in F2	xy	8G	DT	1MPD	WBD	0.920399	19.979
	xy	8G	DT	4MPD	WBD	0.915917	21.119
	xy	8G	DT	4MPD	NBD	0.917450	20.862
	xy	8G	S4	4MPD	NBD	0.926485	19.915
	xyz	28G	DT	1MPD	WBD	0.920769	19.864
12 CRs in F3	xy	8G	DT	1MPD	WBD	0.936857	14.185
	xy	8G	DT	4MPD	WBD	0.933642	14.828
	xy	8G	DT	4MPD	NBD	0.934578	14.801
	xy	8G	S4	4MPD	NBD	0.941992	14.522
	xyz	28G	DT	1MPD	WBD	0.936091	13.996

[a]Subcritical reference, 6 CRs in F1 means six control rods in fuel zone one, etc.

[b]xy means two dimensional xy geometry model with group dependent axial buckling terms. (xyz means three dimensional xyz geometry). All calculations were made in quarter core model without inclusion of blanket narrow drawers in the model.

8G = eight energy groups, 28G = twenty-eight energy groups
DT = diffusion theory, S4 = transport theory with S4 quadrature
1MPD = one mesh per matrix area (55 mm spacing)
4MPD = four meshes per matrix area
WBD = with Benoist Diffusion coefficient
NBD = Isotropic diffusion coefficients

[c]Worth relative to fuel (reference), using β_{eff} = 0.003314.JAIIB29

TABLE 6.18. Comparison of Transport Corrections in xy and r-geometry for ZPPR-13A Control Rod Banks

	xy Model		r Model	
Rod Bank	Transport (S_4) Worth, $	Worth Ratio[a] S4/DT	Transport (S_4) Worth, $	Worth Ratio[a] S4/DT
6 CRs F1	1.81	0.955	1.93	0.968
12 CRs F2	6.56	0.955	7.26	0.965
12 CRs F3	4.79	0.981	5.76	0.979

[a]DT = diffusion theory calculation using the same mesh as in the transport S_4 calculation.

MR2-A22

TABLE 6.19. Higher Order Quadrature and Fine Mesh Effects for Control Rod Worths in ZPPR-13A

	Ratio of Worths		
Rod Bank	S_{16}/S_4[a]	Fine Mesh/ Standard Mesh[b]	Combined S_{16} and Fine Mesh
6 CRs F1	0.998	0.999	0.997
12 CRs F2	0.997	0.997	0.994
12 CRs F3	0.996	0.995	0.991

[a]With standard mesh.

[b]With S_{16} quadrature.

MR2-A22

TABLE 6.20. The Effect of Calculational Improvements on Control Rod Worth C/E Values in ZPPR-13A

	6 CRs in FR1	12 CRs in FR2	12 CRs in FR3
Measured Worth ($)	5.725	19.869	13.559
Reference Model C/E[a]	0.979	1.006	1.047
Model Improvement		**Correction, %**	
All master correction[b]	+0.9	+0.4	-0.2
Mesh[c]	+4.8	+5.7	+4.5
Transport (S4) in xy[d]	-4.5	-4.5	-1.9
Groups, Geometry and Method[e]	-1.1	-1.1	-1.3
Total	+0.1	+0.5	+1.1
Corrected C/E	0.980	1.011	1.059

[a]8 group diffusion theory calculation in xy geometry in one mesh per ZPPR drawer (1MPD) using anisotropic diffusion coefficients. β_{eff} = 0.3294%.

[b]Comparison of full-plan xy model including all drawer masters with the reference homogenized-master model.

[c]Correction from 1MPD to four meshes per drawer (4MPD).

[d]S_4 calculation made with 4MPD.

[e]Comparison of 28 group xyz calculations with reference results. JAII2A2

7.0 SODIUM-VOID REACTIVITY

Zone sodium-voiding experiments were done in phases 13A

7.1 ZPPR-13A

The ZPPR-13A sodium-void experiments were designed principally to provide tests of calculated radial variations, which in the heterogeneous design include complex leakage effects between the fuel and blanket zones. Annular sectors in each fuel zone were voided of sodium over a length of 305 mm (12 in.) on each side of the midplane, with the outer fuel zone (F3) being voided in two radial segments. Symmetric void zones were introduced on each side of the core to permit analysis with a one-eighth core model of the assembly. The sectors in the inner fuel zone (F1) were voided in two steps, ±203 mm (8 in.) and ±305 mm from the midplane. In addition, the entire fuel zone 1 was voided (±305 mm) in order to compare with results from the sectors and also to permit analysis with an rz model for investigation of transport corrections. Following voiding of the fuel zones, contiguous sectors in the two internal blanket zones were voided over a height of ±203 mm. In the last step in the series, sodium was replaced in zone 1 (±203 mm) with the other six zones remaining in the voided condition. This experiment has been variously described as an "inverse voiding" or a "reflood".

The reactor configuration at the start of the voiding sequence is shown in Fig. 7.1. This configuration differed from the reference critical configuration by the replacement of double-column fuel drawers with single-column fuel drawers in locations 1,242-26; 1,255-26; 1,242-73; 1,255-73; 1,246-73; 1,251-73; 1,246-26; 1,251-26; 1,245-56; 1,252-56; 1,245-43; 1,252-43; 1,242-43; 1,255-43; 1,242-56; and 1,255-56. This configuration was 81¢ subcritical.

In the first voiding step, sodium was removed from the first 8 in. of each half in zone 1. In the second step, the axial half height of the void was increased to 12 in. In all subsequent steps in fuel zones, the axial extent of the voids was $\pm$ 12 in. In the blanket zones, the axial extent of the voids was $\pm$ 8 in. Differences between the lengths of sodium-containing cans in the fuel and blanket regions prompted the decision to have the difference in the axial extent of the voids. All steps were cumulative.

The results of the various voiding steps are presented in Table 7.1. All worth determinations were made using the 64 in-core fission counters and the subcritical-source-multiplication technique. The subcritical-source-multiplication measurements were calibrated by making a rod-drop reactivity measurement after voiding zone 7. With all seven zones voided, the reactor was 12¢ subcritical.

There were only two reflood steps. In the first step sodium was added back $\pm$8 in. in zone 1. All the remaining sodium was added back in the second step and the final subcriticality was 78¢. There is a discrepancy of 3¢ in subcriticality between the nominally equivalent configurations before voiding and after reflooding. The source of this discrepancy is not presently known, but the values for the step worths shown in Table 7.1 should still be used as the experiment values.

The uncertainties in the cumulative worths and in the step worths given in Table 7.1 were obtained by combining a 0.2¢ random uncertainty in any reactivity difference due to temperature and table-closure corrections with a 0.8% correlated uncertainty due to detector calibration. The uncertainty in the step worth per kg sodium removed was obtained from the uncertainty in the step worth and a 1% random uncertainty in sodium mass. Uncertainties due to counting statistics are very small compared to other uncertainties and are not included.

The change in steel mass was small for each step and its effect is included in the step worth.

The calculation methods used for analysis in ZPPR-13A are similar to those employed in previous calculations for heterogeneous cores. Processing of the ENDF/B-IV cross section for unit cell heterogeneity with the SDX code used impressed zone- and group-dependent bucklings which were obtained from the zone leakages in prior xyz calculations. For the reference core, these data were the same as those employed for the analysis of reaction rates described earlier. Cross sections for the voided cells were generated by the same method. The bucklings in this case were derived from a second xyz calculation in which all seven zones were voided. Separate macroscopic cross sections were thus produced for single-column and double-column fuel drawers in each of the three fuel zones. A single set of cross sections was used for the internal blanket zones.

An approximate treatment of streaming in the unit cells was included using the Benoist definition of anisotropic diffusion coefficients. Divergence of the diffusion coefficients in the voided region was avoided by smearing of the sodium plate claddings over the total plate thickness. This procedure is consistent with previous sodium-void analysis at ZPPR. However, in contrast to previous applications, for ZPPR-13A we have used the ratios D(Benoist)/ D(heterogeneous) as "diffusion coefficient modifiers" in the DIF3D code. This procedure corrects for the prescription of diffusion coefficients for the heterogeneous cell that is used in the SDX code, in addition to treating plate-cell streaming effects. Previous calculations used the ratio D(Benoist)/ D(homogeneous) in order to provide numerical values for the streaming effects themselves. Test calculations were run for the combined voiding steps 1 and 2 and for step 5 in order to determine the effect of the change in the definition of the ratio. Negligible differences of less than 1% were found for the void reactivities using different definitions, although the diffusion coefficient modifiers differ appreciably in some energy groups.

The calculated void reactivities were obtained with an exact perturbation method using an xyz model with 28 group data. Following a calculation of the real flux for the subcritical reference core, an adjoint calculation was made for each of the void steps that were measured. The traditional "non-leakage" and "leakage terms" were obtained using the VARI3D perturbation code. The worths, in dollars, were defined as $\Delta k/(k_1 k_2 \beta)$, where 1 and 2 refer to the reference and perturbed states, respectively. The value of β_{eff} (0.3295%) was calculated using ENDF/B-V delayed neutron data and an rz model of the reference core. In the experiments, the detector drawers and drawers opposite detectors were not voided of sodium. Due to the asymmetric location of the detectors, those drawers were voided in the calculational model. The calculated results are given in Table 7.2. When comparing the calculated vs. experimental results, this difference was taken into account by normalizing to the mass of sodium that was removed.

The calculated and measured results for the ZPPR-13A sodium-void experiments were processed through the same data analysis code that was used for previous experiments.(15) The calculated reactivity of each step was split into a negative and a positive term; i.e., the sum of the leakage components and the sum of the non-leakage (reaction) components. Through a non-linear fitting procedure, separate leakage and non-leakage bias factors and their covariance matrix were determined. These factors are 0.94 for both terms when only the core void steps are included. Including the blanket void steps reduces the factors to 0.92. These are the factors by which one would multiply the leakage and non-leakage components of a calculated void reactivity in an LMFBR similar to ZPPR-13A, in order to improve the reactivity prediction.

The data were combined with data from smaller heterogeneous assemblies reported in Ref. 15 and the bias factors were re-fit. A leakage bias factor of 0.90 and a non-leakage bias factor of 0.94 were obtained. These are similar to the results reported in Ref. 15.

Table 7.3 compares the calculated (C) and biased calculated (P) results with the measured results (E). Also given are the 1σ uncertainties in the P/E ratios, where the covariance in the bias factors makes the principal contribution. In the fitting process, it is assumed that the approximate calculation procedures introduce net errors that are random on average over many regions of the reactor. Starting with only the contribution from the experimental errors, the covariance matrix is adjusted until a χ^2 test indicates that a reasonable fit is obtained. Note that six of the P/E values in Table 7.3 fall within 1σ of 1.0, and the other two values are within 2σ, even though the range of experimental results includes variations of more than an order of magnitude as well as a change in sign. Nevertheless, errors in the predictions are only about 6% for the major positive void steps.

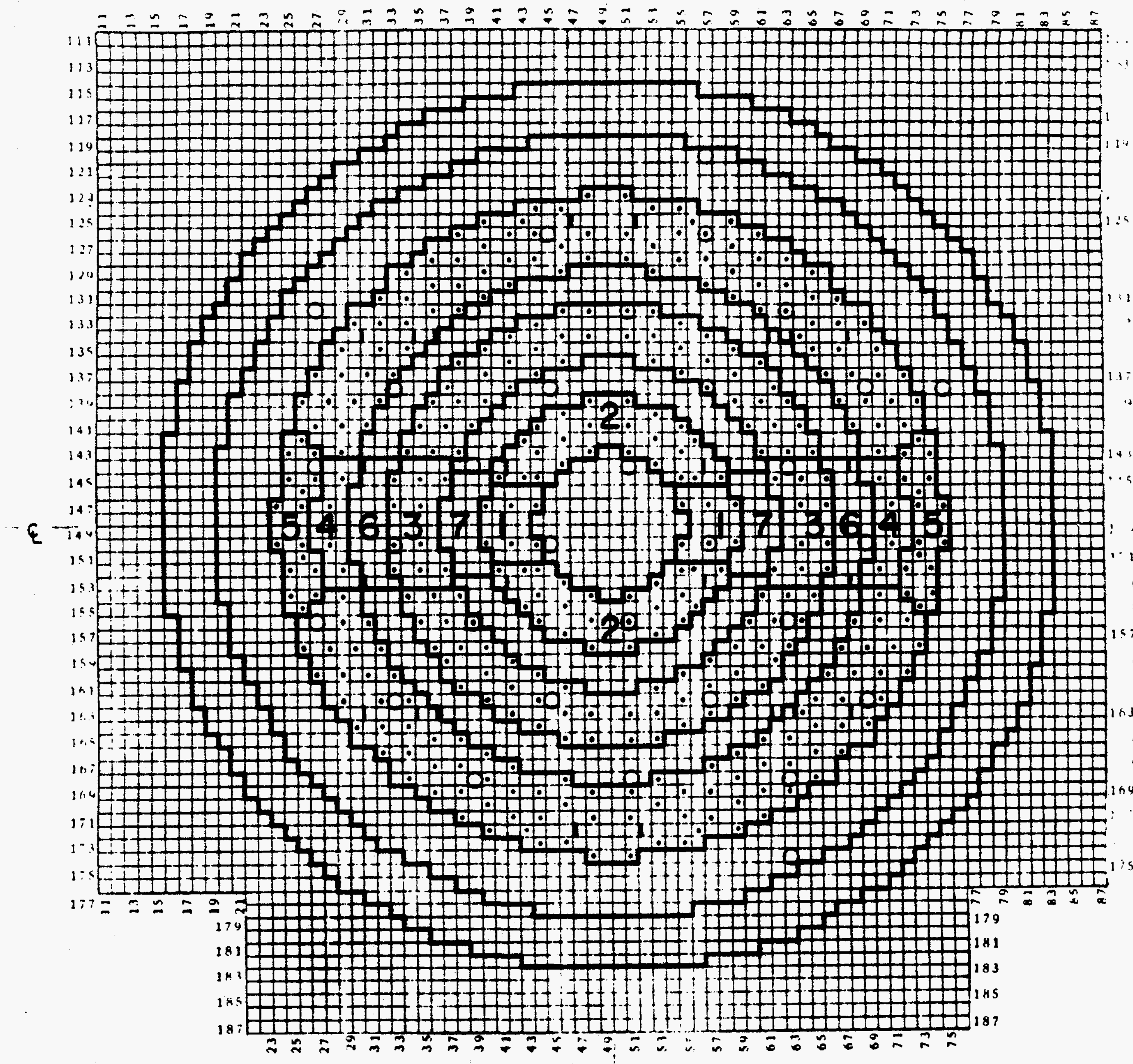

Fig. 7.1. Interface diagram showing the reference configuration for the sodium-voiding experiments and showing the voiding zones in ZPPR-13A. Half 1.

TABLE 7.1. ZPPR-13A Sodium-void Zone Measurement Results

Zone	Height, cm	Mass of Na in Step, kg	Mass of Steel Added in Step, kg	Cumulative Worth, ¢	Step Worth, ¢	Step Worth, ¢/kg Na
1 void	± 20.3	21.82	0.26	7.06 ± 0.21	7.06 ± 0.21	0.324 ± 0.010
1 void	± 20.3- ± 30.5	10.65	0.27	7.68 ± 0.21	0.62 ± 0.20	0.058 ± 0.019
2 void	± 30.5	93.46	1.23	35.75 ± 0.35	28.07 ± 0.30	0.300 ± 0.004
3 void	± 30.5	54.14	0.95	53.88 ± 0.48	18.13 ± 0.25	0.335 ± 0.005
4 void	± 30.5	34.28	0.70	63.36 ± 0.54	9.48 ± 0.21	0.276 ± 0.007
5 void	± 30.5	50.10	0.79	51.94 ± 0.46	-11.42 ± 0.22	-0.228 ± 0.005
6 void	± 20.3	10.85	0.20	61.18 ± 0.53	9.24 ± 0.21	0.852 ± 0.020
7 void	± 20.3	9.45	0.16	69.31 ± 0.59	8.13 ± 0.21	0.860 ± 0.024
1 reflood	± 20.3	21.81	-0.30	60.88 ± 0.53	-8.43 ± 0.21	-0.387 ± 0.008

EA-9

TABLE 7.2. Calculated Sodium-void Reactivity in ZPPR-13A

Step/ Zone[a]	Voided[b] Region, mm	Na Mass, kg/Step	k_{eff}	Worth Components,[c] ¢/kg: Leakage x	Leakage y	Leakage z	Leakage Sum	Non-Leakage	Net	C/E
Reference	---	---	0.975876	---	---	---	---	---	---	---
1/1	203	21.90	0.976104	-0.095	-0.011	-0.050	-0.156	0.491	0.335	1.03
2/1	203-305	10.28	0.976125	-0.069	-0.008	-0.234	-0.311	0.374	0.063	1.09
3/2	305	96.15	0.977017	-0.018	-0.057	-0.107	-0.182	0.477	0.295	0.98
4/3	305	55.51	0.977643	-0.106	-0.007	-0.158	-0.271	0.630	0.359	1.07
5/4	305	35.26	0.978010	-0.013	-0.003	-0.133	-0.149	0.477	0.331	1.20
6/5	305	50.68	0.977632	-0.419	-0.021	-0.078	-0.518	0.281	-0.237	1.04
7/6	203	11.01	0.977970	-0.060	-0.004	-0.048	-0.112	1.084	0.972	1.14
8/7	203	9.94	0.978249	-0.071	-0.005	-0.045	-0.121	1.059	0.938	1.09
9/1[d]	(203)	(21.90)	0.977982	0.092	0.011	0.059	0.162	-0.507	-0.345	0.89

[a]The calculations followed the experimental sequence of steps. Refer to Figs. 7.1 and 7.2.

[b]Relative to midplane, depth into each half of the reactor.

[c]β_{eff} = 0.003295.

[d]In step 9, Na was re-inserted with all other zones voided.

JAI12B25

TABLE 7.3. Comparison of Calculated and Measured Results for the ZPPR-13A Sodium-void Reactivity Experiments

Step[a]	Measured Worth, ¢/kg	C/E	P/E[b]	σ(P/E)
1	0.324 ± 0.010	1.034	0.949	0.067
2	0.058 ± 0.019	1.086	0.985	0.465
3	0.300 ± 0.004	0.983	0.902	0.065
4	0.335 ± 0.005	1.072	0.982	0.078
5	0.276 ± 0.007	1.198	1.099	0.074
6	-0.228 ± 0.005	1.039	0.960	0.125
7	0.852 ± 0.002	1.141	1.048	0.057
8	0.860 ± 0.024	1.091	1.001	0.057

[a]Refer to Figs. 8.1 and 8.2.

[b]Calculation adjusted by bias factors for leakage and non-leakage terms. MR-A20

8.0 ANALYSIS OF ^{238}U REACTIVITY DOPPLER MEASUREMENTS IN ZPPR-13A

The calculation of Doppler worth for the sample is based on first order perturbation theory. The sample is explicitly modelled in the reactor calculation and, the perturbation is defined as the change from reference temperature to elevated temperature cross sections for the sample. In order to normalize the perturbation denominator and integrate over sample length, the axial flux shape is represented as $\phi(xyz) = \phi(xy) \cos B_z$, where B_z is a constant buckling value chosen so that an xy calculation with constant buckling gives the same k_{eff} as the reference case with group- and region-dependent values.

Preparation of the Doppler sample cross section data is based on a pin cell model. A two region pin cell consisting of the Doppler sample at the center surrounded by structural steel, is processed in MC^2-II/SDX for each temperature to produce resonance self-shielded cross sections in an intermediate (156) group structure. For group collapse to the 28 group level, a diffusion calculation is done for a one-dimensional cylindrical model consisting of sample, structure and reactor core. Cross sections are collapsed for each sample temperature.

The core configuration was that of the ZPPR-13A critical reference with the Doppler mechanism and an additional fuel "spike" inserted. Both of these were included in the calculational model. The axial bucklings were derived from the xyz diffusion calculation for the reference core, and anisotropic diffusion coefficients were used. The ZPPR shim rods were not modelled.

The measurements were performed near the center of fuel rings one and two, and toward the outer edge of fuel ring three, the latter dictated by available locations. The experimental values reported here differ slightly from those reported earlier[16] because of adjustment to nominal temperatures for comparison with calculation. The adjustment is accomplished by means of a power-law fit.

The comparison between experiment and calculation for the Doppler reactivity is shown in Table 8.1. The mean C/E results of 0.84, 0.88 and 1.11 in the three fuel rings show the general variation with radius expected from analysis of other parameters. Sample worth data at the reference temperature are presented in Table 8.2. Again, the C/E values have the expected radial variation.

The radial variation of the reactivity Doppler C/E was found to follow the square of the $^{238}U(n,\gamma)$ C/E in ZPPR-11. The ratio of Doppler C/E to the square of the reaction rate C/E was found to be 0.732 ± 0.033 for ZPPR-11B, and 0.738 ± 0.017 for ZPPR-11C. The same analysis for the ZPPR-13A data yields the results shown in Table 8.3. The ratios in fuel ring one (0.77) and fuel ring two (0.78) are consistent and comparable to the results in ZPPR-11.
Fuel ring three shows a significantly higher ratio which is inconsistent with the rest of the data. There are three reasons, in addition to the reaction rate comparison, why the fuel-ring three measurement is suspect. First, in installing the Doppler mechanism at that location, two shim rods had to be removed. Thus, during data acquisition, the reactor was held at power by balancing on six instead of eight shim rods. Experience with the large heterogeneous cores indicates that the resulting flux tilt could significantly influence the result. In addition, the magnitude of the measurement was very small, tending to increase the uncertainties and the flux gradient was very steep at the measurement location, introducing difficulties in modelling. In addition, there is a much larger variation in C/E values for the different temperatures in the fuel ring three measurement. For these reasons, the fuel ring three measurement is felt to be unreliable.

The C/E values in ZPPR-13A are generally comparable to those from ZPPR-11.[17] The results in ZPPR-11B were 0.77 and 0.93 in the inner and outer fuel zones. The results in ZPPR-11C (the EOC core) varied between 0.82 and 0.89. The value in fuel ring two is close to the value obtained at the center of the homogeneous ZPPR-9 core (0.935 $\pm$ 0.007).[1]

TABLE 8.1. Comparison of Measured and Calculated Doppler Reactivities for ZPPR-13A

Temperature, K	Specific Worth,[a] ¢/kg ^{238}U Experiment[b]	Specific Worth,[a] ¢/kg ^{238}U Calculation	C/E
Fuel Ring 1 (153-56)			
500	-0.0119 ± 0.0006	-0.0112	0.938 ± 0.051
650	-0.0214 ± 0.0007	-0.0172	0.803 ± 0.026
800	-0.0263 ± 0.0006	-0.0222	0.844 ± 0.019
950	-0.0312 ± 0.0006	-0.0264	0.846 ± 0.016
1100	-0.0358 ± 0.0006	-0.0299	0.835 ± 0.013
		Mean C/E	0.839 ± 0.014
Fuel Ring 2 (163-52)			
500	-0.0134 ± 0.0006	-0.0134	1.000 ± 0.045
650	-0.0228 ± 0.0006	-0.0205	0.899 ± 0.023
800	-0.0301 ± 0.0006	-0.0264	0.877 ± 0.017
950	-0.0352 ± 0.0006	-0.0314	0.892 ± 0.015
1100	-0.0410 ± 0.0006	-0.0355	0.866 ± 0.013
		Mean C/E	0.884 ± 0.012
Fuel Ring 3 (164-68)			
500	-0.0044 ± 0.0006	-0.0070	1.593 ± 0.221
800	-0.0128 ± 0.0006	-0.0138	1.077 ± 0.051
950	-0.0130 ± 0.0006	-0.0164	1.266 ± 0.060
1100	-0.0167 ± 0.0006	-0.0186	1.114 ± 0.037
		Mean C/E	1.141 ± 0.035

[a]Relative to reference temperature of 300K.

[b]Uncertainties include equal contributions from both end points and 0.0003 temperature uncertainty (equivalent to ±5K in average temperature).

JAII2B18

TABLE 8.2. Comparison of Measured and Calculated Values for ^{238}U Doppler Sample Worth in Fuel Rings of ZPPR-13A

Measurement Locations	Experiment, ¢/kg	Calculation, ¢/kg	C/E
Fuel Ring 1 (153-56)	-0.457 ± 0.001	-0.410	0.897 ± 0.002
Fuel Ring 2 (163-52)	-0.526 ± 0.001	-0.491	0.933 ± 0.002
Fuel Ring 3 (164-68)	-0.0726 ± 0.001	-0.0724	0.997 ± 0.018

TABLE 8.3. Values of Average C/E for ^{238}U Doppler Measurements Compared with Average $(C/E)^2$ for $^{238}U(n,\gamma)$ Foil Measurements in ZPPR-13A

Fuel Ring	$\overline{C/E}$ Doppler Exp.	$(\overline{C/E})^2$ $^{238}U(n,\gamma)^a$	Ratio $\frac{\text{Doppler}}{^{238}U(n,\gamma)}$
1	0.839 ± 0.014	1.084 ± 0.021	0.774 ± 0.025
2	0.884 ± 0.012	1.137 ± 0.030	0.777 ± 0.032
3	1.141 ± 0.035	1.223 ± 0.044	0.933 ± 0.047
	Mean ratio in ZPPR-11B		0.731 ± 0.033
	Mean ratio in ZPPR-11C		0.738 ± 0.017

[a]Value quoted represents the average of all foils in that zone, and is squared for comparisons with the reactivity.

JAII2B19

9.0 SMALL SAMPLE REACTIVITIES

The reactivity worths of small samples of materials were measured in ZPPR-13A using the radial and axial tube method, the long-drawer oscillator and the shim-blade oscillator. Only the results from the radial tube have been analyzed at the present time.

The calculated reactivities were obtained from xyz calculations with 28 group data and included anisotropic diffusion. Homogeneous cell compositions were used in the model (HMM) and the ZPPR shim rods were not represented. Sample-size corrections were calculated with the SARCASM code(18) as a function of position, using the xyz fluxes and adjoints.

A description of the measurements and detailed results are given in Ref. 19. A description of the samples is given in Table 9.1. The calculated and experimental results are shown in Figs. 9.1 to 9.7. The curves shown in the figures are obtained by by a least squares fitting to the fourteen calculated and measured results in the fuel zones along the x-axis traverse. The results of two fittings are shown; the first adjusts the calculated non-leakage and leakage components and the second (dashed-curve) fits to the total worth. For the fissile samples and boron, where the leakage is a small component of the total worth, the two fits are indistinguishable and the bias factor for the non-leakage component is the same as the C/E for the sample worth. For scattering samples (carbon and iron) and DU-6 (^{238}U) the two-component fit produces much improved agreement. One may speculate that some of the large adjustments to the calculated leakage in these cases (40% to 80%) may be associated with streaming effects in the sample tube.

The bias factors for non-leakage components are summarized in Table 9.2. Results for fissile samples and boron are within a few percent of those obtained in ZPPR-9 and ZPPR-10 (also shown in the table). The C/E for ^{239}Pu is 1.20.

The results for ^{235}U, samples U-6 and KSS-1 (named after one of the more illustrious members of the ZPPR analysis group), are about 3% higher. The C/E for boron is much lower at 1.06. It is difficult to draw any conclusions from the results for ^{238}U, iron and carbon because of the large adjustments required to the leakage components. Transport effects are expected to be significant in these cases, based on analysis of ^{238}U fission rates and sodium void reactivity in the heterogeneous cores.

Corrections to the radial traverses for variations in master compositions will increase calculated sample worths (at least for those with small leakage components) in fuel ring 1 relative to fuel ring 3 about 2%. It is clear from Figs. 9.1, 9.2 and 9.3 that this will give some improvement in the fit to the experimental results for the fissile samples. However, the remaining discrepancies of 5% to 10% between the fuel zones are consistent with analysis of control rod worths and reaction rates.

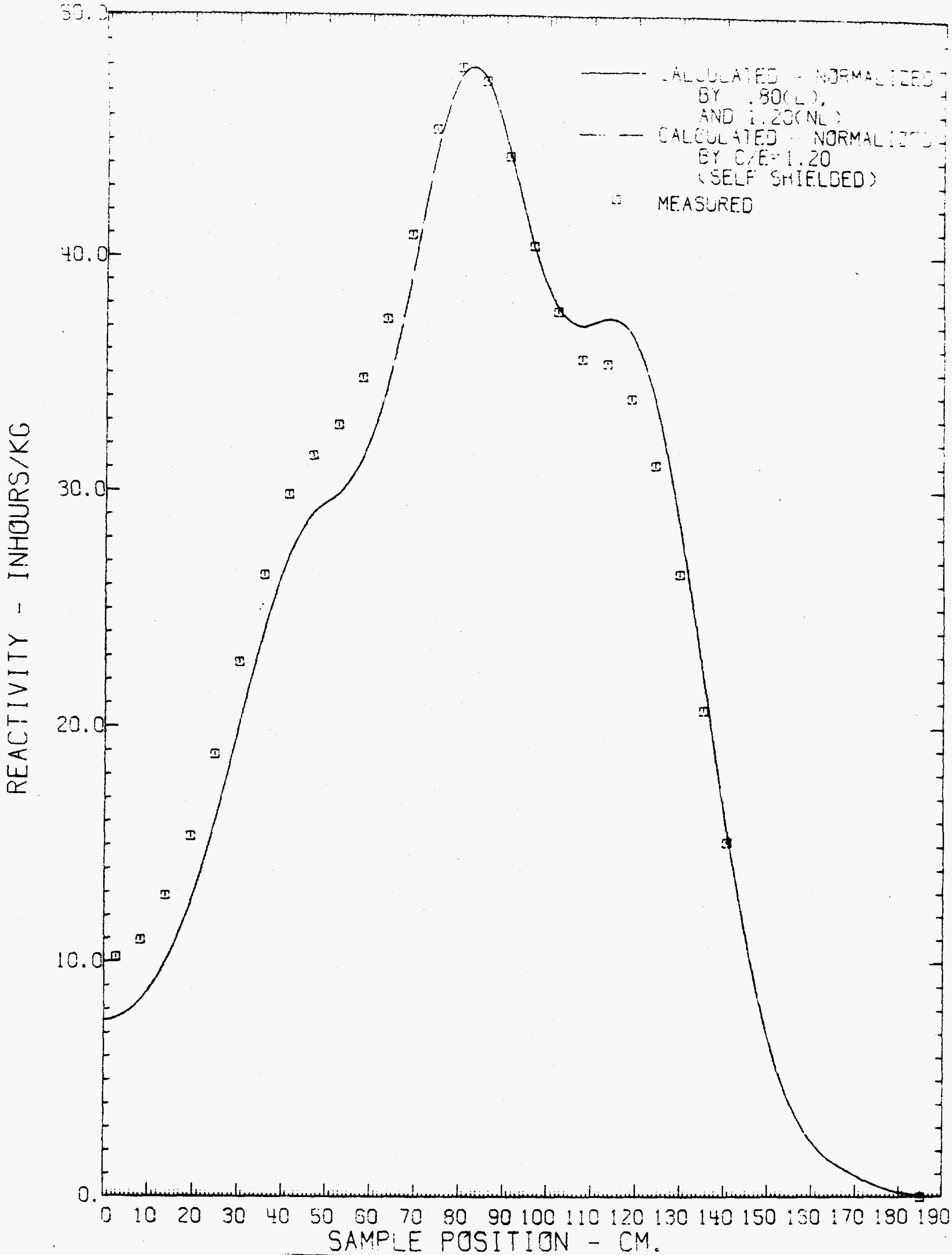

Fig. 9.1. Measured and calculated radial reactivity worth profiles for the PU-30 sample in ZPPR-13A.

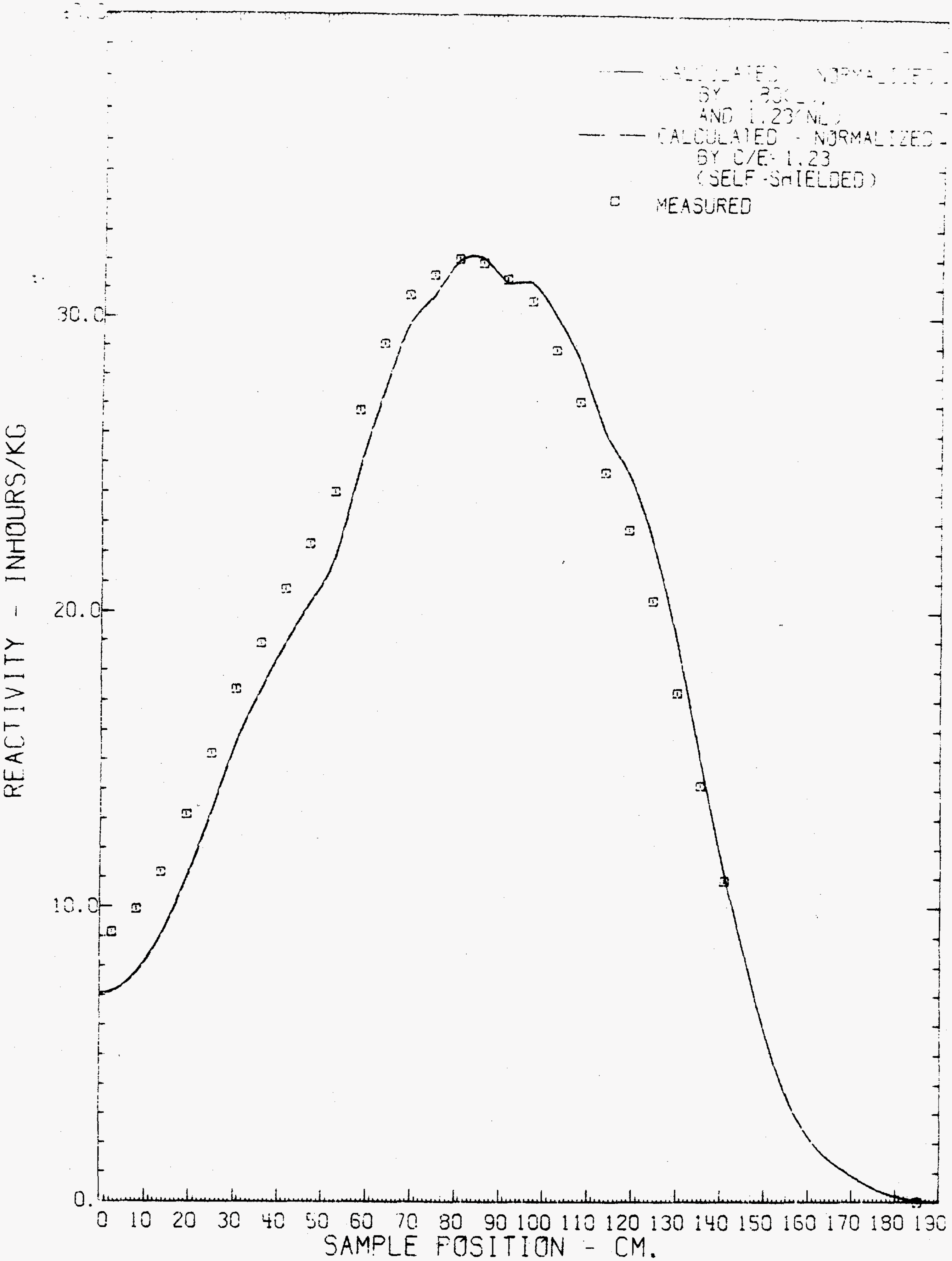

Fig. 9.2. Measured and calculated radial reactivity worth profiles for the U-6 sample in ZPPR-13A.

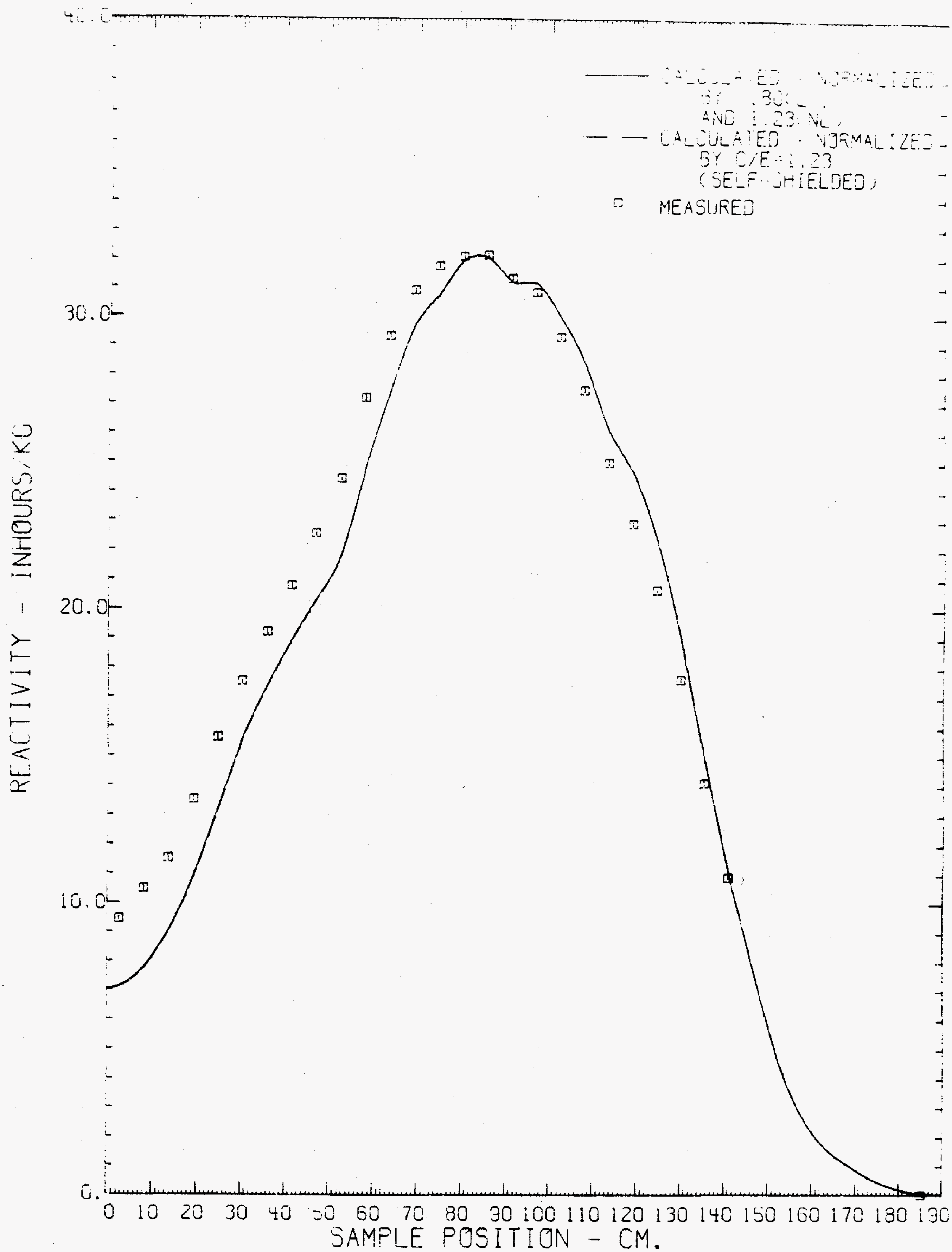

Fig. 9.3. Measured and calculated radial reactivity worth profiles for the KSS-1 sample in ZPPR-13A.

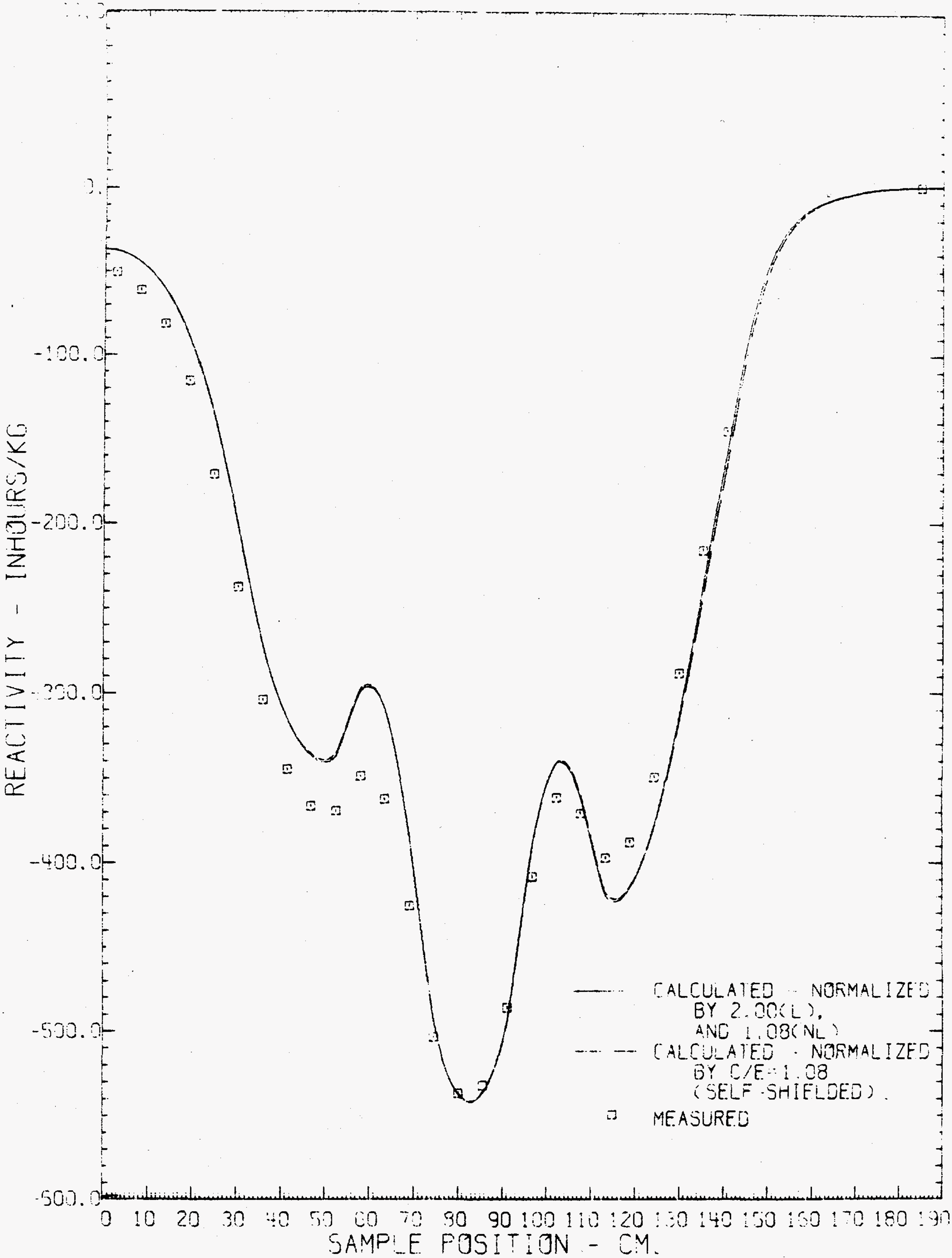

Fig. 9.4. Measured and calculated radial reactivity worth profiles for the B-1 sample in ZPPR-13A.

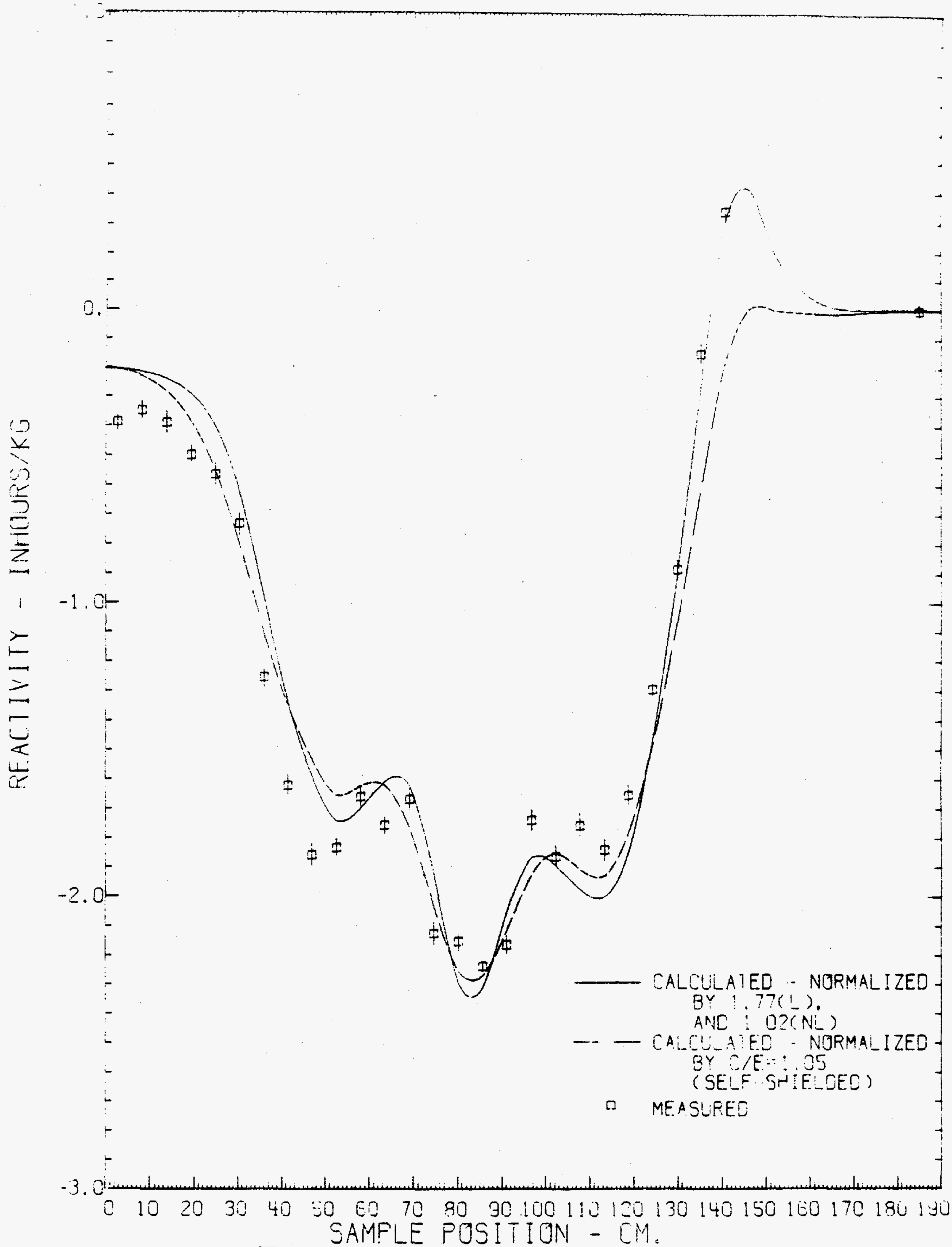

Fig. 9.5. Measured and calculated radial reactivity worth profiles for the DU-6 sample in ZPPR-13A.

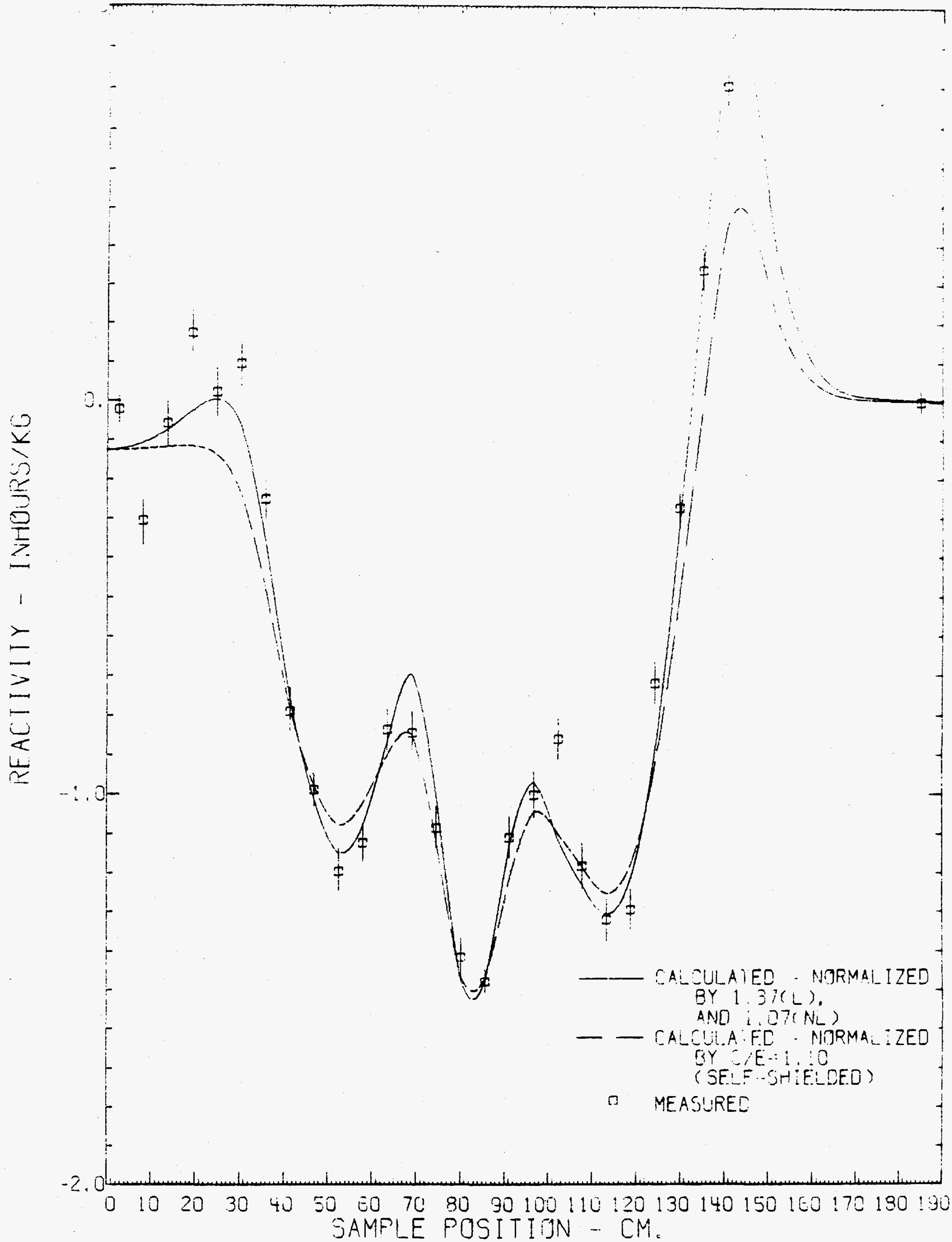

Fig. 9.6. Measured and calculated radial reactivity worth profiles for the Fe-1 sample in ZPPR-13A.

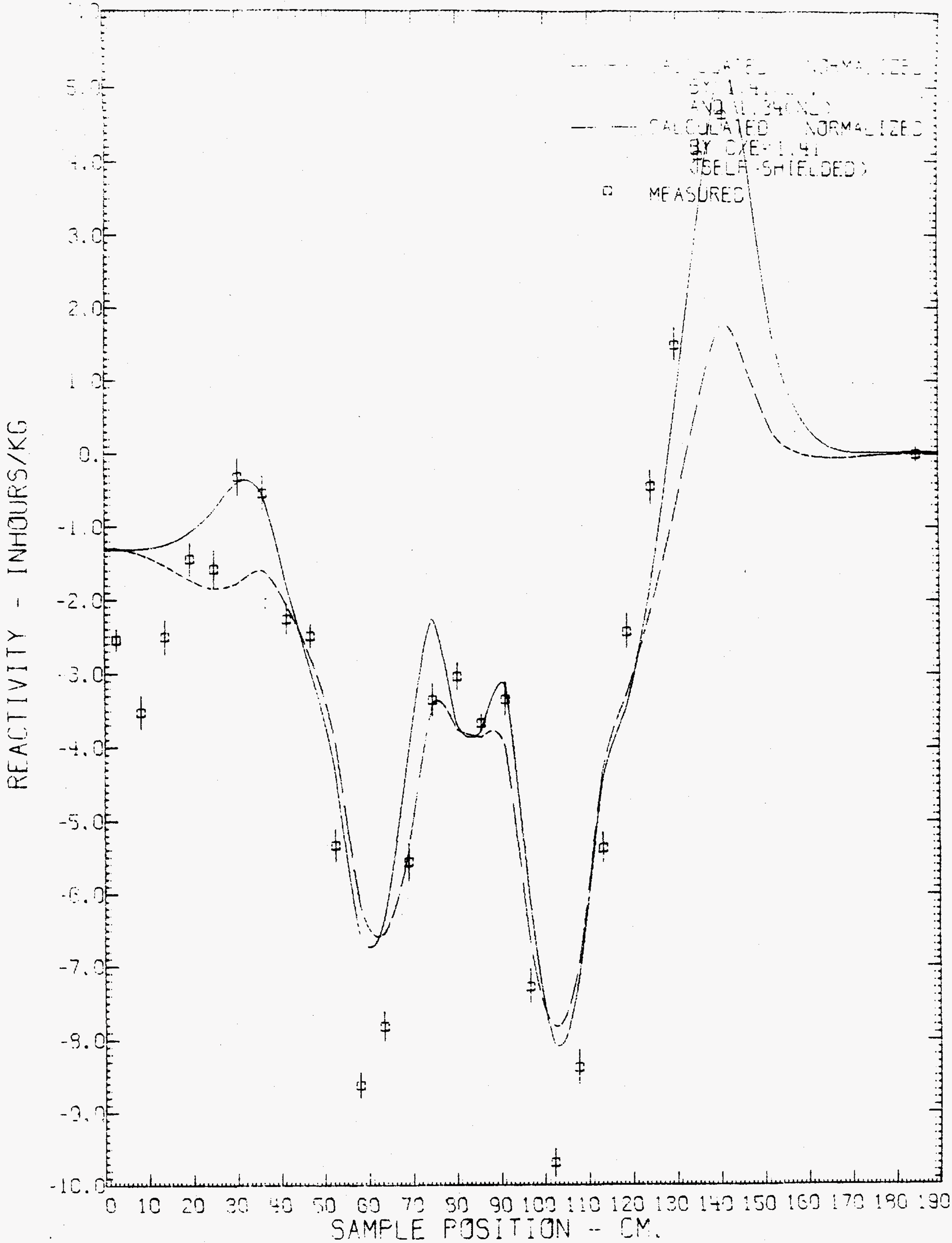

Fig. 9.7. Measured and calculated radial reactivity worth profiles for the C-1 sample in ZPPR-13A.

TABLE 9.1. Description of the Reactivity-Worth Samples Used in ZPPR-13A

Sample	Sample Dimensions, mm Length	O.D.	Sample Mass, g	Capsule Mass, g[a]	Principal Composition Component	wt. %[b]
KSS-1[c]	40.64	6.35	37.42	7.030	^{234}U	0.95
					^{235}U	93.19
					^{236}U	0.30
					^{238}U	5.57
KSS-2	48.67	10.67	---	7.005	Stainless Steel	
B-1	55.22	10.19	4.193	10.521	^{10}B	87.12
					^{11}B	7.38
					O	1.43
					C	0.96
					Si	0.26
					Al	0.05
					H	0.09
Fe-1	55.17	9.88	33.277	10.611	Fe	99.99
C-1	55.22	9.93	8.027	10.672	C	99.99
D-1	66.50	10.75	---	10.668	Stainless Steel	
Pu-30	55.19	7.62	38.091	11.600	^{239}Pu	97.20
					^{240}Pu	1.01
					^{241}Pu	0.04
					Al	0.95
U-6	55.19	7.62	46.889	11.463	^{234}U	0.95
					^{235}U	93.19
					^{236}U	0.26
					^{238}U	5.60
DU-6	55.19	7.62	47.427	11.417	^{235}U	0.21
					^{238}U	99.78
D-13	66.59	10.77	---	11.653	Stainless Steel	

[a]Material is stainless steel.

[b]Total composition less than 100% means that some impurities are not identified.

[c]The uranium in this sample is a stack of 25 foils each 0.25 mm thick fitting inside a steel cylinder.

MR3A-10

TABLE 9.2. Analysis of Reactivity Samples from Radial Traverses in ZPPR-13A and Comparison with Results from ZPPR-9 and ZPPR-10

Sample	Principal Isotope	Non-leakage Adjustment Factor[a]			
		ZPPR-13A	ZPPR-9	ZPPR-10A	ZPPR-10B
Pu-30	^{239}Pu	1.20	1.16	1.17	1.17
U-6	^{235}U	1.23	1.20	1.20	--
KSS-1	^{235}U	1.23	--	--	--
B-1	^{10}B	1.06	1.06	1.06	1.05
DU-6	^{238}U	1.05	1.14	1.14	1.13
FE-1	^{56}Fe	1.07	1.37	--	--
SS-1	(Steel)	--	1.30	1.19	--
C-1	^{12}C	1.34	--	1.55	--

[a]See figures.

JAII2B23

10.0 SUMMARY

Critical Mass

Diffusion theory calculations for ZPPR-13 give k-effective results in the range 0.976 to 0.979.

The results are within 0.2% Δk of those for the smaller heterogeneous cores, ZPPR-7 and ZPPR-11. The small differences may be due as much to changes in cross section processing methods for the unit cells as to differences in core size and configuration.

The diffusion theory k-effective values are between 0.3% Δk and 0.5% Δk lower than for conventional cores. Transport effects are larger in the heterogeneous cores and the corrected value of 0.986 for ZPPR-13A is in good agreement with ZPPR-9 and ZPPR-10.

Reaction Rate Distributions

A distinctive pattern of misprediction of reaction rates as a function of radius is found for all reactions in all cores. The C/E results in the inner zones are 3% to 5% lower than in the outer fuel zone.

The discrepancy is increased by about 0.5% with transport calculations.

Axial distributions show lower values at the top of the core, near the axial blanket interface, by about 1% relative to the core average.

Reaction Rate Ratios

The results are similar to those in all other ZPPR analysis with ENDF/B-IV data. Relative to ^{239}Pu fission, ^{235}U fission is overpredicted by 3% and ^{238}U capture is overpredicted by 6% to 9%.

Diffusion calculations for ^{238}U fission show differences of about 15% between fuel and internal blanket zones. The results are much improved by transport calculations, but a discrepancy of 5% persists in the present analyses.

Control Rod Worths

Predictions of rod worths relative to fuel vary in the range 0.98 (F1), 1.00 (F2) 1.06 (F3).

The radial variations in C/E are about twice those observed for reaction rates. Transport corrections increase the radial discrepancies.

Control rod interaction effects are well predicted with simple diffusion theory calculations.

The worths of CRPs relative to fuel are grossly overpredicted by isotropic diffusion calculations, consistent with previous analyses in other cores.

Results for rod-size, pin geometry and boron enrichment variations are consistent to within 2% using heterogeneity corrections calculated with diffusion theory. Some improvement is anticipated from transport calculations.

Sodium Void Reactivity

The diffusion theory results for zones in ZPPR-13A (C/Es in range 0.98 to 1.20) are reasonably consistent with results from other cores.

Doppler Reactivity

The C/E results in the first and second fuel rings (0.88) are fairly consistent with analyses in ZPPR-9 and ZPPR-11. The result in the the third fuel ring is singularly out of line with other data and is considered to be unreliable.

Sample Traverses

The C/E results for fissile samples of 1.2 are in line with other values from radial tube experiments. The reason for the large discrepancies compared with those from studies in the ANL "diagnostic" cores is presently unexplained and is of considerable interest. The present results for ^{238}U and scattering samples should not be treated seriously due to expectation of substantial transport corrections and possible problems due to leakage in the tube environment.

Cross Section Processing

All results obtained in ZPPR-13 are dependent on the viability of methods used to process cross sections for the cells in the complex environment of the heterogeneous criticals. At this stage it is not clear how much of the error in prediction of spatially-varying parameters is due to ENDF/B-IV data and how much is due to the cell-processing methods need. A Monte Carlo calculation using the VIM code will provide an essential test of the present methods.

Reactor Modelling

The enhanced sensitivities of the large heterogeneous cores has highlighted the need for consideration of fine details in the reactor loadings. Initial results with the "All-master-model" have produced improvements in consistency in the analysis. The first steps have been taken in the automated production of the calculational models from the detailed reactor loading files.

REFERENCES

1. The JUPITER Program: ANL Analysis of ZPPR-9, Report prepared for the First Meeting on JUPITER Program, September 11 and 12, 1980.

2. The JUPITER Program: Analysis of ZPPR-10, Report prepared for the Second Analysis Meeting on JUPITER Program, October 19-26, 1981.

3. M. J. Lineberry, H. F. McFarlane and P. J. Collins, "Physics Assessments of LMFBR Integral parameters," Proc. of the Topical Meeting on Advances in Reactor Physics and Core Thermal Hydraulics, Kiamesha Lake, New York, September 22-24, 1982 NUREG/CP-0034, Vol. 1, p. 1 (1982).

4. T. Ikegami, internal report, (1980), "Relevant sections included in UKAEA/USDOE exchange package."

5. S. G. Carpenter, "Measurements of Control Rod Worths using ZPPR," Proc. of the Specialists Meeting on Control Rod Measurements Technique: Reactivity Worth and Power Distribution, Cadarache, France, 1976, NEACRP-U-75.

6. P. J. Collins and S. B. Brumbach, eds., internal report, (1984), "Relevant sections included in UKAEA/USDOE exchange package."

7. M. J. Lineberry, et al., "Physics Studies of a Heterogeneous Liquid-Metal Fast Breeder Reactor," Nuclear Technology, 44, p. 21 (1979).

8. S. B. Brumbach and P. J. Collins, eds., internal report, (1983), "Relevant sections included in UKAEA/USDOE exchange package."

9. S. B. Brumbach and S. G. Carpenter, internal report, (1983), "Relevant sections included in UKAEA/USDOE exchange package."

10. S. B. Brumbach and P. J. Collins, eds., internal report, (1983), "Relevant sections included in UKAEA/USDOE exchange package."

11. S. B. Brumbach and P. J. Collins, eds., internal report, (1984), "Relevant sections included in UKAEA/USDOE exchange package."

12. R. Avery, "Theory of Coupled Reactors," Proc. Second U.N. Intl. Conf. on Peaceful uses of Atomic Energy, 12, U.N. Publication, p. 186 (1958).

13. D. C. Wade and R. A. Rydin, "An Experimentally Measurable Relationship Between Asymptotic Flux Tilts and Eigenvalue Separation," Dynamics of Nuclear Systems, University of Arizona Press, Tuscon, Arizona (1972).

14. S. B. Brumbach and P. J. Collins, eds., internal report, (1984), "Relevant sections included in UKAEA/USDOE exchange package."

REFERENCES (contd)

15. H. F. McFarlane, et al., "Experimental Studies of Radially Heterogeneous Liquid-Metal Fast Breeder Reactor Critical Assemblies at the Zero Power Plutonium Reactor," Nucl. Sci. and Eng. 87, p. 204 (1984).

16. P. J. Collins and S. B. Brumbach, eds., internal report, (1983), "Relevant sections included in UKAEA/USDOE exchange package."

17. R. E. Kaiser, et al., "Extrapolation of Small Sample Doppler Reactivity Measurements," Proc. of the Topical Meeting on Advances in Reactor Physics and Core Thermal Hydraulics, NUREG/CP-0034 p. 118 (1982).

18. P. J. Collins and R. G. Palmer, "Calculated Size Effects for Reactivity Perturbation Samples in ZPPR," Paper II-38 in Argonne National Laboratory Applied Physics Annual Report July, 1970 to June 30, 1971, ANL-7910, p. 247 (1972).

19. S. B. Brumbach and P. J. Collins, eds., internal report, (1983), "Relevant sections included in UKAEA/USDOE exchange package."

APPENDIX A

Input Data for MC^2 and SDX

The input data for generation of the 226 group library in MC^2-II is shown in Table A.1. The fine group spectrum is generated for the homogeneous composition of the double-fuel-column cells. A number of additional isotopes are added at negligibly low density for editing purposes. Isotopes labelled with an S (e.g. NA23 S) use special resonance shielding treatment for narrow resonances.

A specimen input for SDX is shown in Table A.2. The case shown is the double-fuel-column drawer in fuel ring three. Zone bucklings in 28 groups are applied (on the 09 cards) to the 2082 fine groups of A MCC2, to the intermediate 226 groups of A.INTR and to the 226 groups of A.SEF1D for calculation of a spectrum for group collapse. The special "MODL1B" incorporates a scaling of the input bucklings by a constant factor so as to obtain a k_{eff} of 0.986 for the heterogeneous cell. The SDX runs for the other cells are similar.

```
//CDV4MCC2 JOB (B),USER=B15632,REGION=1400K,CLASS=Y,TIME=060,MSGCLASS A
//*MAIN ORG=RM010,LINES=030,CARDS=000,SYSTEM=S195
//*
//*** B15632.CDV4MCC2
//*
//CD EXEC ARCSP015,
//          VERSION=4,FORMAT=FMT5
//DUMMY1 DD SPACE=(CYL,100,,CONTIG)
//DUMMY2 DD SPACE=(CYL,180,,CONTIG)
//FT06F001 DD SYSOUT=*
//SYSUDUMP DD DUMMY
//FT18F001 DD UNIT=(WRIT6250),
//      DCB=(RECFM=VBS,LRECL=X,BLKSIZE=12280,DEN=4),
//      VOL=(PRIVATE,RETAIN,SER=178816),LABEL=(01,SL),
//      DISP=(NEW,KEEP),
//      DSN=C117.B15632.GPOEL
//FT19F001 DD UNIT=(ALLPERM),
//      DCB=(RECFM=VBS,LRECL=X,BLKSIZE=6136),
//      SPACE=(TRK,(250,10),RLSE),
//      DISP=(OLD,KEEP),
//      DSN=C117.B15632.CDV4226.ISOTXS
//FT37F001 DD UNIT=(SASCR),SUBALLOC=(CYL,(05,01),DUMMY1)
//FT38F001 DD UNIT=(SASCR),SUBALLOC=(CYL,(30,01),DUMMY1)
//FT39F001 DD UNIT=(SASCR),SUBALLOC=(CYL,(55,01),DUMMY1)
//FT40F001 DD UNIT=(SASCR),SUBALLOC=(CYL,(05,01),DUMMY1)
//FT41F001 DD UNIT=(SASCR),SUBALLOC=(CYL,(05,01),DUMMY1)
//FT43F001 DD SUBALLOC=(CYL,(30,01),DUMMY2)
//FT49F001 DD UNIT=(ALLPERM),
//      DCB=(RECFM=VBS,LRECL=X,BLKSIZE=6136),
//      SPACE=(TRK,(01,01)),
//      DISP=(NEW,CATLG),
//      DSN=C117.B15632.CDV42261
//FT50F001 DD UNIT=(WRIT6250),
//      VOL=(PRIVATE,RETAIN,SER=178952),
//      LABEL=(01,SL),
//      DCB=(RECFM=VBS,LRECL=X,BLKSIZE=6136),
//      DISP=(NEW,KEEP),
//      DSN=C117.B15632.CDV42262
//FT52F001 DD SUBALLOC=(CYL,(30,01),DUMMY2)
//FT53F001 DD SUBALLOC=(CYL,(30,01),DUMMY2)
//FT54F001 DD SUBALLOC=(CYL,(30,01),DUMMY2)
//FT55F001 DD SUBALLOC=(CYL,(30,01),DUMMY2)
//FT56F001 DD SUBALLOC=(CYL,(03,01),DUMMY2)
//FT57F001 DD SUBALLOC=(CYL,(03,01),DUMMY2)
//FT58F001 DD SUBALLOC=(CYL,(03,01),DUMMY2)
//FT59F001 DD SUBALLOC=(CYL,(03,01),DUMMY2)
//FT60F001 DD SUBALLOC=(CYL,(03,01),DUMMY2)
//FT61F001 DD SUBALLOC=(CYL,(03,01),DUMMY2)
//FT62F001 DD SPACE=(CYL,(50,5))
//SYSIN DD *
BLOCK=STP015
DATASET=A.STP015
01       000   000   000   000   000   001   001   001   000   000   000
DATASET=A.MCC2
01          VERSION 4, 226 GROUP LIBRARY GENERATION FOR SDX (ZPPR 12,13)
02     120000   000    000
03        001    001    000    010USS226   000   000   000   020   000   000
06          C-12 4        0.0000346          293.00
06          O-16 4        0.0098618          293.00
06          NA23 S        0.0086880          293.00
```

TABLE A.1. Input Data for MC^2

[illegible]	[illegible]	[illegible]000064	293.00
06	[illegible] 4	[illegible]0001840	293.00
[illegible]	[illegible] 3	[illegible]	293.00
06	[illegible]	[illegible]2638	293.00
06	FE 3	[illegible]79308	293.00
06	[illegible] 3	[illegible].0014197	293.00
06	[illegible]	0.0000323	293.00
06	[illegible] 3	0.0004643	293.00
06	U-2354	0.0000112	293.00
06	U-2384	0.0050197	293.00
06	PU2394	0.0017662	293.00
06	PU2404	0.0002338	293.00
06	PU2414	0.0000208	293.00
06	PU2424	0.0000038	293.00
06	AM2414	0.0000153	293.00
00			
06	CL 4	0.0000003	293.00
06	CA 4	0.0000020	293.00
06	CO59 4	0.0000012	293.00
06	PU2384	0.0000011	293.00
00			
06	HYDRGN	1.00000D-12	293.00
06	HE4 4	1.00000D-12	293.00
06	LI-6 4	1.00000D-12	293.00
06	LI-7 4	1.00000D-12	293.00
06	BE-9 3	1.00000D-12	293.00
06	B-10 4	1.00000D-12	293.00
06	B-11 4	1.00000D-12	293.00
06	N-14 4	1.00000D-12	293.00
06	MG 4	1.00000D-12	293.00
06	TI 4	1.00000D-12	293.00
06	V 4	1.00000D-12	293.00
06	NB93 4	1.00000D-12	293.00
06	AG1074	1.00000D-12	293.00
06	AG1094	1.00000D-12	293.00
06	CD 4	1.00000D-12	293.00
06	EU1514	1.00000D-12	293.00
06	EU1534	1.00000D-12	293.00
06	TA1814	1.00000D-12	293.00
06	PB 4	1.00000D-12	293.00
06	TH2324	1.00000D-12	293.00
06	U-2334	1.00000D-12	293.00
06	U-2344	1.00000D-12	293.00
06	U-2364	1.00000D-12	293.00
06	NP2374	1.00000D-12	293.00
06	AM2434	1.00000D-12	293.00

```
09          5.30000E-03 5.35000E-03 2.00000E-05
19      0      0      0      0      0      2
```

TABLE A.1. Input Data for MC^2 (cont.)

```
//DADCF34N JOB (B),USER=B15632,REGION=1250K,TIME=008,CLASS=X,MSGCLASS=A
//*MAIN ORG RM010,LINES=030,CARDS=000,SYSTEM=S195
//*
//*** B15632.DSDXLIB(ADCF34NF) *** DADCF34N
//*
//CX EXEC PGM=IEBGENER
//SYSPRINT DD SYSOUT=*
//SYSUT1 DD UNIT=(READ6250),
//      VOL=(PRIVATE,RETAIN,SER=178952),LABEL=(01,SL),
//      DCB=DEN=4,DISP=(OLD,KEEP),
//      DSN=C117.B15632.CDV42262
//SYSUT2 DD UNIT=(SASCR),
//      DCB=(RECFM=VBS,LRECL=X,BLKSIZE=6136),
//      SPACE=(CYL,(30,05),RLSE),
//      DISP=(NEW,PASS),
//      DSN=&&CDV42262
//SYSIN DD DUMMY
/*
//ZDSDX EXEC ARCSP012,
//*
//*     PRELIB='C116.B09202.SDX.MODLIB',
//*
//      VERSION=4,FORMAT=FMT5,ACCT=N0322
//FT33F001 DD DISP=(SHR),DSN=C117.B15632.CDV42261
//FT33F002 DD DISP=(OLD,DELETE),DSN=&&CDV42262
//FT36F001 DD UNIT=(ALLPERM),
//      DCB=(RECFM=VBS,LRECL=X,BLKSIZE=6136),
//      SPACE=(TRK,(1,1)),
//      DISP=(NEW,CATLG),
//      DSN=C117.B15632.DADCFF3N.V4281
//FT36F002 DD UNIT=(ALLPERM),
//      DCB=(RECFM=VBS,LRECL=X,BLKSIZE=6136),
//      SPACE=(TRK,(20,2),RLSE),
//      DISP=(NEW,CATLG),
//      DSN=C117.B15632.DADCFF3N.V4282
//SYSIN DD *
BLOCK=OLD
DATASET=MCC2F1
DATASET=MCC2F2
DATASET=MCC2F3
DATASET=MCC2F4
DATASET=MCC2F5
DATASET=XS.ISO
BLOCK=STP012
DATASET=A.SDX
01          1       1       0       1
02    CORE
03          1
DATASET=A.MCC2
01            ZPPR ASSY 13 *** HOMOG DOUBLE COLUMN DRAWER ** B**?(G)<F3
02       90000      0       0
03                  0       0       0       0       1       0       0     20
04                      0.0          0.0          0.0          1.35          1.35
06          C-12 4         0.0000345       293.000
06          O-16 4         0.0101694       293.000
06          NA23 S         0.0088144       293.000
06          AL27 4         0.0000063       293.000
06          SI   4         0.0001839       293.000
06          CR   S         0.0031620       293.000
06          MN55 S         0.0002685       293.000
```

TABLE A.2. Input data for SDX.

```
06        FE    3          0.0181507      293.000
06        NI    3          0.0011175      293.000
06        CU    3          0.0000322      293.000
06        MO    3          0.0001644      293.000
06        U-2354           0.0000111      293.000
06        U-2384           0.0050163      293.000
06        PU2394           0.0017677      293.000
06        PU2404           0.0002349      293.000
06        PU2414           0.0000181      293.000
06        PU2424           0.0000038      293.000
06        AM2414           0.0000175      293.000
09            +0.007704         0.0           0.0  0001  0102
09            +0.007976         0.0           0.0  0103  0162
09            +0.006931         0.0           0.0  0163  0222
09            +0.006722         0.0           0.0  0223  0282
09            +0.005721         0.0           0.0  0283  0342
09            +0.003510         0.0           0.0  0343  0402
09            +0.003491         0.0           0.0  0403  0462
09            +0.001734         0.0           0.0  0463  0522
09            +0.001680         0.0           0.0  0523  0582
09            +0.000595         0.0           0.0  0583  0642
09            -0.000032         0.0           0.0  0643  0702
09            -0.000538         0.0           0.0  0703  0762
09            +0.000313         0.0           0.0  0763  0822
09            -0.000810         0.0           0.0  0823  0882
09            -0.003426         0.0           0.0  0883  0942
09            -0.003093         0.0           0.0  0943  1002
09            -0.009027         0.0           0.0  1003  1062
09            -0.001920         0.0           0.0  1063  1122
09            -0.004827         0.0           0.0  1123  1182
09            -0.007621         0.0           0.0  1183  1242
09            -0.013989         0.0           0.0  1243  1302
09            -0.021085         0.0           0.0  1303  1362
09            -0.028858         0.0           0.0  1363  1422
09            -0.052053         0.0           0.0  1423  1482
09            -0.100486         0.0           0.0  1483  1542
09            -0.047015         0.0           0.0  1543  1602
09            -0.072890         0.0           0.0  1603  1782
09            -0.036386         0.0           0.0  1783  2082
12    U-2354
12    U-2384
12    PU2394
12    PU2404
12    PU2414
12    PU2424
12    AM2414
DATASET=A.INTR
01          ZPPR ASSY 13 *** DOUBLE COL FUEL  WITH B**(G)<F3
02             0 90000      0      0
03             0      0      0      0      0      0      0      0      0      0
04          0.00000D 00 1.00000D-03 1.00000D-04 0.00000D 00 1.00000D 00
05             0      0      0      0      0      0
09            +0.007704                               001    036
09            +0.007976                               037    049
09            +0.006931                               050    066
09            +0.006722                               067    080
09            +0.005721                               081    093
09            +0.003510                               094    105
09            +0.003491                               106    116
09            +0.001734                               117    128
```

TABLEA.2. Input data for SDX (cont.)

```
09          +0.001680                               129   140
09          +0.000595                               141   144
09          -0.000032                               145   150
09          -0.000538                               151   157
09          +0.000313                               158   164
09          -0.000810                               165   168
09          -0.003426                               169   172
09          -0.003093                               173   178
09          -0.009027                               179   185
09          -0.001920                               186   191
09          -0.004827                               192   193
09          -0.007621                               194   195
09          -0.013989                               196   197
09          -0.021085                               198   199
09          -0.028858                               200   201
09          -0.052053                               202   203
09          -0.100486                               204   205
09          -0.047015                               206   207
09          -0.072890                               208   213
09          -0.036386                               214   226
10      1.00000D-03 9.60000D-01
DATASET=A.NIP
01          ZPPR ASSY 13 ** DOUBLE COLUMN FUEL DRAWER
03              10
04              11    11
06    MPD1          0.0      0.44450     1
06    NAQ1      0.44450      1.07950     1
06    FOX1      1.07950      1.39700     1
06    CLD1      1.39700      1.43510     1
06    ZPU1      1.43510      1.99390     1
06    CLD2      1.99390      2.03200     1
06    FOX2      2.03200      2.34950     1
06    NAH1      2.34950      3.61950     1
06    FOX3      3.61950      3.93700     1
06    CLD3      3.93700      3.97510     1
06    ZPU2      3.97510      4.53390     1
06    CLD4      4.53390      4.57200     1
06    FOX4      4.57200      4.88950     1
06    NAQ2      4.88950      5.52450     1
14          ZPUX  PU2394  0.010200  PU2404  0.001357  PU2414  0.000163
14          ZPUX  PU2424  0.000023  AM2414  0.000059  U-2354  0.000064
14          ZPUX  U-2384  0.028974  MO    S 0.002615
14          NAQX  CR    S 0.003105  NI    S 0.001485  MN55 S  0.000244
14          NAQX  SI    4 0.000155  MO    S 0.000017  CU    4 0.000026
14          NAQX  NA23 S  0.021902  C-12 4  0.000019  FE    S 0.010747
14          NAHX  CR    S 0.002129  NI    S 0.000993  MN55 S  0.000174
14          NAHX  SI    4 0.000110  MO    S 0.000014  CU    4 0.000021
14          NAHX  NA23 S  0.021902  C-12 4  0.000019  FE    S 0.007391
14          CLDX  C-12 4  0.000019  FE    S 0.059971  CR    S 0.017428
14          CLDX  NI    S 0.008691  MN55 S  0.001279  SI    4 0.000841
14          CLDX  MO    S 0.000055  CU    4 0.000108  AL27 4  0.000067
14          FOXX  C-12 4  0.000019  O-16 4  0.046632  FE    S 0.035770
14          FOXX  CR    S 0.001152  NI    S 0.000502  MN55 S  0.000103
14          FOXX  SI    4 0.000063  MO    S 0.000012  CU    4 0.000015
14          MPDX  C-12 4  0.000248  FE    S 0.053590  CR    S 0.015251
14          MPDX  NI    S 0.006694  MN55 S  0.001360  SI    4 0.000809
14          MPDX  MO    S 0.000151  CU    4 0.000210
15    MPDX  MPD1
15    FOXX  FOX1  FOX2
15    FOXX  FOX3  FOX4
```

TABLE A.2. Input data for SDX (cont.)

```
15    CLDX  CLD1  CLD2
15    CLDX  CLD3  CLD4
15    NAQX  NAQ1
15    NAQX  NAQ2
15    NAHX  NAH1
15    ZPUX  ZPU1
15    ZPUX  ZPU2
DATASET=A.CPSE
01            IN-PLATE FOR BENOIST D-MOD GEN
02      30000      0      0
03    C-12 4FUEL        C H
03    O-16 4FUEL        O H
03    NA23 SFUEL        NAH
03    AL27 4FUEL        ALH
03    SI   4FUEL        SIH
03    CR   SFUEL        CRH
03    MN55 SFUEL        MNH
03    FE   SFUEL        FEH
03    NI   SFUEL        NIH
03    CU   4FUEL        CUH
03    MO   SFUEL        MOH
03    U-2354FUEL        U5H   ZPU1  U5Z1
03    U-2384FUEL        U8H   ZPU1  U8Z1
03    PU2394FUEL        P9H   ZPU1  P9Z1
03    PU2404FUEL        P0H   ZPU1  P0Z1
03    PU2414FUEL        P1H   ZPU1  P1Z1
03    PU2424FUEL        P2H   ZPU1  P2Z1
03    AM2414FUEL        A1H   ZPU1  A1Z1
03    U-2354FUEL        U5H   ZPU2  U5Z2
03    U-2384FUEL        U8H   ZPU2  U8Z2
03    PU2394FUEL        P9H   ZPU2  P9Z2
03    PU2404FUEL        P0H   ZPU2  P0Z2
03    PU2414FUEL        P1H   ZPU2  P1Z2
03    PU2424FUEL        P2H   ZPU2  P2Z2
03    AM2414FUEL        A1H   ZPU2  A1Z2
NOSORT=A.SEF1D
100000     0      0      0      1      1
    18   226      1
C-12 4  O-16 4  NA23 S  AL27 4  SI    4  CR    S  MN55 S  FE    S  NI    S  CU    4
MO    S  U-2354  U-2384  PU2394  PU2404  PU2414  PU2424  AM2414
    2     0     0     0     0     0     0     0     0     0     0     0     0     0     0     0
 0.0000345 0.0101694 0.0088144 0.0000063 0.0001839 0.0031620
 0.0002685 0.0181607 0.0014175 0.0000322 0.0004644 0.0000111
 0.0050163 0.0017677 0.0002349 0.0000181 0.0000038 0.0000175
         0        0.5    0.0001        5.0        0.0        0.0        0.0
   16     1     0    10     0     1     1     1     3     5     5     3   0.0     0     1     3
09              +0.007704                           001    036    1
09              +0.007976                           037    049    2
09              +0.006931                           050    066    3
09              +0.006722                           067    080    4
09              +0.005721                           081    093    5
09              +0.003510                           094    105    6
09              +0.003491                           106    116    7
09              +0.001734                           117    128    8
09              +0.001680                           129    140    9
09              +0.000595                           141    144    10
09              -0.000032                           145    150    11
09              -0.000538                           151    157    12
09              +0.000313                           158    164    13
09              -0.000810                           165    168    14
```

TABLE A.2. Input data for SDX (cont.)

```
[illegible]         -0.003[illegible]                                    16[illegible]   [illegible]   [illegible]
09                  -0.00[illegible]93                                   173    178    16
09                  -0.009027                                            179    185    17
09                  -0.001920                                            186    191    18
09                  -0.00[illegible]                                     192    193    19
09                  -0.0[illegible]621                                   194    195    20
09                  -0.013989                                            196    197    21
09                  -0.021085                                            198    199    22
09                  -0.028858                                            200    201    23
09                  -0.052053                                            202    203    24
09                  -0.100486                                            204    205    25
09                  -0.047015                                            206    207    26
09                  -0.072890                                            208    213    27
09                  -0.036386                                            214    226    28
    28      1      0      0
   36    13    17    14    13    12    11    12    12    04    06    07
   07    04    04    06    07    06    02    02    02    02    02    02
   02    02    06    13
FUEL
C D
O U
NAD
ALD
STD
CRD
MND
FED
NID
CUD
MOD
U5D
U8D
P9D
P0D
P1D
P2D
A1D
PU2394  U-2384
```

TABLE A.2. Input data for SDX. (cont.)

APPENDIX B

The homogenized atom densities used in the ZPPR-13 analysis are presented in this appendix. Tables B.1, B.2 and B.3 give the densities for ZPPR-13A,

The atom densities for the control-rod drawers and control-rod-position drawers are given in Table B.4. Drawers without buttons were used in all measurements in ZPPR-13A

TABLE B.1. Homogenized Drawer Compositions for ZPPR-13A (10^{24} At/cm^3)

	Single Col. Fuel 0-18 in.	Double Col. Fuel 0-18 in.	Internal and Radial Blankets				Radial Refl. 0-36 in.	Matrix Tubes
			0-18 in.	18-28 in.	28-29 in.	29-31 in.		
C	0.0000335	0.0000345	0.0000317	0.0000317	0.0000317	0.0000319	0.0002481	0.0000186
O	0.0139736	0.0101694	0.0222897	0.0222897	0.0000003	0.0000003	---	---
Na	0.0090188	0.0088144	0.0041382	0.0041382	0.0041814	0.0041335	---	---
Si	0.0001579	0.0001839	0.0001386	0.0001386	0.0001391	0.0001397	0.0006011	0.0000676
Al	0.0000040	0.0000063	0.0000024	0.0000024	0.0000025	0.0000025	---	---
Mn	0.0002305	0.0002685	0.0001992	0.0001992	0.0001998	0.0002540	0.0012705	0.0001048
Cr	0.0026941	0.0031620	0.0023224	0.0023224	0.0023337	0.0056522	0.0135216	0.0011764
Fe	0.0131312	0.0181607	0.0082918	0.0082918	0.0083338	0.0207125	0.0587994	0.0042335
Ni	0.0011794	0.0014175	0.0009994	0.0009994	0.0010043	0.0024565	0.0058834	0.0004751
Cu	0.0000295	0.0000322	0.0000289	0.0000289	0.0000289	0.0000291	0.0000320	0.0000171
Mo	0.0002407	0.0004644	0.0000137	0.0000137	0.0000137	0.0000137	0.0000164	0.0000081
^{235}U	0.0000126	0.0000111	0.0000287	0.0000287	0.0000636	0.0000434	---	---
^{238}U	0.0058083	0.0050163	0.0131978	0.0131978	0.0291505	0.0193358	---	---
^{238}Pu	0.0000004	0.0000010	---	---	---	---	---	---
^{239}Pu	0.0008898	0.0017677	---	---	---	---	---	---
^{240}Pu	0.0001180	0.0002339	---	---	---	---	---	---
$^{241}Pu^{a}$	0.0000082	0.0000181	---	---	---	---	---	---
^{242}Pu	0.0000016	0.0000037	---	---	---	---	---	---
$^{241}Am^{a}$	0.0000089	0.0000175	---	---	---	---	---	---

JAII3A29

TABLE B.1. Homogenized Drawer Compositions for ZPPR-13A (10^{24} At/cm^3) (cont.)

	Axial Blanket 18-28 in.[b]	Axial Blanket 18-28 in.[c]	Axial Blanket 28-29 in.[b]	Axial Blanket 28-29 in.[c]	Axial Blank t 29-31 in.[b]	29-31 in.[c]	Iron Block Refl.	Steel Refl.
C	0.0000332	0.0000619	0.0000331	0.0000617	0.0000570	0.0000858	0.0005874	0.0002182
O	0.0142813	0.0088277	0.0054643	0.0000006	0.0054449	0.0000006	---	---
Na	0.0092968	0.0090981	0.0094191	0.0089800	0.0093394	0.0089800	---	---
Si	0.0001444	0.0002397	0.0001439	0.0002403	0.0002238	0.0003212	0.0001115	0.0008379
Al	0.0000028	0.0000027	0.0000028	0.0000028	0.0000028	0.0000028	---	---
Mn	0.0002061	0.0003731	0.0002053	0.0003739	0.0003243	0.0004944	0.0006791	0.0014769
Cr	0.0024051	0.0041119	0.0024004	0.0041313	0.0040282	0.0057751	0.0019487	0.0145968
Fe	0.0123703	0.0147299	0.0123621	0.0147976	0.0184370	0.0209428	0.0768471	0.0517614
Ni	0.0010349	0.0018039	0.0010325	0.0018140	0.0017752	0.0025642	0.0007863	0.0064583
Cu	0.0000279	0.0000279	0.0000278	0.0000280	0.0000471	0.0000473	0.0000256	0.0000185
Mo	0.0000127	0.0000128	0.0000127	0.0000127	0.0000226	0.0000227	0.0000127	0.0000090
^{235}U	0.0000179	0.0000179	0.0000320	0.0000318	0.0000217	0.0000217	---	---
^{238}U	0.0081644	0.0081649	0.0145622	0.0145321	0.0096843	0.0097138	---	---
^{238}Pu	---	---	---	---	---	---	---	---
^{239}Pu	---	---	---	---	---	---	---	---
^{240}Pu	---	---	---	---	---	---	---	---
^{241}Pu	---	---	---	---	---	---	---	---
^{242}Pu	---	---	---	---	---	---	---	---
^{241}Am	---	---	---	---	---	---	---	---

[a]Decayed to 6-1-82.

[b]Axial blanket behind double column fuel.

[c]Axial blanket behind single column fuel.

JAI13B30

APPENDIX C: Detailed Reaction Rate Analysis for ZPPR-13A

The results are grouped according to the different traverses, radial or axial and special experiments. For convenience, some results are duplicated among the tables.

Tables C.1 and C.2:	Traverses at the x and y axes for all four reactions.
Tables C.3 to C.6:	Comparison of ^{235}U in symmetric positions at the axes, at 30° and at 60° to the axes.
Table C.7:	^{235}U fission at 15°, 45°, 75° to the x-axis.
Table C.8:	Special measurements in the radial reflector.
Table C.9:	^{235}U fission foil for fission chamber calibration.
Tables C.10 and C.11:	Axial traverses in 147-42 and 147-27.
Tables C.12 to C.14:	Axial traverses for ^{235}U fission.
Tables C.15 and C.16:	Reaction rate ratios at the axes.
Tables C.17 and C.18:	Reaction rate ratios from the axial traverses.

TABLE C.1. ZPPR-13A : REACTION RATES MEASURED ALONG THE X-AXIS

MATRIX POSITION	ZONE	239PU(N,F) EXP. A	239PU(N,F) C/E	235U(N,F) EXP. A	235U(N,F) C/E	238U(N,G) EXP. A	238U(N,G) C/E	238U(N,F) B EXP. A	238U(N,F) B C/E
149 50	CB	4.260	0.973	5.131	1.006	0.6138	1.036	0.0185	0.877
148 50	CB	4.357	0.951	5.140	1.004	0.6111	1.041	0.0189	0.859
149 49	CB	4.341	0.954	5.180	0.995	0.6113	1.040	0.0185	0.878
148 49	CB	4.248	0.975	5.164	0.999	0.6065	1.048	0.0189	0.860
147 49	CB	4.473	0.959	5.306	1.000	0.6268	1.050	0.0220	0.883
147 48	CB	4.588	0.966	5.429	1.003	0.6521	1.041	0.0255	0.897
148 47	CB	4.669	0.980	5.524	1.011	0.6649	1.053	0.0289	0.919
148 46	CB	5.095	0.979	5.981	0.996	0.7207	1.049	0.0378	1.065
148 45	CB	5.610	0.975	6.324	1.003	0.7739	1.057	0.0612	1.052
148 44	CB	6.118	0.980	6.557	1.020	0.8217	1.051	0.1006	1.045
147 44	F1 S	6.146	0.958	6.492	1.021	0.8763	1.034	0.1421	0.948
147 43	F1	6.434	0.971	6.684	1.004	0.8544	1.067	0.2089	0.895
147 42	F1 S	6.717	0.999	6.915	1.022	0.9121	1.053	0.2009	0.958
147 41	F1	6.895	0.974	7.235	0.996	0.9277	1.060	0.2250	0.893
147 40	F1 S	7.023	0.968	7.576	1.012	1.0090	1.048	0.1666	0.911
147 39	B1	7.222	0.984	7.987	1.012	1.0130	1.046	0.0951	1.054
147 38	B1	7.350	0.992	8.155	1.018	1.0330	1.055	0.0910	1.072
147 37	B1	7.559	0.998	8.198	1.022	1.0330	1.059	0.1267	1.050
147 36	F2	7.567	0.997	7.977	1.020	1.0250	1.086	0.2419	0.884
147 35	F2 S	7.709	1.015	7.940	1.045	1.0560	1.060	0.2397	0.946
147 34	F2	7.654	1.007	7.942	1.029	1.0120	1.094	0.2618	0.919
147 33	F2 S	7.403	1.017	7.901	1.047	1.0500	1.078	0.2020	0.931
147 32	B2	7.343	1.016	7.936	1.058	1.0210	1.079	0.1102	1.045
147 31	B2	6.985	1.040	7.797	1.061	1.0050	1.083	0.0846	1.118
147 30	B2	6.847	1.048	7.551	1.062	0.9617	1.093	0.1028	1.106
147 29	F3	6.764	1.022	7.061	1.058	0.9143	1.117	0.2050	0.919
147 28	F3 S	6.611	1.045	6.765	1.069	0.8874	1.089	0.1988	1.032
147 27	F3 C	6.431	1.039	6.315	1.070	0.7932	1.140	0.2261	0.981
147 26	F3 S	5.818	1.047	5.897	1.066	0.7578	1.099	0.1838	1.030
147 25	F3	5.102	1.059	5.257	1.071	0.6627	1.135	0.1773	0.977
147 24	F3 S	4.388	1.023	4.646	1.062	0.6026	1.109	0.1125	0.979
147 23	RB	3.628	1.037	3.934	1.083	0.4870	1.125	0.0493	1.112
147 22	RB	2.911	1.016	3.255	1.069	0.3947	1.116	0.0262	1.049
147 21	RB	2.339	1.009	2.667	1.065	0.3114	1.109	0.0141	1.004
147 20	RB	2.095	0.967	2.321	1.057	0.2540	1.088	0.0079	0.952

A UNITS OF 10-18 REACTIONS PER ATOM PER SECOND AT A REACTOR POWER OF APPROXIMATELY 1 WATT. THE 239PU FOILS WERE LOCATED AT 90.8 MM FROM THE MIDPLANE,THE 235U FOILS AT 63.1 MM AND THE 238U FOILS AT 77.0 MM .

B STATISTICAL UNCERTAINTIES FOR MEASUREMENT OF 238U FISSION RANGE FROM 3% TO 7% WITH PENETRATION IN THE CENTRAL BLANKET AND FROM 3% TO 20% WITH PENETRATION IN THE RADIAL BLANKET.

C AXIAL TRAVERSE LOCATION, ALL FOILS WERE AT 77.0 MM FROM THE MIDPLANE

TABLE C.2. ZPPR-13A : REACTION RATES MEASURED ALONG THE Y-AXIS

MATRIX POSITION	ZONE	239PU(N,F) EXP. A	239PU(N,F) C/E	235U(N,F) EXP. A	235U(N,F) C/E	238U(N,G) EXP. A	238U(N,G) C/E	238U(N,F) B EXP. A	238U(N,F) B C/E
149 50	CB	4.260	0.973	5.131	1.006	0.6138	1.036	0.0185	0.877
149 49	CB	4.341	0.954	5.180	0.995	0.6113	1.040	0.0185	0.878
148 50	CB	4.357	0.951	5.140	1.004	0.6111	1.041	0.0189	0.859
148 49	CB	4.248	0.975	5.164	0.999	0.6065	1.048	0.0189	0.860
147 49	CB	4.473	0.959	5.306	1.000	0.6268	1.050	0.0220	0.883
147 48	CB	4.588	0.966	5.429	1.003	0.6521	1.041	0.0255	0.897
146 49	CB	4.802	0.953	5.523	1.011	0.6701	1.045	0.0284	0.940
145 49	CB	5.145	0.967	5.894	1.008	0.7207	1.046	0.0382	1.056
144 49	CB	5.597	0.971	6.266	1.006	0.7858	1.033	0.0595	1.082
143 49	CB	6.035	0.983	6.558	1.009	0.8195	1.042	0.1003	1.046
143 48	F1 S	6.002	0.970	6.511	1.008	0.8761	1.023	0.1443	0.926
142 48	F1	6.376	0.971	6.643	1.001	0.8472	1.067	0.2124	0.873
141 48	F1 S	6.639	0.985	6.909	1.012	0.9130	1.035	0.2065	0.908
140 48	F1	6.727	0.976	7.078	1.000	0.9152	1.056	0.2233	0.867
139 48	F1 S	6.807	0.972	7.439	1.004	0.9928	1.039	0.1631	0.900
138 48	B1	6.954	0.992	7.820	1.003	0.9812	1.049	0.0891	1.084
137 48	B1	7.202	0.978	7.922	1.012	1.0070	1.045	0.0886	1.069
136 48	B1	7.413	0.979	7.960	1.012	1.0090	1.043	0.1247	1.031
135 48	F2	7.459	0.972	7.699	1.011	1.0080	1.055	0.2407	0.873
134 48	F2 S	7.469	0.995	7.733	1.022	1.0170	1.048	0.2247	0.956
133 48	F2	7.479	0.972	7.563	1.021	0.9811	1.068	0.2542	0.884
132 48	F2 S	7.142	0.989	7.626	1.022	1.0250	1.043	0.1905	0.908
131 48	B2	6.921	1.005	7.576	1.036	0.9715	1.061	0.0995	1.053
130 48	B2	6.659	1.010	7.294	1.053	0.9422	1.074	0.0762	1.124
129 48	B2	6.522	1.012	7.136	1.038	0.9074	1.069	0.0934	1.099
128 48	F3 S	6.407	0.995	6.679	1.043	0.8988	1.054	0.1683	0.954
127 48	F3	6.350	0.982	6.236	1.046	0.7929	1.104	0.2176	0.912
126 48	F3 S	5.952	1.009	5.962	1.043	0.7733	1.068	0.1915	0.969
125 48	F3	5.434	1.009	5.475	1.030	0.6838	1.093	0.1954	0.953
124 48	F3	4.787	1.008	4.842	1.040	0.6163	1.092	0.1677	0.923
123 48	F3 S	4.071	1.002	4.323	1.040	0.5616	1.085	0.1032	0.964
122 48	RB	3.382	1.013	3.667	1.060	0.4566	1.094	0.0471	1.037
121 48	RB	2.768	0.975	3.034	1.047	0.3713	1.082	0.0230	1.068
120 48	RB	2.215	0.978	2.506	1.041	0.2935	1.078	0.0129	0.990
119 48	RB	1.933	0.979	2.187	1.045	0.2385	1.071	0.0084	0.812

A UNITS OF 10-18 REACTIONS PER ATOM PER SECOND AT A REACTOR POWER OF APPROXIMATELY 1 WATT. THE 239PU FOILS WERE LOCATED AT 90.8 MM FROM THE MIDPLANE,THE 235U FOILS AT 63.1 MM AND THE 238U FOILS AT 77.0 MM.

B STATISTICAL UNCERTAINTIES FOR MEASUREMENT OF 238U FISSION RANGE FROM 3% TO 7% WITH PENETRATION IN THE CENTRAL BLANKET AND FROM 3% TO 20% WITH PENETRATION IN THE RADIAL BLANKET.

TABLE C.3. ZPPR-13A: MEASUREMENTS OF 235U FISSION RATES IN SYMMETRIC POSITIONS ALONG THE X-AXIS

MATRIX POSITION	ZONE	EXP. A	C/E	MEAN C/E (S.D.) B	MATRIX POSITION	ZONE	EXP. A	C/E	MEAN C/E (S.D.) B
ULH QUADRANT					URH QUADRANT				
147 44	F1 S	6.492	1.021		147 55	F1 S	6.539	1.016	
147 43	F1	6.684	1.004		147 56	F1	6.651	1.010	
147 42	F1 S	6.915	1.022		147 57	F1 S	7.024	1.015	
147 41	F1	7.235	0.996	1.011	147 58	F1	7.173	1.007	1.011
147 40	F1 S	7.576	1.012	(0.011)	147 59	F1 S	7.620	1.008	(0.004)
147 39	B1	7.987	1.012		147 60	B1	8.012	1.011	
147 38	B1	8.155	1.018	1.017	147 61	B1	8.017	1.038	1.024
147 37	B1	8.198	1.022	(0.005)	147 62	B1	8.211	1.023	(0.014)
147 36	F2	7.977	1.020		147 63	F2	8.016	1.018	
147 35	F2 S	7.940	1.045		147 64	F2 S	8.036	1.036	
147 34	F2	7.942	1.029	1.035	147 65	F2	7.933	1.033	1.031
147 33	F2 S	7.901	1.047	(0.013)	147 66	F2 S	8.025	1.035	(0.008)
147 32	B2	7.936	1.058		147 67	B2	7.929	1.063	
147 31	B2	7.797	1.061	1.060	147 68	B2	7.773	1.068	1.066
147 30	B2	7.551	1.062	(0.002)	147 69	B2	7.546	1.067	(0.003)
147 29	F3	7.061	1.058		147 70	F3	7.138	1.045	
147 28	F3 S	6.765	1.069		147 71	F3 S	6.894	1.058	
147 27	F3	6.315	1.070		147 72	F3	6.431	1.055	
147 26	F3 S	5.897	1.066		147 73	F3 S	5.956	1.060	
147 25	F3	5.257	1.071	1.066	147 74	F3	5.334	1.060	1.055
147 24	F3 S	4.646	1.062	(0.005)	147 75	F3 S	4.718	1.050	(0.006)
147 23	RB	3.934	1.083		147 76	RB	3.992	1.072	
147 22	RB	3.255	1.069		147 77	RB	3.321	1.052	
147 21	RB	2.667	1.065	1.069	147 78	RB	2.770	1.029	1.054
147 20	RB	2.321	1.057	(0.011)	147 79	RB	2.319	1.062	(0.018)

A UNITS OF 10-18 FISSIONS PER ATOM PER SECOND AT A REACTOR POWER OF APPROXIMATELY 1 WATT. THE 235U FOILS WERE LOCATED 63.1 MM FROM THE MIDPLANE. ULH QUADRANT=UPPER-LEFT-HAND QUADRANT OF THE ZPPR HALF-1, ETC.

B STANDARD DEVIATION OF THE C/E DISTRIBUTION

TABLE C.4 . ZPPR-13A: MEASUREMENTS OF 235U FISSION RATES IN SYMMETRIC POSITIONS ALONG THE Y-AXIS

MATRIX POSITION	ZONE	EXP. A	C/E	MEAN C/E (S.D.) B	MATRIX POSITION	ZONE	EXP. A	C/E	MEAN C/E (S.D.) B
ULH QUADRANT					LLH QUADRANT				
143 48	F1 S	6.511	1.008		154 48	F1 S	6.419	1.019	
142 48	F1	6.643	1.001		155 48	F1	6.589	1.006	
141 48	F1 S	6.909	1.012		156 48	F1 S	6.819	1.022	
140 48	F1	7.078	1.000	1.005	157 48	F1	6.982	1.010	1.013
139 48	F1 S	7.439	1.004	(0.005)	158 48	F1 S	7.369	1.010	(0.007)
138 48	B1	7.820	1.003		159 48	B1	7.623	1.025	
137 48	B1	7.922	1.012	1.009	160 48	B1	7.809	1.022	1.029
136 48	B1	7.960	1.012	(0.005)	161 48	B1	7.722	1.039	(0.009)
135 48	F2	7.699	1.011		162 48	F2	7.479	1.037	
134 48	F2 S	7.733	1.022		163 48	F2 S	7.531	1.045	
133 48	F2	7.563	1.021	1.019	164 48	F2	7.465	1.031	1.039
132 48	F2 S	7.626	1.022	(0.005)	165 48	F2 S	7.440	1.044	(0.007)
131 48	B2	7.576	1.036		166 48	B2	7.372	1.060	
130 48	B2	7.294	1.053	1.042	167 48	B2	7.237	1.057	1.062
129 48	B2	7.136	1.038	(0.009)	168 48	B2	6.901	1.070	(0.007)
128 48	F3 S	6.679	1.043		169 48	F3 S	6.694	1.037	
127 48	F3	6.236	1.046		170 48	F3	6.260	1.040	
126 48	F3 S	5.962	1.043		171 48	F3 S	6.033	1.038	
125 48	F3	5.475	1.030		172 48	F3	5.362	1.048	
124 48	F3	4.842	1.040	1.040	173 48	F3	4.748	1.057	1.046
123 48	F3 S	4.323	1.040	(0.006)	174 48	F3 S	4.248	1.054	(0.009)
122 48	RB	3.667	1.060		175 48	RB	3.656	1.059	
121 48	RB	3.034	1.047		176 48	RB	2.987	1.060	
120 48	RB	2.506	1.041	1.048	177 48	RB	2.455	1.058	1.061
119 48	RB	2.187	1.045	(0.008)	178 48	RB	2.136	1.066	(0.004)

A UNITS OF 10-18 FISSIONS PER ATOM PER SECOND AT A REACTOR POWER OF APPROXIMATELY 1 WATT. THE 235U FOILS WERE LOCATED 63.1 MM FROM THE MIDPLANE.ULH QUADRANT=UPPER-LEFT-HAND QUADRANT OF THE ZPPR HALF-1, ETC.

B STANDARD DEVIATION OF THE C/E DISTRIBUTION

TABLE C.5 . ZPPR-13A: MEASUREMENTS OF 235U FISSION RATES IN SYMMETRIC POSITIONS AT 30-DEGREES TO THE X-AXIS

MATRIX POSITION	ZONE	A EXP.	C/E	MEAN C/E (S.D.) B	MATRIX POSITION	ZONE	A EXP.	C/E	MEAN C/E (S.D.) B
ULH QUADRANT					URH QUADRANT				
145 44	F1 S	6.676	1.014		145 55	F1 S	6.606	1.027	
144 43	F1	6.923	1.007	1.010	144 56	F1	6.863	1.017	1.014
143 42	F1	7.233	1.008	(0.004)	143 57	F1	7.310	0.999	(0.014)
143 41	B1	7.688	1.022		143 58	B1	7.730	1.018	
143 40	B1	8.162	0.999	1.020	143 59	B1	8.014	1.019	1.022
142 39	B1	8.053	1.038	(0.020)	142 60	B1	8.140	1.030	(0.007)
142 38	F2	7.990	1.014		142 61	F2	8.098	1.004	
141 37	F2 S	7.977	1.034		141 62	F2 S	7.979	1.038	
141 36	F2	7.854	1.033	1.025	141 63	F2	7.964	1.022	1.020
140 35	F2	7.865	1.020	(0.010)	140 64	F2	7.919	1.017	(0.014)
139 34	B2	7.884	1.043	1.037	139 65	B2	7.998	1.033	1.035
139 33	B2	7.803	1.031	--	139 66	B2	7.794	1.037	--
138 32	F3	7.193	1.028		138 67	F3	7.224	1.028	
137 31	F3 S	6.575	1.045		137 68	F3 S	6.726	1.027	
137 30	F3	6.238	1.057		137 69	F3	6.384	1.037	
137 29	F3 S	5.784	1.063		137 70	F3 S	5.914	1.044	
136 28	F3	4.894	1.068	1.052	136 71	F3	4.945	1.061	1.039
135 28	F3	4.610	1.053	(0.014)	135 71	F3	4.699	1.039	(0.012)

A UNITS OF 10-18 FISSIONS PER ATOM PER SECOND AT A REACTOR POWER OF APPROXIMATELY 1 WATT. THE 235U FOILS WERE LOCATED 63.1 MM FROM THE MIDPLANE.ULH QUADRANT=UPPER-LEFT-HAND QUADRANT OF THE ZPPR HALF-1, ETC.

B STANDARD DEVIATION OF THE C/E DISTRIBUTION

TABLE C.6. ZPPR-13A: MEASUREMENTS OF 235U FISSION RATES IN SYMMETRIC POSITIONS AT 60-DEGREES TO THE X-AXIS

MATRIX POSITION	ZONE	EXP. A	C/E	MEAN C/E (S.D.) B	MATRIX POSITION	ZONE	EXP. A	C/E	MEAN C/E (S.D.) B
ULH QUADRANT					URH QUADRANT				
143 46	F1	6.610	0.999		143 53	F1	6.667	0.992	
142 46	F1 S	6.880	1.010	1.004	142 53	F1 S	6.934	1.003	0.993
141 45	F1	7.070	1.004	(0.006)	141 54	F1	7.216	0.985	(0.009)
140 44	B1	7.730	1.008		140 55	B1	7.716	1.012	
139 44	B1	8.007	1.003	1.010	139 55	B1	7.934	1.013	1.011
138 43	B1	8.071	1.018	(0.008)	138 56	B1	8.175	1.007	(0.003)
137 43	F2	7.844	1.011		137 56	F2	7.986	0.995	
136 42	F2 S	7.807	1.035		136 57	F2 S	7.937	1.021	
135 42	F2	7.704	1.027	1.021	135 57	F2	7.720	1.028	1.013
134 41	F2	7.745	1.009	(0.013)	134 58	F2	7.791	1.007	(0.015)
133 40	B2	7.798	1.026	1.032	133 59	B2	7.759	1.036	1.039
132 40	B2	7.507	1.037	--	132 59	B2	7.499	1.042	--
131 40	F3 S	7.263	1.016		131 59	F3 S	7.284	1.017	
130 39	F3	6.515	1.030		130 59	F3	6.739	1.034	
129 38	F3	6.028	1.052		129 61	F3	6.134	1.038	
128 38	F3 S	5.593	1.057		128 61	F3 S	5.673	1.047	
127 37	F3	4.761	1.055	1.044	127 62	F3	4.837	1.044	1.036
127 36	F3	4.446	1.055	(0.017)	127 63	F3	4.538	1.037	(0.011)

A UNITS OF 10-18 FISSIONS PER ATOM PER SECOND AT A REACTOR POWER OF APPROXIMATELY 1 WATT. THE 235U FOILS WERE LOCATED 63.1 MM FROM THE MIDPLANE. ULH QUADRANT=UPPER-LEFT-HAND QUADRANT OF THE ZPPR HALF-1, ETC.

B STANDARD DEVIATION OF THE C/E DISTRIBUTION.

TABLE C.7. ZPPR-13A: MEASUREMENTS OF 235U FISSION RATES AT 15-,45- AND 75-DEGREES TO THE X-AXIS

MATRIX POSITION	ZONE	EXP. A	C/E	MEAN C/E (S.D.) B
ULH QUADRANT AT 15-DEGREES				
142 30	F3	7.082	1.046	
140 29	F3	6.487	1.055	
141 28	F3	6.256	1.058	
141 27	F3 S	5.723	1.065	
141 26	F3	5.174	1.056	1.057
140 26	F3	4.913	1.060	(0.006)
ULH QUADRANT AT 45-DEGREES				
133 36	F3	6.848	1.050	
133 35	F3	6.722	1.044	
132 35	F3	6.581	1.027	
132 34	F3	6.236	1.040	
132 33	F3	5.669	1.049	
131 33	F3	5.419	1.048	1.044
131 32	F3 S	5.042	1.052	(0.009)
ULH QUADRANT AT 75-DEGREES				
129 44	F3	6.809	1.018	
128 44	F3 S	6.520	1.034	
127 43	F3	6.018	1.034	
126 43	F3	5.559	1.037	
125 42	F3	4.791	1.054	1.039
125 41	F3	4.578	1.054	(0.014)

A UNITS OF 10-18 FISSIONS PER ATOM PER SECOND AT A REACTOR POWER OF APPROXIMATELY 1 WATT. THE 235U FOILS WERE LOCATED 63.1 MM FROM THE MIDPLANE.ULH QUADRANT=UPPER-LEFT-HAND QUADRANT OF THE ZPPR HALF-1, ETC.
B STANDARD DEVIATION OF THE C/E DISTRIBUTION.

TABLE C.8. ZPPR-13A: SPECIAL 235U(N,F) MEASUREMENTS IN THE RADIAL REFLECTOR

MATRIX POSITION	ZONE[A]	X-AXIS POSITIONS Z,MM	EXP.[B]	C/E	MATRIX POSITION	ZONE[A]	Y-AXIS POSITIONS Z,MM	EXP.[B]	C/E
148 17	RR T	12.3	1.537	1.059	116 48	RR T	12.3	1.230	1.041
148 17	RR T	26.2	1.524	1.066	116 48	RR T	26.2	1.231	1.038
148 17	RR T	40.0	1.527	1.062	116 48	RR T	40.0	1.236	1.032
148 17	RR B	12.3	1.528	1.069	116 48	RR B	12.3	1.488	1.139
148 17	RR B	26.2	1.523	1.070	116 48	RR B	26.2	1.487	1.138
148 17	RR B	40.0	1.538	1.057	116 48	RR B	40.0	1.503	1.124
181 48	RR T	12.3	1.598	1.072	148 82	RR T	12.3	1.554	1.053
181 48	RR T	26.2	1.590	1.076	148 82	RR T	26.2	1.549	1.054
181 48	RR T	40.0	1.581	1.080	148 82	RR T	40.0	1.552	1.050
181 48	RR B	12.3	1.350	0.955	148 82	RR B	12.3	1.553	1.056
181 48	RR B	26.2	1.330	0.968	148 82	RR B	26.2	1.551	1.056
181 48	RR B	40.0	1.333	0.964	148 82	RR B	40.0	1.548	1.055

A ZONE RR =RADIAL REFLECTOR. T = IN FOIL HOLDER LOCATION NEAR TOP OF DRAWER (12.1 MM ABOVE DRAWER CENTRE). B = IN FOIL HOLDER LOCATION NEAR BOTTOM OF DRAWER (12.1 MM BELOW DRAWER CENTR

B UNITS OF 10-18 FISSIONS PER ATOM PER SECOND AT A REACTOR POWER OF APPROXIMATELY 1 WATT.

TABLE C.9. ZPPR-13A: 235U FISSION MEASURED IN POSITIONS SYMMETRIC TO IN-CORE FISSION CHAMBERS

MATRIX POSITION	ZONE	EXP. A	C/E	MEAN C/E (S.D.) B	MATRIX POSITION	ZONE	EXP. A	C/E	MEAN C/E (S.D.) B
150 51	CB	5.343	1.006		126 51	F3 S	5.793	1.045	
244 51	CB	6.391	1.005	1.004	226 57	F3 S	5.231	1.031	
250 45	CB	6.333	1.002	(0.002)	232 63	F3 S	6.621	1.032	
					132 69	F3	4.295	1.027	
143 56	F1	7.133	1.000		238 69	F3	6.441	1.044	
250 57	F1 S	6.988	1.017		144 69	F3	7.277	1.019	
256 51	F1 S	6.797	1.009		150 75	F3 S	4.816	1.058	
156 45	F1	7.053	0.992	1.000	156 69	F3	6.960	1.037	
144 45	F1	6.675	0.984	(0.013)	262 69	F3	5.650	1.060	
					268 63	F3	5.572	1.060	
138 51	B1	7.846	1.002		168 57	F3	6.649	1.029	
156 57	B1	7.668	1.035		174 51	F3 S	4.404	1.042	
150 39	B1	8.003	1.007		168 45	F3	6.888	1.016	
244 39	B1	8.035	1.026	1.018	268 39	F3	6.236	1.038	
238 45	B1	7.903	1.021	(0.014)	168 33	F3	4.493	1.041	
					262 33	F3	6.694	1.039	
232 51	F2 S	7.660	1.009		256 27	F3 S	5.859	1.066	
238 57	F2 S	8.000	1.008		150 27	F3	6.319	1.068	
244 63	F2	7.980	1.019		244 27	F3	6.058	1.051	
150 63	F2	7.969	1.019		138 27	F3	4.888	1.057	
256 63	F2	7.897	1.023		132 33	F3	5.669	1.049	
262 57	F2	7.708	1.022		126 39	F3	4.692	1.027	1.042
162 51	F2	7.665	1.005		226 45	F3	5.586	1.033	(0.015)
262 45	F2	7.614	1.018						
256 39	F2 S	8.065	1.016						
250 33	F2 S	7.905	1.040	1.019					
138 39	F2	7.780	1.027	(0.010)					
					220 57	RB	2.138	1.093	
132 57	B2	7.661	1.024		126 63	RB	3.820	1.060	
138 63	B2	8.030	1.035		238 75	RB	3.050	1.056	
250 69	B2	7.570	1.050		274 63	RB	2.464	1.059	
160 63	B2	8.051	1.024		162 27	RB	4.033	1.074	1.069
268 51	B2	7.031	1.056		232 27	RB	2.764	1.069	(0.014)
162 39	B2	7.800	1.041						
156 33	B2	7.816	1.049						
144 33	B2	7.977	1.047						
238 33	B2	7.501	1.038						
232 39	B2	7.268	1.032	1.039					
132 45	B2	7.665	1.030	(0.011)					

A UNITS OF 10-18 FISSIONS PER ATOM PER SECOND AT A REACTOR POWER OF APPROXIMATELY 1 WATT. THE 235U FOILS WERE LOCATED 63.1 MM FROM THE MIDPLANE.

B STANDARD DEVIATION OF THE C/E DISTRIBUTION FOR THE SELECTED GROUPS.

TABLE C.10. ZPPR-13A: AXIAL TRAVERSES IN MATRIX 147-42

MATRIX POSITION	ZONE	Z,MM	239PU(N,F) EXP.A	239PU(N,F) C/E	235U(N,F) EXP.A	235U(N,F) C/E	238U(N,G) EXP.A	238U(N,G) C/E	238U(N,F) EXP.A	238U(N,F) C/E
147 42	F1 S	63.1	--	--	6.918	1.029	--	--	--	--
147 42	F1 S	77.0	6.717	0.999	6.915	1.022	0.9121	1.053	0.2009	0.958
147 42	F1 S	127.8	6.541	0.993	6.714	1.019	0.8990	1.035	0.1932	0.964
147 42	F1 S	204.0	6.085	0.983	6.229	1.014	0.8317	1.033	0.1689	1.013
147 42	F1 S	280.2	5.372	0.982	5.489	1.019	0.7355	1.037	0.1555	0.960
147 42	F1 S	331.0	4.848	0.972	4.902	1.028	0.6783	1.015	0.1413	0.926
147 42	F1 S	381.8	4.265	0.963	4.472	1.001	0.5987	1.025	0.1168	0.928
147 42	F1 S	432.6	3.571	0.983	3.956	1.005	0.5364	1.017	0.0888	0.908
147 42	AB	483.4	3.307	0.975	3.602	1.023	0.4450	1.062	0.0456	0.954
147 42	AB	534.2	2.801	0.988	3.197	1.018	0.3860	1.059	0.0252	0.960 B
147 42	AB	610.4	2.169	0.965	2.517	1.003	0.2935	1.052	0.0122	0.851 B
147 42	AB	686.6	1.592	0.951	1.815	1.016	0.2107	1.041	0.0060	0.773 B
CORE REGION - MEAN				0.982		1.017		1.031		0.951
(S.D.)				(0.012)		(0.010)		(0.013)		(0.035)

A UNITS OF 10-18 REACTIONS PER ATOM PER SECOND AT A REACTOR POWER OF APPROXIMATELY 1 WATT.
B STATISTICAL UNCERTAINTIES ARE 3% TO 20% FOR 238U FISSION AT THESE LOCATIONS

TABLE C.11. ZPPR-13A: AXIAL TRAVERSES IN MATRIX 147-27

MATRIX POSITION	ZONE	Z,MM	239PU(N,F) EXP.A	239PU(N,F) C/E	235U(N,F) EXP.A	235U(N,F) C/E	238U(N,G) EXP.A	238U(N,G) C/E	238U(N,F) EXP.A	238U(N,F) C/E
147 27	F3	77.0	6.431	1.039	6.315	1.070	0.7932	1.140	0.2261	0.981
147 27	F3	127.8	6.271	1.031	6.120	1.069	0.7729	1.133	0.2244	0.956
147 27	F3	204.0	5.706	1.043	5.664	1.065	0.7176	1.126	0.2038	0.966
147 27	F3	280.2	5.167	1.012	5.074	1.050	0.6467	1.107	0.1801	0.953
147 27	F3	331.0	4.587	1.016	4.564	1.048	0.5803	1.112	0.1600	0.937
147 27	F3	381.8	3.984	1.016	4.025	1.050	0.5243	1.094	0.1324	0.938
147 27	F3	432.6	3.361	1.023	3.554	1.045	0.4474	1.138	0.0990	0.930
147 27	AB	483.4	3.050	1.009	3.190	1.074	0.4117	1.070	0.0445	1.056 B
147 27	AB	534.2	2.522	1.039	2.860	1.054	0.3593	1.062	0.0247	1.064 B
147 27	AB	610.4	1.983	0.993	2.204	1.061	0.2690	1.073	0.0125	0.894 B
147 27	AB	686.6	1.419	0.999	1.625	1.057	0.1925	1.070	0.0077	0.636 B
CORE REGION - MEAN				1.026		1.057		1.121		0.952
(S.D.)				(0.012)		(0.011)		(0.017)		(0.018)

A UNITS OF 10-18 REACTIONS PER ATOM PER SECOND AT A REACTOR POWER OF APPROXIMATELY 1 WATT.
B STATISTICAL UNCERTAINTIES ARE 3% TO 20% FOR 238U FISSION AT THESE LOCATIONS

TABLE C.12. ZPPR-13A: AXIAL TRAVERSES FOR 235U(N,F) IN FUEL RING 3 NEAR TO THE AXES

	MATRIX POSITION 147-27		MATRIX POSITION 147-72		MATRIX POSITION 126-48		MATRIX POSITION 171-48	
Z,MM A	EXP. B	C/E	EXP. B	C/E	EXP. B	C/E	EXP. B	C/E
	ULH QUADRANT		URH QUADRANT		ULH QUADRANT		LLH QUADRANT	
12.9	6.437	1.069	6.556	1.054	5.971	1.033	6.121	1.041
12.9	6.435	1.072	6.567	1.055	6.098	1.032	5.956	1.053
12.9	6.398	1.080	6.566	1.057	6.173	1.036	5.882	1.045
63.1	--	--	6.478	1.056	5.962	1.043	5.923	1.047
77.0	6.315	1.070	6.431	1.055	5.873	1.031	6.033	1.038
127.8	6.120	1.069	6.211	1.058	5.647	1.038	5.789	1.047
204.0	5.664	1.065	5.731	1.057	5.193	1.042	5.320	1.051
280.2	5.074	1.050	5.082	1.053	4.611	1.038	4.721	1.048
331.0	4.564	1.048	4.612	1.042	4.165	1.033	4.247	1.048
381.8	4.025	1.050	4.065	1.044	3.705	1.029	3.774	1.045
432.6	3.554	1.045	3.626	1.029	3.257	1.035	3.345	1.042
CORE REGION MEAN		1.062		1.051		1.035		1.046
(S.D.)		(0.012)		(0.009)		(0.004)		(0.004)

A THE THREE MEASUREMENTS AT Z=12.9 MM WERE RESPECTIVELY 12.1 MM ABOVE THE DRAWER CENTRE, AT THE DRAWER CENTRE AND 12.9 MM BELOW THE DRAWER CENTRE (ALONG THE Y-DIMENSION). MATRIX POSITIONS 126-48 AND 171-48 WERE SINGLE-FUEL-COLUMN DRAWERS.

B UNITS OF 10-18 FISSIONS PER ATOM PER SECOND AT A REACTOR POWER OF APPROXIMATELY 1 WATT. ULH QUADRANT = UPPER-LEFT-HAND QUADRANT OF ZPPR HALF-ONE ETC.

TABLE C.13. ZPPR-13A: AXIAL TRAVERSES FOR 235U(N,F) IN FUEL RING 3 AT 30-DEGREES TO THE X-AXIS

	MATRIX POSITION 137-31		MATRIX POSITION 137-68		MATRIX POSITION 160-68		MATRIX POSITION 160-31	
Z,MM A	EXP. B	C/E	EXP. B	C/E	EXP. B	C/E	EXP. B	C/E
	ULH QUADRANT		URH QUADRANT		LRH QUADRANT		LLH QUADRANT	
12.9	6.664	1.050	6.704	1.049	6.839	1.044	6.663	1.064
12.9	6.732	1.050	6.811	1.042	6.831	1.038	6.658	1.058
12.9	6.803	1.046	6.811	1.049	6.667	1.053	6.540	1.066
63.1	6.640	1.052	--	--	--	--	--	--
77.0	6.575	1.045	6.726	1.027	6.665	1.053	6.486	1.074
127.8	6.341	1.049	--	--	--	--	--	--
204.0	5.877	1.044	--	--	--	--	--	--
280.2	5.190	1.044	5.230	1.041	5.256	1.053	5.222	1.053
331.0	4.679	1.040	4.703	1.039	4.719	1.054	4.750	1.040
381.8	4.134	1.039	4.161	1.037	4.190	1.049	4.191	1.042
432.6	3.630	1.039	--	--	--	--	--	--
CORE REGION MEAN		1.045		1.041		1.049		1.057
(S.D.)		(0.005)		(0.008)		(0.006)		(0.013)

A THE THREE MEASUREMENTS AT Z=12.9 MM WERE RESPECTIVELY 12.1 MM ABOVE THE DRAWER CENTRE, AT THE DRAWER CENTRE AND 12.9 MM BELOW THE DRAWER CENTRE (ALONG THE Y-DIMENSION). MATRIX POSITIONS 126-48 AND 171-48 WERE SINGLE-FUEL-COLUMN DRAWERS.

B UNITS OF 10-18 FISSIONS PER ATOM PER SECOND AT A REACTOR POWER OF APPROXIMATELY 1 WATT. ULH QUADRANT = UPPER-LEFT-HAND QUADRANT OF ZPPR HALF-ONE ETC.

TABLE C.14. ZPPR-13A: AXIAL TRAVERSES FOR 235U(N,F) IN FUEL RING 3 AT 60-DEGREES TO THE X-AXIS

	MATRIX POSITION 130-39		MATRIX POSITION 130-60		MATRIX POSITION 167-60		MATRIX POSITION 167-39	
Z,MM A	EXP. B	C/E	EXP. B	C/E	EXP. B	C/E	EXP. B	C/E
	ULH QUADRANT		URH QUADRANT		LRH QUADRANT		LLH QUADRANT	
12.9	6.853	1.018	6.762	1.036	6.606	1.036	6.502	1.045
63.1	6.652	1.025	--	--	--	--	--	--
77.0	6.515	1.030	6.496	1.037	6.601	1.040	6.592	1.034
127.8	6.185	1.050	--	--	--	--	--	--
204.0	5.819	1.029	--	--	--	--	--	--
280.2	5.177	1.023	5.195	1.024	5.264	1.030	5.250	1.025
331.0	4.669	1.019	4.658	1.026	4.747	1.027	4.751	1.018
381.8	4.122	1.020	4.147	1.019	4.195	1.026	4.191	1.020
432.6	3.673	1.008	--	--	--	--	--	--
CORE REGION MEAN		1.025		1.029		1.034		1.033
(S.D.)		(0.010)		(0.006)		(0.007)		(0.013)

A UNITS OF 10-18 FISSIONS PER ATOM PER SECOND AT A REACTOR POWER OF APPROXIMATELY 1 WATT. ULH QUADRANT = UPPER-LEFT-HAND QUADRANT OF ZPPR HALF-ONE, ETC.

TABLE C.15. ZPPR-13A : REACTION RATE RATIOS ALONG THE X-AXIS

MATRIX POSITION	ZONE	235U(N,F)/239PU(N,F) EXP.	235U(N,F)/239PU(N,F) C/E	238U(N,G)/239PU(N,F) EXP.	238U(N,G)/239PU(N,F) C/E	238U(N,F)/239PU(N,F) EXP.	238U(N,F)/239PU(N,F) C/E
149 50	CB	1.204	1.034	0.1441	1.065	0.00435	0.901
148 50	CB	1.180	1.056	0.1403	1.095	0.00434	0.903
149 49	CB	1.193	1.043	0.1408	1.090	0.00426	0.920
148 49	CB	1.216	1.025	0.1428	1.075	0.00444	0.882
147 49	CB	1.186	1.043	0.1401	1.095	0.00492	0.921
147 48	CB	1.183	1.038	0.1421	1.078	0.00557	0.929
148 47	CB	1.183	1.032	0.1424	1.074	0.00619	0.938
148 46	CB	1.174	1.017	0.1415	1.072	0.00742	1.088
148 45	CB	1.127	1.029	0.1380	1.084	0.01090	1.079
148 44	CB	1.072	1.041	0.1343	1.072	0.01644	1.066
147 44	F1 S	1.056	1.066	0.1426	1.079	0.02312	0.990
147 43	F1	1.039	1.034	0.1328	1.099	0.03247	0.922
147 42	F1 S	1.029	1.023	0.1358	1.054	0.02991	0.959
147 41	F1	1.049	1.023	0.1345	1.088	0.03263	0.917
147 40	F1 S	1.079	1.045	0.1437	1.083	0.02372	0.941
147 39	B1	1.106	1.028	0.1403	1.063	0.01317	1.071
147 38	B1	1.110	1.026	0.1405	1.064	0.01238	1.081
147 37	B1	1.085	1.024	0.1367	1.061	0.01676	1.052
147 36	F2	1.054	1.023	0.1355	1.089	0.03197	0.887
147 35	F2 S	1.030	1.030	0.1370	1.044	0.03109	0.932
147 34	F2	1.038	1.022	0.1322	1.086	0.03420	0.913
147 33	F2 S	1.067	1.029	0.1418	1.060	0.02729	0.915
147 32	B2	1.081	1.041	0.1390	1.062	0.01501	1.029
147 31	B2	1.116	1.020	0.1439	1.041	0.01211	1.075
147 30	B2	1.103	1.013	0.1405	1.043	0.01501	1.055
147 29	F3	1.044	1.035	0.1352	1.093	0.03031	0.899
147 28	F3 S	1.023	1.023	0.1342	1.042	0.03007	0.988
147 27	F3 A	X.XXX	X.XXX	X.XXXX	X.XXX	X.XXXXX	X.XXX
147 26	F3 S	1.014	1.018	0.1303	1.050	0.03159	0.984
147 25	F3	1.030	1.011	0.1299	1.072	0.03475	0.923
147 24	F3 S	1.059	1.038	0.1373	1.084	0.02564	0.957
147 23	RB	1.084	1.044	0.1342	1.085	0.01358	1.072
147 22	RB	1.118	1.052	0.1356	1.098	0.00901	1.032
147 21	RB	1.140	1.056	0.1331	1.099	0.00605	0.995
147 20	RB	1.108	1.093	0.1212	1.125	0.00379	0.984
A AXIAL TRAVERSE LOCATION		0.982	1.030	0.1233	1.097	0.03516	0.944

TABLE C.16. ZPPR-13A: REACTION RATE RATIOS ALONG THE Y-AXIS

MATRIX POSITION	ZONE	235U(N,F)/239PU(N,F) EXP.	235U(N,F)/239PU(N,F) C/E	238U(N,G)/239PU(N,F) EXP.	238U(N,G)/239PU(N,F) C/E	238U(N,F)/239PU(N,F) EXP.	238U(N,F)/239PU(N,F) C/E
149 50	CB	1.204	1.034	0.1441	1.065	0.00435	0.901
149 49	CB	1.193	1.043	0.1408	1.090	0.00426	0.920
148 50	CB	1.180	1.056	0.1403	1.095	0.00434	0.903
148 49	CB	1.216	1.025	0.1428	1.075	0.00444	0.882
147 49	CB	1.186	1.043	0.1401	1.095	0.00492	0.921
147 48	CB	1.183	1.038	0.1421	1.078	0.00557	0.929
146 49	CB	1.150	1.061	0.1395	1.097	0.00592	0.986
145 49	CB	1.146	1.042	0.1401	1.082	0.00743	1.092
144 49	CB	1.120	1.036	0.1404	1.064	0.01063	1.114
143 49	CB	1.087	1.026	0.1358	1.060	0.01662	1.064
143 48	F1 S	1.085	1.039	0.1460	1.055	0.02404	0.955
142 48	F1	1.042	1.031	0.1329	1.099	0.03331	0.899
141 48	F1 S	1.041	1.027	0.1375	1.051	0.03110	0.922
140 48	F1	1.052	1.025	0.1360	1.082	0.03319	0.888
139 48	F1 S	1.093	1.033	0.1458	1.069	0.02396	0.926
138 48	B1	1.125	1.011	0.1411	1.057	0.01282	1.093
137 48	B1	1.100	1.035	0.1398	1.069	0.01230	1.093
136 48	B1	1.074	1.034	0.1361	1.065	0.01682	1.053
135 48	F2	1.032	1.040	0.1351	1.085	0.03227	0.898
134 48	F2 S	1.035	1.027	0.1362	1.053	0.03008	0.961
133 48	F2	1.011	1.050	0.1312	1.099	0.03399	0.909
132 48	F2 S	1.068	1.033	0.1435	1.055	0.02667	0.918
131 48	B2	1.095	1.031	0.1404	1.056	0.01438	1.048
130 48	B2	1.095	1.043	0.1415	1.063	0.01144	1.113
129 48	B2	1.094	1.026	0.1391	1.056	0.01432	1.086
128 48	F3 S	1.042	1.048	0.1403	1.059	0.02627	0.959
127 48	F3	0.982	1.065	0.1249	1.124	0.03427	0.929
126 48	F3 S	1.002	1.034	0.1299	1.058	0.03217	0.960
125 48	F3	1.008	1.021	0.1258	1.083	0.03596	0.944
124 48	F3	1.011	1.032	0.1287	1.083	0.03503	0.916
123 48	F3 S	1.062	1.038	0.1380	1.083	0.02535	0.962
122 48	RB	1.084	1.046	0.1350	1.080	0.01393	1.024
121 48	RB	1.096	1.074	0.1341	1.110	0.00832	1.095
120 48	RB	1.131	1.064	0.1325	1.102	0.00581	1.012
119 48	RB	1.131	1.067	0.1234	1.094	0.00432	0.829

TABLE C.17. ZPPR-13A: REACTION RATE RATIOS IN MATRIX 147-42

MATRIX POSITION	ZONE	Z(MM)	235U(N,F)/239PU(N,F) EXP.	235U(N,F)/239PU(N,F) C/E	238U(N,G)/239PU(N,F) EXP.	238U(N,G)/239PU(N,F) C/E	238U(N,F)/239PU(N,F) EXP.	238U(N,F)/239PU(N,F) C/E
147 42	Fl S	77.0	1.029	1.023	0.1358	1.054	0.02991	0.959
147 42	Fl S	127.8	1.026	1.026	0.1374	1.042	0.02954	0.971
147 42	Fl S	204.0	1.024	1.032	0.1367	1.051	0.02776	1.033
147 42	Fl S	280.2	1.022	1.038	0.1369	1.056	0.02895	0.978
147 42	Fl S	331.0	1.011	1.058	0.1399	1.044	0.02915	0.953
147 42	Fl S	381.8	1.049	1.039	0.1404	1.064	0.02739	0.964
147 42	Fl S	432.6	1.108	1.022	0.1502	1.035	0.02488	0.924
147 42	AB	483.4	1.089	1.049	0.1346	1.089	0.01380	0.978
147 42	AB	534.2	1.141	1.030	0.1378	1.072	0.00901	0.972
147 42	AB	610.4	1.160	1.039	0.1353	1.090	0.00562	0.882
147 42	AB	686.6	1.140	1.068	0.1323	1.095	0.00374	0.813
CORE REGION - MEAN				1.034		1.049		0.969
(S.D.)				(0.012)		(0.010)		(0.032)

TABLE C.18. ZPPR-13A: REACTION RATE RATIOS IN MATRIX 147-27

MATRIX POSITION	ZONE	Z(MM)	235U(N,F)/239PU(N,F) EXP.	235U(N,F)/239PU(N,F) C/E	238U(N,G)/239PU(N,F) EXP.	238U(N,G)/239PU(N,F) C/E	238U(N,F)/239PU(N,F) EXP.	238U(N,F)/239PU(N,F) C/E
147 27	F3	77.0	0.983	1.030	0.1233	1.097	0.03516	0.944
147 27	F3	127.8	0.979	1.037	0.1232	1.099	0.03578	0.927
147 27	F3	204.0	0.997	1.021	0.1258	1.080	0.03572	0.926
147 27	F3	280.2	0.986	1.038	0.1252	1.094	0.03486	0.942
147 27	F3	331.0	1.000	1.031	0.1265	1.094	0.03488	0.922
147 27	F3	381.8	1.008	1.033	0.1316	1.077	0.03323	0.923
147 27	F3	432.6	1.055	1.022	0.1331	1.112	0.02945	0.909
147 27	AB	483.4	1.046	1.064	0.1350	1.060	0.01460	1.047
147 27	AB	534.2	1.134	1.014	0.1425	1.022	0.00981	1.024
147 27	AB	610.4	1.111	1.068	0.1357	1.081	0.00630	0.900
147 27	AB	686.6	1.137	1.058	0.1347	1.071	0.00538	0.637
CORE REGION - MEAN				1.030		1.093		0.928
(S.D.)				(0.007)		(0.012)		(0.012)

TABLE D.12. ZPPR-13A: AXIAL TRAVERSES IN MATRIX 148-49

MATRIX POSITION	ZONE	Z,MM	235U(N,F) EXP. A	235U(N,F) C/E	238U(N,G) EXP. A	238U(N,G) C/E	238U(N,F) B EXP. A	238U(N,F) B C/E
148 49	CB	77.0	6.300	1.019	0.7518	1.060	0.0214	0.934
148 49	CB	127.8	6.177	1.007	0.7356	1.049	0.0216	0.894
148 49	CB	204.0	5.698	1.012	0.6776	1.054	0.0167	1.058
148 49	CB	280.2	4.983	1.034	0.6024	1.054	0.0147	1.047
148 49	CB	331.0	4.654	1.003	0.5496	1.043	0.0132	1.034
148 49	CB	381.8	4.177	0.996	0.4845	1.048	0.0107	1.088
148 49	CB	432.6	3.647	0.997	0.4209	1.047	0.0111	0.857
148 49	CB	483.4	3.180	0.980	0.3601	1.040	0.0101	0.744
148 49	CB	534.2	2.672	0.979	0.2989	1.042	0.0072	0.792
148 49	CB	610.4	1.936	0.991	0.2215	1.020	0.0057	0.615
148 49	CB	686.6	1.345	0.961	0.1516	1.000	0.0050	0.413
0 - 458 MM		MEAN		1.010		1.051		0.987
		(S.D.)		(0.013)		(0.006)		(0.091)

A UNITS OF 10-18 REACTIONS PER ATOM PER SECOND AT A REACTOR POWER OF APPROXIMATELY 1 WATT.
B STATISTICAL UNCERTAINTIES FOR 238U FISSION RANGE FROM 6% NEAR THE MIDPLANE TO 18% AT 687 MM.

TABLE D.13. ZPPR-13A: AXIAL TRAVERSES IN MATRIX 148-34

MATRIX POSITION	ZONE	Z,MM	235U(N,F) EXP. A	235U(N,F) C/E	238U(N,G) EXP. A	238U(N,G) C/E	238U(N,F) B EXP. A	238U(N,F) B C/E
148 34	F2 S	77.0 C	8.558	1.027	1.1510	1.045	0.2191	0.948
148 34	F2 S	127.8	8.316	1.011	1.1590 D	1.006	0.1949	1.030 D
148 34	F2 S	204.0	7.675	1.012	1.0330	1.043	0.1962	0.942
148 34	F2 S	280.2	6.750	1.021	0.9187	1.043	0.1677	0.963
148 34	F2 S	331.0	6.126	1.016	0.8422	1.029	0.1456	0.972
148 34	F2 S	381.8	5.486	1.009	0.7509	1.029	0.1267	0.930
148 34	F2 S	432.6	4.878	1.007	0.6620	1.036	0.0939	0.940
148 34	AB	483.4	4.408	1.036	0.5521	1.064	0.0448	1.064
148 34	AB	534.2	3.888	1.033	0.4702	1.075	0.0260	1.034
148 34	AB	610.4	3.057	1.015	0.3658	1.040	0.0147	0.798
148 34	AB	686.6	2.187	1.035	0.2590	1.042	0.0069	0.763
0 - 458 MM		MEAN (S.D.)		1.015 (0.007)		1.038 (0.007)		0.949 (0.016)

A UNITS OF 10-18 REACTIONS PER ATOM PER SECOND AT A REACTOR POWER OF APPROXIMATELY 1 WATT.

B STATISTICAL UNCERTAINTIES FOR 238U FISSION IN THE AXIAL BLANKET RANGE FROM 3% TO 20%.

C THE 235U FOIL WAS LOCATED AT Z=63.1 MM, THE 238U FOIL WAS LOCATED AT Z=77.0 MM.

D THESE FOILS WERE LOCATED AT THE END OF A FUEL PLATE. THE FOIL/CELL-AVERAGE FACTORS ARE NOT APPROPRIATE AND THE DATA SHOULD BE DISCARDED.

TABLE D.14. ZPPR-13A: AXIAL TRAVERSES IN MATRIX 148-31

MATRIX POSITION	ZONE	Z,MM	235U(N,F) EXP. A	235U(N,F) C/E	238U(N,G) EXP. A	238U(N,G) C/E	238U(N,F) B EXP. A	238U(N,F) B C/E
148 31	B2	77.0 C	7.820	1.043	0.9947	1.076	0.0770	1.124
148 31	B2	127.8	7.681	1.023	0.9696	1.069	0.0761	1.099
148 31	B2	204.0	7.122	1.021	0.8972	1.067	0.0713	1.077
148 31	B2	280.2	6.281	1.030	0.7925	1.072	0.0618	1.081
148 31	B2	331.0	5.595	1.045	0.7193	1.064	0.0531	1.097
148 31	B2	381.8	5.001	1.040	0.6358	1.065	0.0460	1.051
148 31	B2	432.6	4.379	1.042	0.5598	1.052	0.0356	1.042
148 31	B2	483.4	3.910	1.010	0.4744	1.060	0.0268	0.963
148 31	B2	534.2	3.285	1.020	0.3923	1.071	0.0185	0.907
148 31	B2	610.4	2.456	1.017	0.2895	1.058	0.0095	0.884
148 31	B2	686.6	1.700	1.014	0.1924	1.081	0.0063	0.643
0 - 458 MM		MEAN (S.D.)		1.035 (0.010)		1.066 (0.008)		1.082 (0.028)

A UNITS OF 10-18 REACTIONS PER ATOM PER SECOND AT A REACTOR POWER OF APPROXIMATELY 1 WATT.

B STATISTICAL UNCERTAINTIES FOR 238U FISSION IN THE AXIAL BLANKET RANGE FROM 3% TO 20%.

C THE 235U FOIL WAS LOCATED AT Z=63.1 MM, THE 238U FOIL WAS LOCATED AT Z=77.0 MM.

TABLE D.15. ZPPR-13A: REACTION RATE RATIOS ALONG THE X-AXIS

MATRIX POSITION	ZONE	235U(N,F)/239PU(N,F) EXP.	C/E	238U(N,G)/239PU(N,F) EXP.	C/E	238U(N,F)/239PU(N,F) EXP.	C/E
148 43	F1	1.073	1.016	0.1389	1.074	0.03054	0.917
148 42	F1	1.009	1.063	0.1317	1.109	0.03237	0.938
148 41	F1 S	1.050	1.043	0.1412	1.059	0.02762	0.949
148 40	F1	1.052	1.055	0.1406	1.097	0.02727	0.944
148 36	F2 S	1.098	1.030	0.1479	1.055	0.02365	0.956
148 35	F2	1.079	1.013	0.1380	1.090	0.03196	0.877
148 34	F2 S	1.088	1.012	0.1463	1.030	0.02785	0.934
148 33	F2	1.084	1.019	0.1416	1.082	0.02879	0.918
148 29	F3	1.060	1.035	0.1381	1.093	0.02938	0.894
148 28	F3	1.015	1.045	0.1290	1.112	0.03347	0.922
148 27	F3 S	1.040	1.015	0.1360	1.041	0.03089	0.949
148 26	F3	1.030	1.020	0.1279	1.103	0.03292	0.963
148 25	F3 S	1.019	1.052	0.1343	1.074	0.02815	0.992
148 24	F3	1.067	1.020	0.1394	1.068	0.03060	0.899